National Library of Canada
Acquisitions and Bibliographic Services Branch
395 Wellington Street
Ottawa, Ontario
K1A 0N4

Bibliothèque nationale du Canada
Direction des acquisitions et des services bibliographiques
395, rue Wellington
Ottawa (Ontario)
K1A 0N4

Your file Votre référence

Our file Notre référence

NOTICE

The quality of this microform is heavily dependent upon the quality of the original thesis submitted for microfilming. Every effort has been made to ensure the highest quality of reproduction possible.

If pages are missing, contact the university which granted the degree.

Some pages may have indistinct print especially if the original pages were typed with a poor typewriter ribbon or if the university sent us an inferior photocopy.

AVIS

La qualité de cette microforme dépend grandement de la qualité de la thèse soumise au microfilmage. Nous avons tout fait pour assurer une qualité supérieure de reproduction.

S'il manque des pages, veuillez communiquer avec l'université qui a conféré le grade.

La qualité d'impression de certaines pages peut laisser à désirer, surtout si les pages originales ont été dactylographiées à l'aide d'un ruban usé ou si l'université nous a fait parvenir une photocopie de qualité inférieure.

Canada

FIELD PERFORMANCE OF HIGH EFFICIENCY GAS-FIRED HEATING SYSTEMS

Peter Monastiriakos

A Thesis
in
The Centre for Building Studies

Presented in Partial Fulfilment of the Requirements
for the Degree of Master of Engineering at
Concordia University
Montreal, Quebec, Canada

May 1994

ISBN 0-315-97608-X

ABSTRACT

Field Performance of High Efficiency Gas-Fired Heating Systems

Peter Monastiriakos

The relative performance of three high efficiency gas-fired heating systems installed in a three story row townhouse in the downtown Montreal area, is assessed. The systems are compared systematically from the point of view of both physical, cost and operational characteristics.

In order to assess the relative performance of the three systems, various operational characteristics were compared. These include: normal daily operation, typical cyclic operation, warm up-cool down tests, and steady-state efficiency. In addition to steady-state efficiency, these test results reveal the transient and cyclic behaviour of the three systems.

From the long-term monitoring of the heating systems, several seasonal performance characteristics were assessed. These include : seasonal frequency distributions for cycle times, average outdoor temperature vs. cycle time, room temperature fluctuations, seasonal gas consumption,

and the cumulative seasonal efficiency.

Of the three heating systems, the hydronic boiler is widely used in residential applications. It is for this reason that the hydronic heating system was chosen as a candidate system for analytical study. To this end, a transient model of a hydronic heating system is developed. Predictions from the model are compared with the experimental data. Using the developed model, improved control strategies have been proposed which give good room temperature control.

ACKNOWLEDGEMENTS

I wish to express my deepest gratitude and appreciation to Dr. M. Zaheer-uddin for his initiation of the present work, his great patience and guidance throughout my undergraduate and graduate studies.

This project was a collaborative effort jointly initiated by Paul Fazio on behalf of the Centre for Building Studies and Mr. Pierre Gauthier on behalf of Gaz Metropolitain Inc. The equipment, facility and support provided by Gaz Metropolitain as well as the financial assistance received is greatly appreciated.

I also would like thank my parents and sister for their relentless support and encouragement in my most difficult and sometimes frustrating hours. Special thanks and appreciation go to my wife Anastasia Radiotis for her great support and patience. Also, for giving me the greatest gift of all: a brand new, healthy son.

I would also like to thank all the friends and colleagues I have made over the years at the Centre for Building Studies for their support.

And finally, I would like to thank God for the good health and opportunity that he has given to me, without whom none of this is possible.

This thesis is dedicated to my late uncle Peter Lambrinakos, and late grandfather Demetrios Marinos both whom I miss dearly and are in my thoughts everyday. May God bless both of you.

TABLE OF CONTENTS

TABLE OF CONTENTS

TABLE OF CONTENTS

TABLE OF CONTENTS

LIST OF FIGURES

LIST OF FIGURES

LIST OF FIGURES

LIST OF FIGURES

LIST OF TABLES

LIST OF TABLES

NOMENCLATURE

A air-side area of the baseboard unit (m^2)

A_f fin surface area (m^2)

A_{lt} water-side heat transfer area per unit length

A_o sum of fin and bare tube area per unit length (m^2/m)

A_d perimeter of the DHW coil (m)

A_{po} outside perimeter of DHW coil (m)

A_{pi} inside perimeter of DHW coil (m)

a_b heat loss coefficient of the boiler jacket (J/s·°C)

a_{dhw} heat loss coefficient of the DHW tank jacket (J/s·°C)

a_z heat loss coefficient of the space or zone (J/s·°C)

C_b boiler thermal capacity (J/°C)

C_c Thermal capacity of DHW coil per unit length (J/m·°C)

$C_{c,w}$ Thermal capacity of the return water in the DHW coil (J/°C)

C_f specific heat of fin material (J/kg·°C)

c_t Thermal capacity of tube material per unit length (J/m·°C)

c_{pw} specific heat of water (J/kg·°C)

C_z thermal capacity of the space or zone (J/°C)

C_{dhw} thermal capacity of water in DHW storage tank (J/°C)

d_i inside tube diameter (m)

d outside tube diameter (m)

e output error vector

h_{it} heat transfer coefficient from DHW coil surface ($J/s \cdot m^2 \cdot °C$)

h_{ta} air-side heat transfer coefficient ($J/s \cdot m^2 \cdot °C$)

h_t heat transfer coefficient from DHW coil surface ($J/s \cdot m^2 \cdot °C$)

K_w conductivity of water ($J/s \cdot °C \cdot m$)

K_f conductivity of fin ($J/s \cdot °C \cdot m$)

l_c length of coil (m)

l_r length of baseboard radiator (m)

l_f height of fin (m)

m_{dhw} mass flow rate of DHW (kg/s)

m_w mass of water in radiator circuit per unit length (kg/m)

m_f mass of fin per unit length (kg/m)

m_t mass of tube per unit length (kg/m)

P_{rw} Prandtl number (dimensionless)

R_{ew} Reynolds number (dimensionless)

T_a outdoor air temperature (°C)

T_b boiler temperature (°C)

T_t baseboard fin-tube temperature (°C)

T_t average baseboard fin-tube temperature (°C)

T_{dhw} DHW temperature (°C)

T_∞ city water temperature (°C)

T_e boiler-room temperature (°C)

T_c DHW coil temperature (°C)

$T_{c,w}$ temperature of water in DHW coil (°C)

T_z zone temperature (°C)

t time (s)

U_1 normalized flow rate of water in baseboard circuit (dimensionless)

U_2 normalized input capacity of the burner (dimensionless)

U_3 normalized flow rate of water in DHW coil (dimensionless)

U_{1max} maximum rated capacity of U_1 (kg/s)

U_{2max} maximum rated capacity of U_2 (kg/s)

U_{3max} maximum rated capicity of U_3 (kg/s)

V_w velocity of water in baseboard radiator circuit (m/s)

y length coordinate (m)

y_f thickness of fin (m)

GREEK LETTERS

α flue-loss coefficient (dimensionless)

η_f fin eficiency (dimensionless)

ε overall effectiveness of the fin-tube surface (dimensionless)

CHAPTER 1

INTRODUCTION AND LITERATURE REVIEW

1.1 Introduction

After the oil embargo of 1973, many western nations adopted very strict and stringent policies towards more efficient energy use. Substantial public awareness campaigns and private efforts were put into planning, research and development, and in service programs to conserve energy in buildings.

Many strategies were developed to help make buildings more energy efficient. Such methods included: making building envelope tighter thus decreasing the heating/cooling loads (infiltration); making better use of building mass to help in decreasing the space load; utilizing the sun and solar design strategies (both passive and active); switching from oil to a more readily available source of energy such as natural gas; utilizing more efficient HVAC system components.

The attention of this study is focused on the usage of natural gas as a combustion fuel for space heating. Here, in Canada, natural gas accounts for 40 percent of fuel used for space heating, and is expected to increase proportionally with the growing multiple-unit building sector [1].

The choice of natural gas for space heating is recommended, but there is need for improving the efficiency of existing gas-fired heating systems. This is regarded as one of the most important step towards energy conservation. In this regard, the high efficiency gas-heating systems, employing condensing and/or heat pipe [2] technology, are seen as potential candidates for upgrading existing systems. Although these systems are presently available and utilized, there is a lack of systematic field data particularly in the context of multiple-unit apartment buildings [3].

Recognizing this lack of field data on high efficiency gas heating systems, a research program was initiated at Concordia University in collaboration with Gas Metropolitain Inc. This program involved a fully renovated three storey apartment building located in downtown Montreal. This building was equipped with three different heating systems installed on each floor, which were instrumented and monitored for two consecutive heating seasons (winter 1987-88 and winter 1988-89). The three heating systems included: a condensing warm-air furnace on the first floor; a zone adjustable modular system located on the second floor; an integrated hydronic boiler located on the third floor.

1.2 Literature Review

The literature review can be divided into three distinct yet related sections. The first section describes and quotes various studies which were conducted upon gas-heating systems, including how some variables were measured. The second section covers various mathematical models utilized in the estimation of system efficiencies and seasonal fuel consumptions. The final part of the survey reviews various standards which are used to assess various heating systems' performance characteristics.

1.2.1 Review of Previous Studies

In single and two family homes, the state of existing central furnace installation is one of several factors contributing to energy consumption for space heating. Other factors are the size and quality of construction of the dwelling, its level of insulation (R-value), degree of tightness, the climate and the occupants' lifestyle.

Improvement of energy use efficiency of such installations can be accomplished in several ways, but usually, by replacement with similar but higher efficiency equipment or by retrofitting either the existing heating system (for better adjustment or sizing) or its energy distribution system (ductwork, hot water piping, etc).

A three year program, known as SHEIP, (Space Heating Efficiency Improvement Program) was initiated whereby over 2650 test sites were monitored by 67 participating gas companies from 48 states and one province [4,5]. Retrofit options were chosen as potentially useful since they can increase the furnace on-time thus operating near full load efficiency, or increase the full load (steady-state) furnace efficiency, or reduce house air lost through the chimney during burner off periods.

Various retrofit options included: derating fuel only, derating fuel and air, addition of vent restriction, addition of vent dampers, and the installation of electronic ignitions. The results showed that vent dampers were most effective in homes with heated basements and full communication between the furnace and the home, reducing the consumption of natural gas for space heating by 10-15% [5].

Another study [6] of 150 low-income family detached residences in Illinois was reviewed. These homes experienced furnace retrofits which had a ceiling cost of $300.00 per dwelling.

The test sites were divided into three distinct climatic zones, the first being the coldest with 7000 HDD (Heating Degree Day), the second with 5200 HDD, and the third with 3800 HDD. The various methods of retrofit

included furnace tune-up, service and repair, and in some cases, replacement. Each furnace was retrofitted by one or more of the following options such as installation of an intermittent ignition device (IID) and installation of thermal vent dampers. The breakdown of retrofits and their corresponding savings can be seen in Table 1.1.

Table 1.1 Retrofits and measured gas savings.

Retrofit Option	Gas Consumption Savings (%)
13 point tune up	0-3
Tune up + IID	4.8
Tune up + IID + thermal vent dampers	10.1
Tune up + thermal vent dampers	5.6

In a separate field study [7], it is shown how furnaces equipped with vent dampers have reported 3-10% energy savings per year.

Another such study was conducted by Gable and Koenig [8]. They found that energy savings and efficiency improvements were obtainable when certain improvements were incorporated into a residential gas-fired heating system. They found that when steady-state efficiency increased from 75 to 84%, a 6.6% increase in seasonal efficiency resulted. They also found that oversizing affects the seasonal efficiency. When an 80000 BH

unit was replaced by a larger 125000 BH unit, the seasonal efficiency dropped by 2.5%. It was also shown that occupant lifestyles and operating schedule played a large role in fuel consumption. The use of 5 °F night set-back between the hours of 11:00 P.M. and 6:00 A.M. resulted in a 7% operating cost savings from the base year.

It should be noted that seasonal efficiency is always less than rated efficiency or steady-state efficiency of a heating system. Both the steady-state and seasonal efficiency are important in assessing the performance of a gas-fired heating system. The steady-state efficiency determines the effectiveness of the combustion side of the heat balance or input, while the seasonal efficiency is based upon the usable heat or output side.

Another study conducted by Hise and Holman [9] showed that furnaces which utilize pilot lights corresponding to 1 ft^3/hr, accounts for 5-10% of the total seasonal fuel consumption. They also found that a furnace which has an oversize factor of 2, which they say is quite common, requires 8-10% more fuel than a unit of correct size. Also, an installation that has uninsulated ducts passing through an unheated crawlspace or attic, will lose 1.5 BH/ft^2 of duct per degree of temperature difference between the duct and the outside. This can amount to 40% of the furnace output under mild conditions and can easily be much greater. In some

cases [10] only 50% of energy entering the duct actually emerges from the register under normal operation. The adjustment of the fan switch does affect the cyclic efficiency, and the conventional high-temperature setting of this switch can reduce the seasonal efficiency performance by as much as 8%.

Steady state efficiency tests are easy to conduct. They require only the temperature profile of the flue gas, and the CO_2/O_2 concentration of the flue gases during a full load test, and in most cases, this rated efficiency is given by the manufacturer. On the other hand, seasonal efficiency measurements are difficult to obtain and require much money and much of time to conduct. Elaborate and costly data acquisition systems must be connected to monitor an installed heating system. For this reason, many researchers have developed [11,12,13] various techniques which correlate seasonal efficiency with steady-state efficiency and various other empirical parameters which are readily available.

One method by which off-cycle losses can be quantified is described in as study conducted by Kweller [14]. The tracer gas method is adopted by DOE to measure these losses. The alternative method uses a controlled flow of gas to a small gas fuelled burner to simulate normal flue or stack temperature previously measured during a cool down test. The tracer gas

method involves measuring mass flow and temperature in the stack during a cool-down period. The product of stack mass flow, specific heat of air, and temperature rise above room air when integrated over the burner off cycle period is equivalent to the off cycle loss.

The alternative method uses a controlled flow of gas to a small Bunsen burner in order to duplicate normal stack temperatures that would exist during a cool down test from steady-state conditions. The amount of energy metered to the burner during this test is equivalent to the normal stack heat lost from residual heat stored in the heat exchanger and lost through the chimney during an off-cycle. This result is within 5% of the losses as calculated by DOE-2.

In another study, Bonne [15] looks at the effect of increasing cycling frequency of furnace/boiler efficiency and operating costs. One of the findings showed that energy losses were higher with increased cycling rates. This is namely due to: the average off-period flue gas temperature increases, which leads to higher flue enthalpy losses; the higher flue-gas temperature cause higher flue and stack velocities removing more heat from the heat exchanger and infiltrating more air from outside to the environment near the furnace or boiler; lowering steady-state efficiency.

Various benefits to higher cycling rates reported in the literature can be summarized follows: the average on period flue gas temperature decreases leading to lower flue enthalpy losses during on cycle; lower flue on temperature causes lower flue and/or stack flows relatively to the steady-state on period; larger relative heat exchanger, thus bursts of high cycling rates spread the fuel input over a larger period of time resulting in a more favourable ratio of heat transfer surface per unit of firing rate; the circulation fan or pump operating time generally increases if the on-delay is smaller than the off-delay since the ratio of fan or pump operating time to burner operating time then increases, this ratio then becomes more favourable in extracting greater energy from the heat exchanger, at the expense of higher electric consumption.

Assuming that the scope is to maintain an unchanged room temperature, it was found that increasing the cycling frequency reduces average on-period flue temperatures, increases average off-period flue temperatures and increases the operating time and cost of the circulation pump or fan. Other indirect influences were also found: lower room temperature because of thermostat droop or because the system is not able to deliver the required heat, reduced duct losses to unheated space, but increased house infiltration because of longer circulating fan operation, shortened life or increased maintenance cost of all switches, relays, valves

and parts involved in mechanical, electrical or thermal cycling when the system turns on and off.

Another study conducted by Bonne and Patani [16] discuss various benefits and drawbacks for modulating and on-off control. Table 1.2 lists the benefits and shortcomings for the above mentioned control systems.

The key to understanding the modulating vs. cycling alternative is contained in the higher steady-state efficiency achievable with the modulation (assuming that excess air can be held constant), on one hand vs. the longer operating hours on the other. Operating costs may be higher if the fuel savings are overshadowed by increased electrical consumption.

Table 1.2 Modulating vs. on-off controls.

Modulating Control
- saves fuel ie. fuel efficiency is higher if excess air is kept constant. - saves costs only if increased electric consumption does not mask fuel savings. - achievable small load swings lead to improved process control or comfort.
On-Off Control
- shorter equipment operating times. - uses less electric energy. - does not require fuel and air modulation controls. - more efficient than fuel only modulation.

Kweller [14] found that energy savings from 6-20% were achievable from the increase in efficiency with both fuel and combustion air modulation, over the conventional single stage on-off control.

Another documented case [2] discusses various design alternatives for the development of a high-efficiency gas-fired, warm air heating system utilizing heat pipe technology. Becker and Searight found that 10% of fuel input energy appears as water vapour or latent heat in the combustion products. This heat is difficult to recover due to low temperature differences across the heat exchanger. To recover this heat adds greatly to the heat exchanger size and inturn to its cost. To increase the thermal efficiency from 85 to 95% requires more than doubling the heat exchanger area. In addition, when operating in the condensing mode, heat exchanger material must be selected to be compatible with the acidity of the condensate.

The final field study by Caron and Wilson [17] presents the field test results on the water-heating performance of integrated systems under actual usage conditions. Field tests were performed at 24 residential sites over a two year period. Integrated systems were installed side by side with existing conventional water heaters, and performance was monitored for alternating weekly periods in the summer. Analysis of the data indicated

that the non-condensing integral systems produce hot water at an efficiency from 49 to 54% range at 64.3 gallons/day at 90 °F, which is comparable to the conventional hot water heater. The efficiency of the condensing integrating system is 58% which compares to the performance of energy-conserving water heaters.

One problem that was discovered was the very high stand-by losses. This was mainly due to excessive cycling caused by undersized water heating coil, and because of cooling of residual hot water left in the transferlines. This was a function of pipe length which also determines the volume of stored hot water subject to energy loss.

1.2.2 Review of Mathematical Models

The next part of the literature review deals with various papers on mathematical modelling of furnaces and boilers, utilized in computer simulation models. Some models are developed by various researchers and their simplicity or complexity varies according to its application.

The first such paper dealt with a computer simulation model developed by Claus and Stephan [18]. In this model, the thermal state of the boiler was calculated by using the method of indirect determination of boiler efficiency. All the variables were measured on a test bench under

standard conditions. Since the flue gas temperature profile and the air temperature at the outlet of the boiler are easily determined, it was possible to calculate the losses through the chimney during the burner-on and burner-off periods. Another assumption that was utilized was that since the temperatures and the heat transfer within the boiler are not known, the boiler is considered as an ideal storage unit with an evenly distributed temperature.

The application of this semi-analytic model was to investigate the effects of various parameters on the behaviour of the boiler and the energy consumption of the boiler. Simple boiler models are insufficient since the effects of various parameters must be known in advance. Purely analytic models cannot be applied to various boiler constructions without developing a new model for each type of boiler. Furthermore, such models do not show more accuracy because of the uncertainties concerning the heat transfer in the combustion chamber.

Malstrom et al. [19] developed a boiler model primarily to be used as part of a larger HVAC simulation model, and thus it was kept as simple as possible. The model developed was based upon previous work by Claus and Stephan (1984), and was kept simple in order to avoid iterations and thus minimizing the computer time.

The flue gas and ventilation losses were computed, assuming first order lag transients approaching constant air temperatures, respectively when the burner starts and stops. Corrections were made for flue gas temperature changes due to wind pressure and chimney temperature dependence on burner intermittency. The environmental (jacket losses) to the plant room were divided into two parts, one dependant on mean boiler water temperature and one on burner operation. The heat content of the boiler was calculated by means of a resulting heat capacity for the boiler and its water, thus the total heat content was represented by one temperature which was the set water (aquastat) temperature.

The model has been compared within the Annex 10 "system simulation" of the International Energy Agency (IEA). In spite of its simplifications, it achieved good accuracy for both calculation of fuel consumption and for calculation of temperature variations of the boiler water.

Another model was developed by Lebrun et al. [20]. In this work, a simplified dynamic model of a hydronic boiler was developed. Its results were analyzed and compared to information gained through the use of a steady-state model in two very different operating conditions. The first condition consisted of standardized lab tests, while the second utilized a

real building studied within the framework of the IEA Annex 10.

As far as energy calculation was concerned, the steady-state evaluation of the boiler performance over a long period was quite satisfactory. The use of a dynamic model did not allow more accuracy in energy calculations, but was necessary in specific problems such as control or integration of the boiler in a complete building and system simulation.

In another study, Pedersen et al. [21] developed a mechanistic first order lag model for warm air furnace. The study followed the format for model presentation as was obtained by the System Simulation Subcommittee of T.C. 4.7 of ASHRAE.

The model was based upon a hot and cold airstreams exchanging heat with the metal walls. By using a lumped parameter analysis, the heat transfer rates to the air and the products of combustion were determined by the effectiveness of the individual heat exchanger. Data was shown along with a first order lag function fitted to the steady-state efficiency determined separately. The resulting behaviour followed a first order lag function.

Kusuda et al. [22] developed three gas furnace models to handle

different operational methods including a pilot light, an intermittent ignition device and a stack damper. By calculating the part load correction factor and multiplying it by the steady-state efficiency, an estimate of the seasonal efficiency was obtained.

A quadratic model was specified similar to that used in DOE-2 and through regression analysis, the coefficients were evaluated. The DOE-2 model calculates the part load ratios (PLR) and efficiency on an hourly basis, whereas the simplified model makes only one calculation to explain the PLR and efficiency for the entire year. The results obtained using the seasonal models were within 5% of those calculated hourly by DOE-2.

1.2.3 Heating System Standards

Under the heading of heating system standards, there exist many different subgroupings. One such subgroupings looks at system performance from the point of view of various norms and regulations. For instance, a gas-fired heating system must have a rated efficiency of at least 75%, according to ANSI/ASHRAE Standard 103, in order to be accepted by the American Gas Association.

Other standards such as CAN1-2.3-M84, and ANSI/ASHRAE Standard 103 describe various ways in which steady-state efficiency tests

are performed.

The last type of standard is utilized to help in the process of mathematical modelling and computer simulation. Such standards are outlined by the International Energy Agency (IEA) Annex 10, by the System Simulation Subcommittee of T.C. 4.7 of ASHRAE, and by DIN 4705 in Germany.

1.3 Scope and Objectives of the Present Work

The literature review shows that field data on high efficiency gas-fired heating systems is lacking. Also a systematic comparison of the performance of different gas-fired heating systems subjected to similar environmental conditions over an extended time such as a heating season is not done. With this as the motivation, an experimental study was carried out. The specific objectives of this research study are:

1. To monitor and gather in-situ field performance data on three different high efficiency gas-fired heating systems, namely (a) a warm-air furnace, (b) a zone adjustable modular heating system, and (c) a hydronic heating system.
2. Compare the cyclic and daily operating characteristics of the heating systems.
3. Evaluate and compare the steady state efficiency.

4. Compare the seasonal efficiency of the heating systems.

The above four objectives are designed to evaluate the relative performance of the three heating systems using performance attributes which are applicable to all heating systems. However, the transient response characteristics of the heating systems are influenced by several design and operating parameters. To study the transient response of the heating system subject to variations in outdoor temperatures, it will be necessary to develop validated models of the heating systems and carry out simulation runs. To this end, it is proposed to develop an analytical model of a hydronic heating system and validate the model using measured data. The rationale for choosing the hydronic heating system over the other two systems was due to the fact that it is an integrated system in that it is designed to supply both space heating and domestic hot water needs of residential houses. It has been reported [23] that such combined systems offer a 20-25 % economic advantage over the conventional separate systems. Therefore, further objectives of this study are :

(A) develop an analytical model of a hydronic heating system,

(B) validate the model using measured data, and

(C) carry out simulation runs using the validated model to study efficient operating strategies to achieve good room temperature control.

CHAPTER 2

TEST FACILITY, HEATING SYSTEMS AND INSTRUMENTATION

In this chapter the test facility and the instrumentation are described. Also included are various calculations which were performed and are essential prior to data analysis and system evaluation. The main focus of this chapter is to describe where and how data was collected, and also to introduce the pertinent background information required for the major data analysis in the subsequent chapters.

There are four basic parts to this chapter: General building description; the building's envelope; heating systems' specifications (ie. rated output capacities, rated input capacities, flow rates, etc...); the data acquisition system and the instrumentation utilized for the various tests and a comparison of physical characteristics and costs of the heating systems.

2.1 General Building Description

The test facility is a three storey townhouse which is characteristic of late 19th to early 20th century Victorian Architecture. It is located in the central east district of downtown Montreal (45° 30'N, 73° 35'W, HDD=8203), on a residential block of similar dwellings. A typical block consists of two rows of houses, separated by a service lane or alley. The homes consist of

approximately 3900 ft^2 (362 m^2) of habitable space (1300 ft^2 per floor)(121 m^2). The facility shares two side or common walls with the adjacent buildings as do all other homes on the block. An elevation of the building as well as a plan view for each floor, are shown in Figure 2.1 and Figure 2.2.

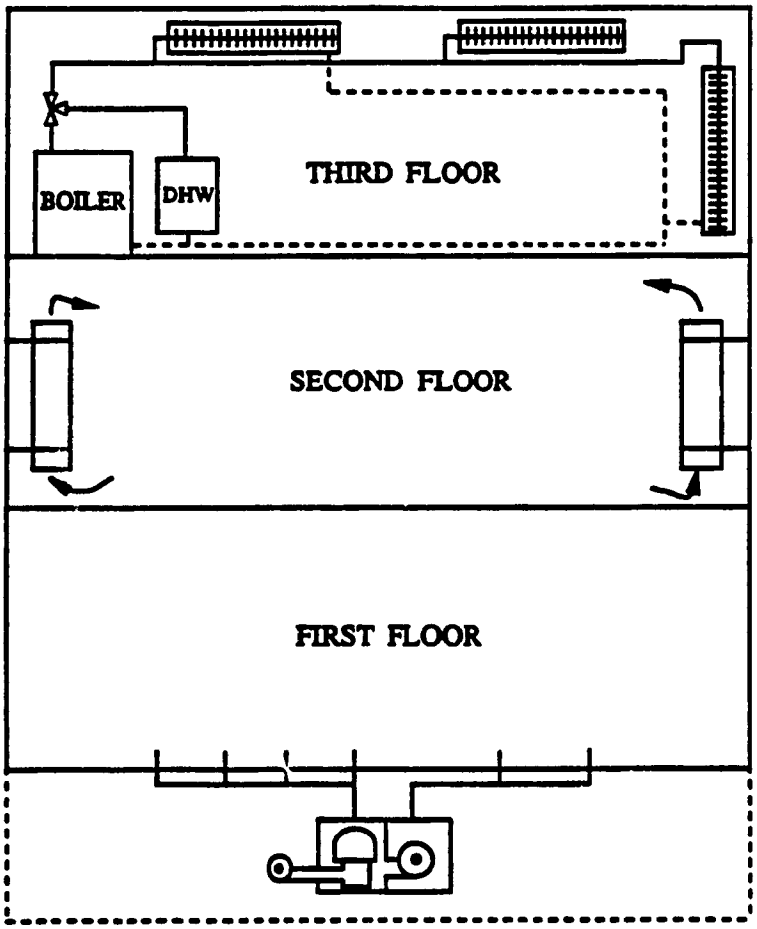

Figure 2.1 Heating systems and their respective floors.

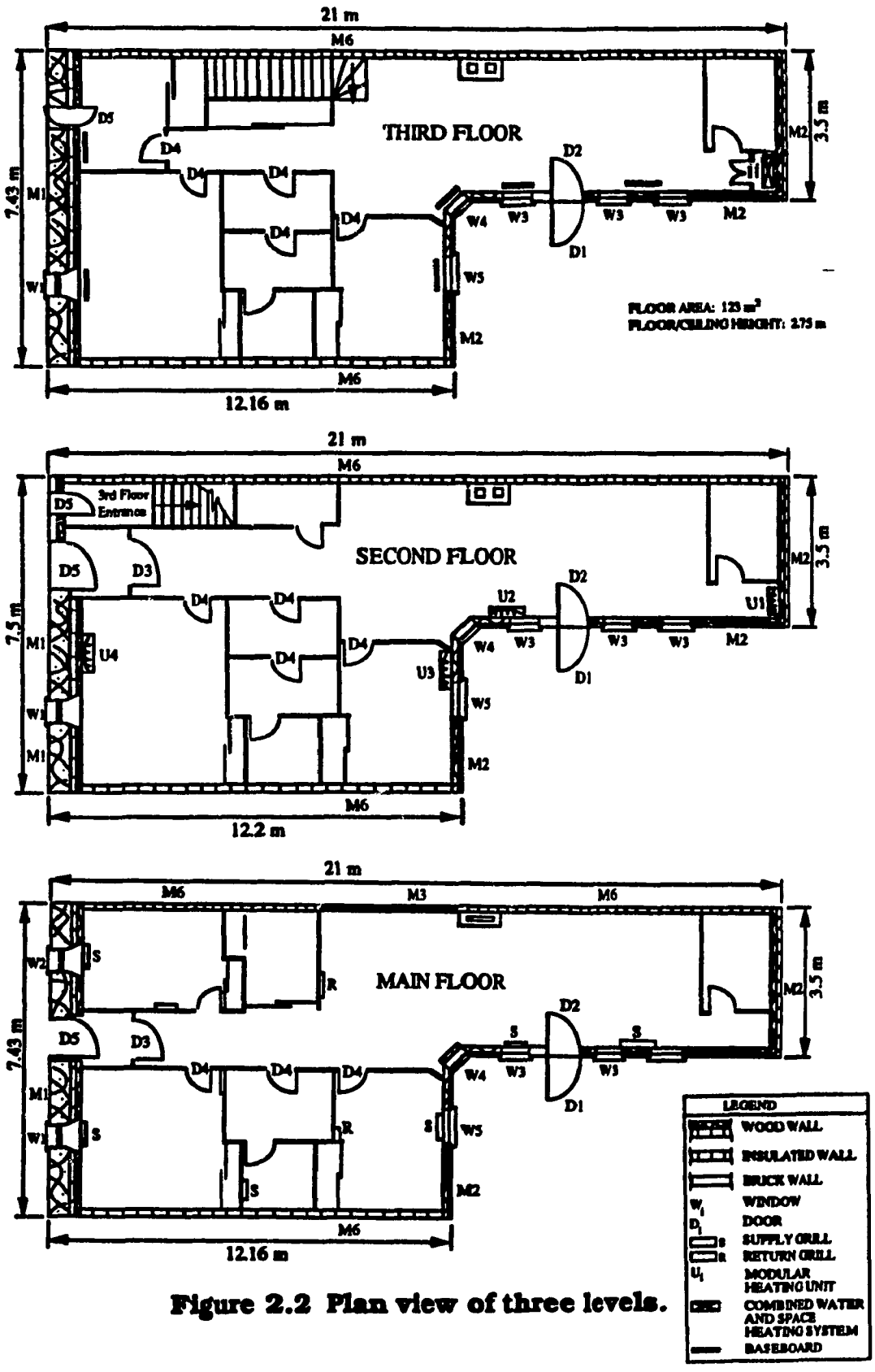

Figure 2.2 Plan view of three levels.

Each floor or flat in the building was completely furnished although not inhabited. The rationale behind this was to attain as much as possible all the furnishings typical of a two adult, one child family. This was intended to represent a real-life situation in which the thermal mass effects of both furnishings and the building itself, would contribute to the building dynamics. Some of the furnishings included on each floor were: gas-operated ranges, a clothes washer and dryer, and a refrigerator. The first two floors were equipped with gas-fired domestic hot water heaters, or DHW, which worked independently of the space heating. The third floor however, utilized an integrated hydronic boiler which supplied both the space heating and domestic hot water.

2.2 Building Envelope and Thermal Properties

The envelope of the building had been retrofitted prior to the installation of the heating systems and subsequently the test period. Loose fitting windows, leaky doors, and a very poorly insulated exterior envelope were renovated with the primary intention of increasing the overall resistance, or R-value, of the envelope. Minor alterations were also performed on some interior partitions, which did not alter the architectural integrity of the original layout.

From the architectural drawings, the conductances of each element

of the building and the overall heat loss coefficient for each floor were computed using material properties given in ASHRAE [24]. The results of these calculations are given in Tables 2.1 through 2.3.

Table 2.1 Wall composition of floor 1.

Element	ASHRAE CODE	Orient.	Area ft^2	U-value (BH/ft^2)
Stone Facade (M1)	A0,C11,B10,B12, E3,E1,E0	NE	203.4	0.079
Back Wall (M2)	A0,A7,B1,B9,E3, B10,B4,E3,E0	SW,NW,W	431.1	0.060
Side Wall (M3)	E0,A7	NW	225.0	1.250
Side Wall (M6)	E0,B7,E1,A7	NW,SE	945.1	0.650
Window (W1)		NE	30.3	0.490
Window (W5)		SW	21.8	0.490
Window (W3)		NW	47.1	0.490
Window (W4)		W	26.7	0.490
Window (W2)		NE	17.3	0.490
Door (D1)		NW	23.9	0.335
Door (D5)		NE	25.7	0.338
Floor	E0,B8,B10,E0		1323.0	0.201

Table 2.2 Wall composition floor 2.

Element	ASHRAE CODE	Orient.	Area (ft^2)	U-value (BH/ft^2)
Stone Facade (M1)	A0,C11,B10,B12 E3,E1,E0	NE	194.9	0.079
Back Wall (M2)	A0,A7,B1,B9,E3 B10,B4,E3,E0	SW,NW,W	431.1	0.060
Side Wall (M3)	E0,A7	NW		1.250
Side Wall (M6)	E0,B7,E1,A7	NW,SE	1170.1	0.650
Window (W1)		NE	30.3	0.490
Window (W5)		SW	21.8	0.490
Window (W3)		NW	47.1	0.490
Window (W4)		W	26.7	0.490
Window (W2)		NE		0.490
Door (D1)		NW	23.9	0.335
Door (D5)		NE	51.4	0.338
Floor	E0,B8,B10,E0		1323.0	0.201

Table 2.3 Wall composition floor 3.

Element	ASHRAE CODE	Orient.	Area(ft^2)	U-value (BH/ft^2)
Stone Facade (M1)	A0,C11,B10,B12 E3,E1,E0	NE	221.6	0.079
Back Wall (M2)	A0,A7,B1,B9,E3 B10,B4,E3,E0	SW,NW,W	431.1	0.060
Side Wall (M3)	E0,A7	NW		1.250
Side Wall (M6)	E0,B7,E1,A7	NW,SE	1170.1	0.650
Window (W1)		NE	28.8	0.490
Window (W5)		SW	21.8	0.490
Window (W3)		NW	47.1	0.490
Window (W4)		W	26.7	0.490
Window (W2)		NE		0.490
Door (D1)		NW	23.9	0.335
Door (D5)		NE	25.7	0.338
Skylight			7.2	0.70
Ceiling	A0,E2,E3,B5,B9 E0		1323.0	0.030
Floor	E0,B8,B10,E0		1323.0	0.201

The R-values of various building components can be compared to various suggested values for energy savings by Quebec Law O.C. 89-83, CMHC Energy Efficient Housing Construction, and ASHRAE Standard 90.1 (1989). A summary of these values can be found in Table 2.4.

Table 2.4 Recommended heat loss coefficients.

Component	ASHRAE 90.1 Umax ($W/m^2°C$)	Quebec O.C. 89-83 Umax ($W/m^2°C$)
Glazing	2.555	2.857
Walls	0.227	0.294
Roofs	0.136	0.189
Doors	-	1.428

From the calculations, we see that the R-value of the envelope components, falls within the prescribed limits as outlined by Quebec Law for energy conservation. It should be noted that these prescribed R-values are recommended values for new construction only, and that it is quite a difficult task to attain these values when renovating old homes.

As shown in Table 2.5, there are some differences in the magnitudes of the heat loss coefficients for each floor. With the addition of basement heat loss, the overall UA-value of the first floor is about 40 % higher than the third floor.

Table 2.5 Calculated heat loss coefficients.

Floor	(UA) Value (BH/°F)	(UA) Value (W/°C)
1	468	247
2	208	110
3	269	142

Similarly, the third floor UA-value is about 20 % higher than the second floor. This is expected since the ceiling/roof assembly on that particular floor is exposed to outdoor ambient conditions. Furthermore, the roof of the third floor also contains a skylight, which acts as a radiative sink to the clear night sky.

By assuming -16 °F and 15 mph wind speed as design conditions for Montreal, the peak heating loads for each floor were calculated. These values were as follows: floor 1-45000 BH, Floor 2-20000 BH, and Floor 3-35000 BH.

2.3 Heating Systems

For the sake of comparison, three different gas-fired heating systems were installed, one per floor. Each system utilized a different means of warming the space. On the first floor was installed a warm-air condensing furnace. On the second floor a modular, direct-vent, non-condensing unit

was installed. On the uppermost floor, an integrated DHW-space heating hydronic boiler was installed.

2.3.1 Warm-Air Furnace

The first floor was equipped with a gas-fired forced-air furnace, which was installed in the basement of the dwelling. The manufacturer's specifications are given in Table 2.6.

The ducts were also installed in the basement just below the floor. The distribution of the air consists of seven supply outlets which are floor mounted, and four return air grilles which were located in strategic locations at the bottom of the room walls. The location of the various supply and return grilles can be seen in Figure 2.3. It should be noted that there is no make-up fresh air connected to the return side of the system. In other words, air infiltration was the only means of make-up fresh air for the main floor.

Table 2.6 Specifications of warm-air furnace.

Description	
Make	Coleman
Country of Origin	U.S.A
Model	2960-656
Input (BH)	65000
Output (BH)	57500
Manifold Pressure (" w.g.)	3.5
Max. Natural gas Pressure @ supply inlet (" w.g.)	7.0
Min. Natural gas Pressure @ supply inlet (" w.g.)	5.0
Max. External Static Pressure (" w.g.)	0.5
Temperature Rise (°F)	25-55
Max. Outlet Air Temperature (°F)	150
Ignition Type	spark
Venting Type	mechanical
Control Type	on/off
Condensing H-X	yes
Motor Hp	1/3
Max. Current Motor (amps)	9.2

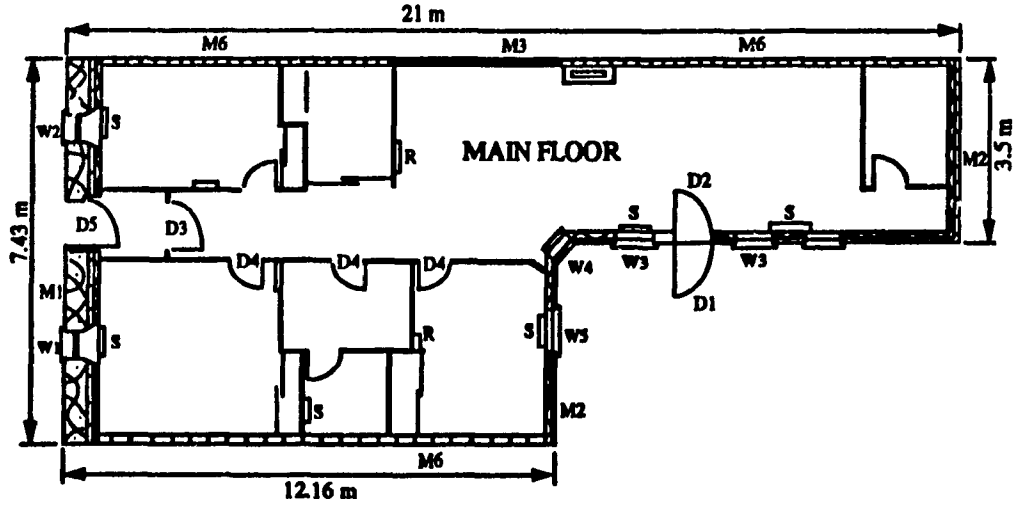

Figure 2.3 Location of supply/return grilles.

The warm air furnace had a condensing heat exchanger and therefore arrangements were made to collect and dispose of the condensate. A mechanical vent was employed to minimize the on and off cycle losses, and also to expel the relatively cool and heavier flue gases from the exhaust pipe to the outdoors.

The forced air furnace was also equipped with both a humidity control and an electronic air cleaner. The humidity controller was set at approximately 45% throughout the duration of the heating season. It should also be noted that the furnace was controlled via a wall-mounted programmable thermostat, which was located in the living room. This

thermostat allowed for testing various operating strategies such as night set back and set forward.

Several sensors were installed to measure temperatures, mass flow rates etc. These are shown in Figure 2.4. The gas meter (G), records both the rate of gas consumption and also the total gas consumed. The output heat delivered was calculated by measuring the supply air pressure (P) in the supply duct and the temperature of the supply and return air (T). The room thermostat controls the on-off cycling of the furnace according to the space load imposed on the system. A flue-gas analyzer was also utilized to determine the percent constituent of carbon dioxide and oxygen in the flue gases (CO_2/O_2 sensors). The temperature of the flue gas was also recorded (sensor T in flue pipe).

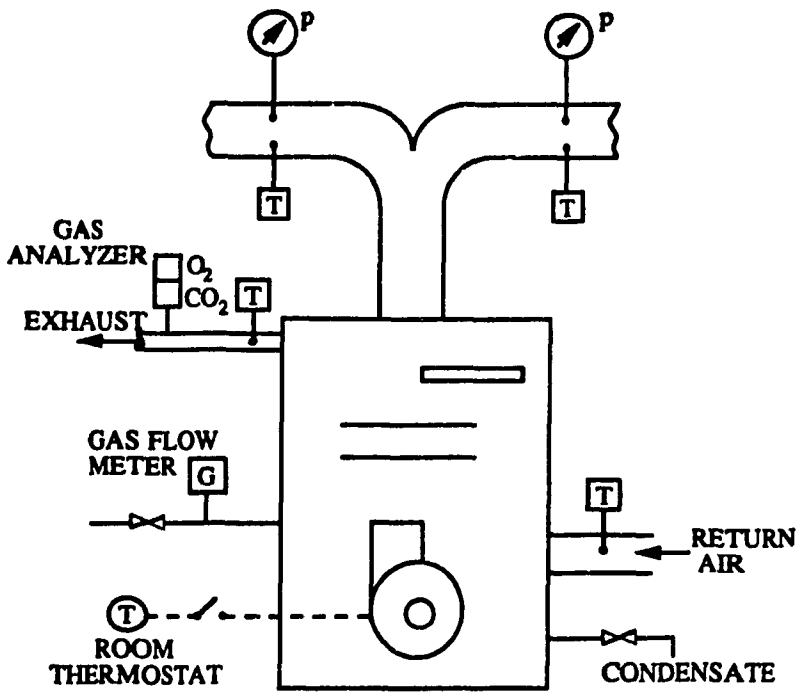

Figure 2.4 Schematic of the warm-air furnace.

2.3.2 Zone Adjustable Modular System

The modular heating system, which also consumed natural gas as the combustible fuel, was installed on the second floor. This system was the smallest of the three units and required multiple units to satisfy the thermal load for the second floor. Figure 2.5 shows the location of the modular units. This system was designed to transfer the heat of combustion passively to the room air by natural convection and/or radiation. It should be noted that of the 3 heating systems utilized, this one did not require any auxiliary energy, such as electricity, for its operation.

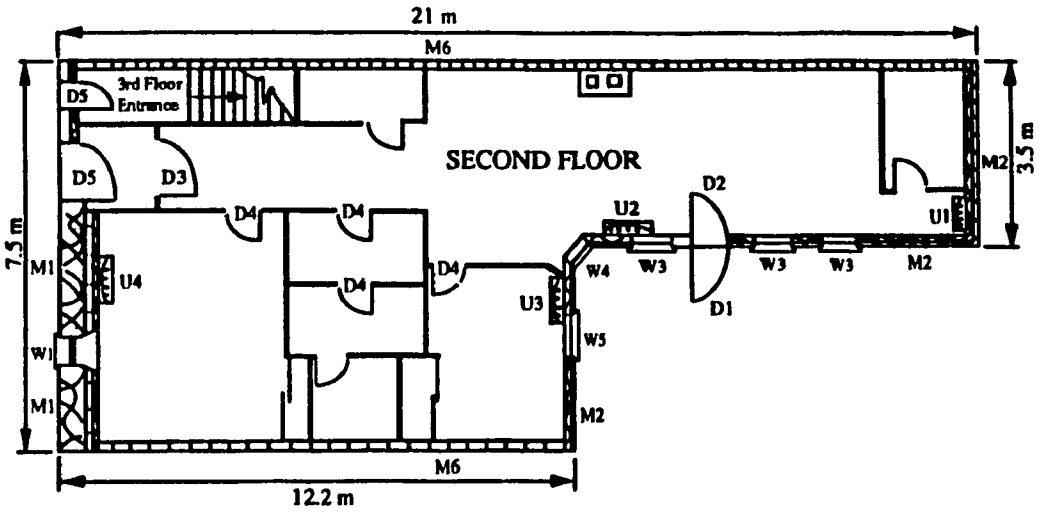

Figure 2.5 Location of modular units.

As its name implies, the modular system "modulates" according to the load imposed on it. That is to say, the control action of the modular heating system is not of the simple on-off control. The modular system employs a modulating valve to control the supply of natural gas to the burner. This system is also of the direct-vent type, and was installed on the exterior walls of the dwelling, so that the flue gases could be exhausted to the outdoors. The specifications of the modular system can be seen in Table 2.7. Although this unit is not of the condensing type perse, it did have a tube-in-tube heat exchanger in the exhaust. The cold outdoor

combustion air was drawn in through a vent pipe which passes over the hot exhaust air. Thus, some heat exchange did occur.

Table 2.7 Specifications of modular units.

Description	
Make	Auer
Country of Origin	France
Model	
Input (BH)	13200
Output (BH)	10200
Ignition Type	pilot
Venting Type	direct
Control Type	modulating
Condensing H-X	no
Manifold Pressure (" w.g.)	3.2
Max. Natural Pressure @ supply inlet (" w.g.)	7.0

A schematic diagram illustrating the type and the location of the installed sensors on the system are shown in Figure 2.6. The flow rate of the natural gas (G), the flue gas constituents (CO_2/O_2 sensors), and the temperature of the flue gases (T) were recorded to determine the various system performance characteristics. Figure 2.7 shows the placement of various thermocouples on, above and below the heat exchanger surface, which were also utilized to assess the temperature gradients across the modular system.

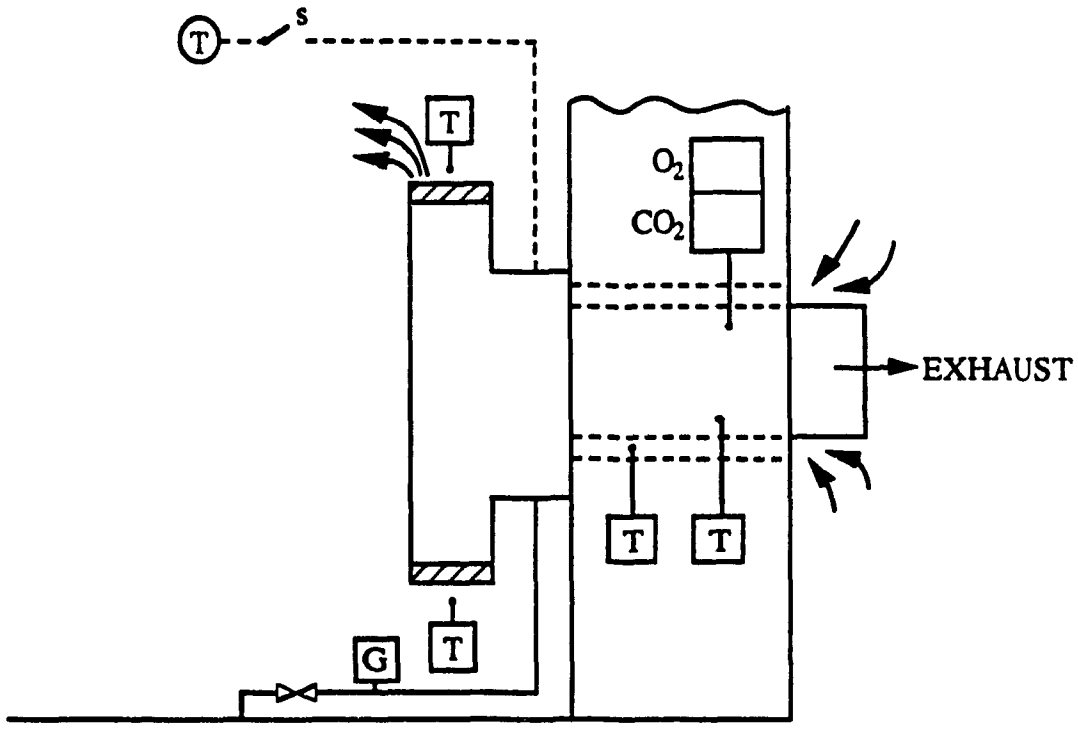

Figure 2.6 Schematic of modular units.

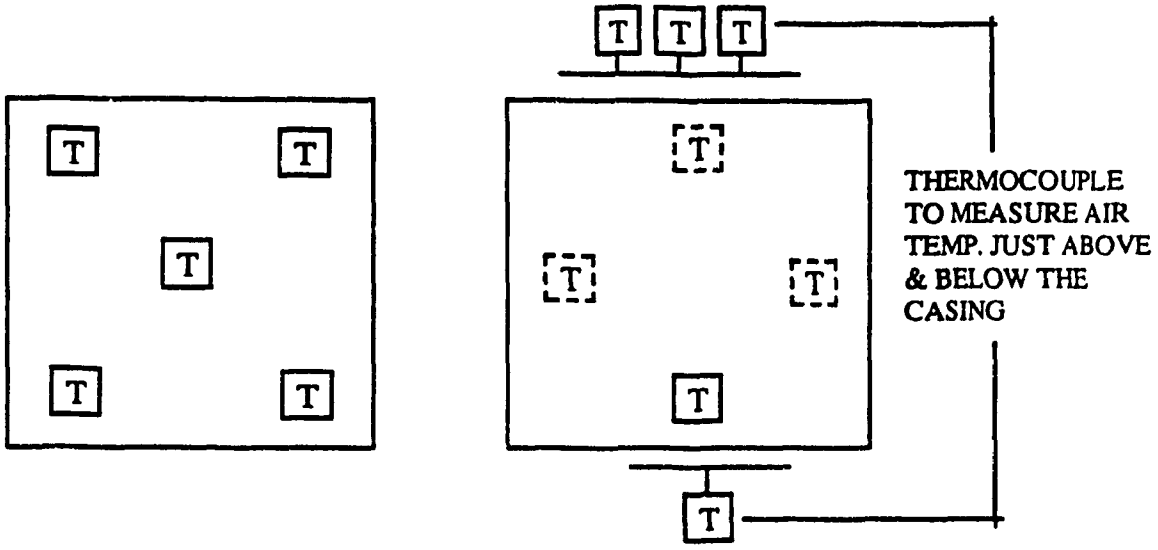

Figure 2.7 Thermocouple location on modular casing.

2.3.3 Integrated Hydronic Boiler

An electronic ignition, direct-vent hydronic boiler was installed on the third floor of the test facility. This system is referred to as "integrated", because it combined both the space heating load and DHW load simultaneously. This unit was also wall mounted as was the modular system. The hot water boiler had a pump that circulated hot water to baseboard heaters via a two-pipe reverse return system. The heat transfer mechanism to the room air occurred by means of natural convection and/or radiation. Seven baseboards were located on the third floor as shown in Figure 2.8. The specifications of the boiler can be seen in Table 2.8.

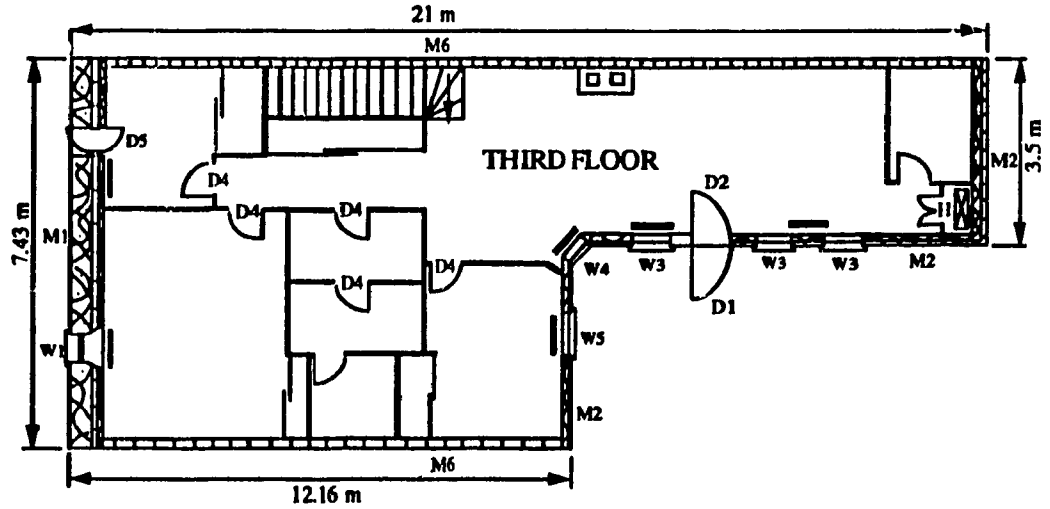

Figure 2.8 Location of radiators.

Table 2.8 Specifications of hydronic boiler.

Description	
Make	Celtic
Country of Origin	France
Model	50FF
Input (BH)	50000
Output (BH)	42000
Ignition Type	spark
Venting Type	direct
Control Type	on/off
Condensing H-X	yes
Water Pump Rate (gpm)	2.4
Manifold Pressure (" w.g.)	2.5
Max. Natural Pressure @ supply inlet (" w.g.)	7.0

Depending on the demand, either DHW or space heating, a three way valve controlled the direction of the hot water. At any given time the hot water was directed to either the radiator circuit to fulfil the necessary space load, or to the DHW coil. It was determined during testing, that if heat was required simultaneously for the space and for DHW, there was no clear priority. The three way valve shuttled back and forth between the DHW coil and the space heating coil, and if the space demand was quite high, it often was not met.

A schematic diagram of the type of sensors and their location is shown in Figure 2.9. As in the other two systems,

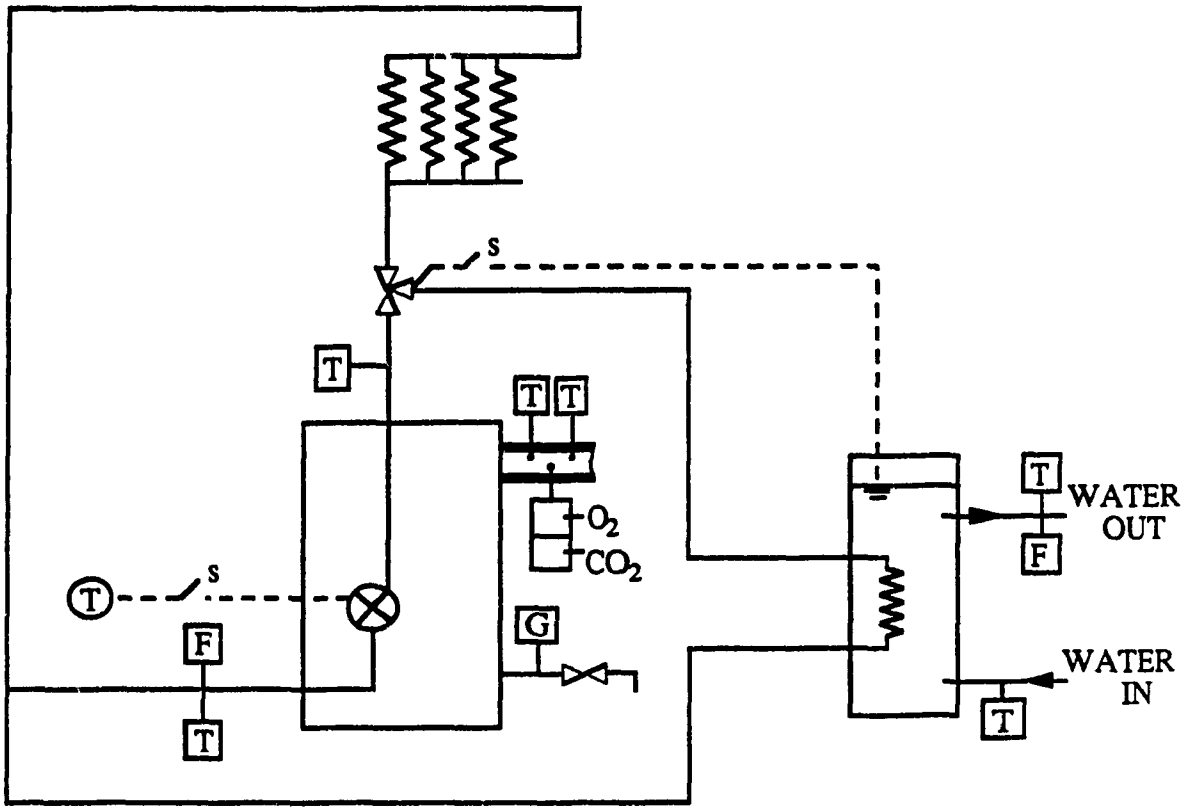

Figure 2.9 Schematic of the hydronic boiler.

the input-side of the heat balance consisted of a gas flow meter (G). On the output-side, water flow meters (F), on both radiator and DHW coils, as well

as their respective hot water temperatures (T) were measured and recorded. The return water temperature (T return) was also recorded. Like the warm-air furnace, the boiler is controlled via a wall mounted programmable room thermostat. It should also be noted that flue gas analysis (CO_2/O_2 sensors), as well as flue gas temperatures, were also recorded to study the steady-state efficiency of the system.

2.4 Data Acquisition System

Since numerous data points were monitored, an elaborate data acquisition system (DAS), was developed [25]. At each sample time about 120 variables were monitored and recorded. For this purpose, the programmable data acquisition computer (SAFE 8000), a personal computer (IBM AT), and a communications modem, constituted the main elements in the fully automated DAS. The data collecting frequency varied from 20 seconds to 1 hour. Periodically, the modem would transmit raw data to the Centre for Building Studies where it was stored on the VAX 11/785, a mainframe computer.

In order to facilitate the collection of data, the monitored data was broken down into various experiments called data TYPES. This thesis focuses on the efficiency measurements, which were identified as data Type 1 and Type 6 as shown in Table 2.9. Table 2.10 and 2.11 show the

physical location of the sensors and the corresponding channel numbers in the DAS.

Table 2.9 Data type and experiments.

Experiment Type	Data Type	Description
Thermal Efficiency	Type 1	Efficiency Measurements
	Type 6	Room, Outside Temperatures.
Thermal Comfort	Type 6	Room, Outside Temperatures.
	Type 8	Thermal Comfort Room
	Type 9	Thermal Comfort Room
	Type 10	Anemometers
	Type 11	PMV-Meters
Air Quality	Type 6	Room, Outside Temperatures.
	Type 14	IAQ Gas Analysis

Table 2.10 Type 1 monitored data.

Identification	SAFE in	Description
Thermocouple 1	Ain(1)	Furnace: Supply duct A
2	(2)	Supply duct B
3	(3)	Return Duct
4	(4)	Flue
5	(5)	Modular: Vent
6	(6)	Air In
7-9	(7-9)	Air Out
10-14	(10-14)	Heat Exchanger
15-17	(15-17)	Casing: Inside
18	(18)	Casing: Outside
19	(19)	Flue
20	(20)	Boiler: Return Water
21	(21)	Supply Radiators
22	(22)	Supply Coil
23	(23)	DHW Side: Hot
24	(24)	Cold
25	(25)	Flue
26	(26)	Vent
Analog 1	Ain(96)	Furnace: Supply Duct A Pressure
2	(97)	Supply Duct B Pressure
3	(98)	Flue Gases: % Oxygen
4	(99)	% Carbon Dioxide
Interrupt 1	Irq(16)	Furnace: Burner relay
2	(17)	Gas Meter
3	(18)	Modular: Gas Meter
4	(19)	Boiler: Gas Meter
5	(20)	Burner/Pump Relay
6	(21)	Aquastat/Valve Relay
Digital 1	Din(16)	Boiler: Water Flow Radiator Side
2	(18)	Water Flow DHW Side

Table 2.11 Type 6 monitored data.

Identification	SAFE in	Description
T.C. 27	Ain(27)	Outdoor Temperature
28	(28)	Basement Temperature
Multiplex 129	M129	Bedroom First Floor
130	M130	Bedroom Second Floor
131	M131	Bedroom Third Floor
132	M132	Hall First Floor
133	M133	Hall Second Floor
134	M134	Hall Third Floor
135	M135	Bathroom First Floor
136	M136	Bathroom Second Floor
137	M137	Bathroom Third Floor
138	M138	Living Room First Floor
139	M139	Living Room Second Floor
140	M140	Living Room Third Floor
Analog 8	Ain(103)	Pyhremometer 1
9	(104)	Barometric Pressure (" w.g)
10	(105)	Wind Velocity (mph)
11	(106)	Pyhremometer 2
12	(107)	Wind Direction (degrees from N)
13	(108)	Relative Humidity Outdoors
14	(109)	Relative Humidity Floor 1
15	(110)	Relative Humidity Floor 2
16	(111)	Relative Humidity Floor 3

2.5 Instrumentation, Calibration and Accuracy

The inputs, such as thermocouple signals, digital on-off signals and analog (pressure transducer output), were read through assigned channel inputs on the DAS as discussed in the previous section. In most cases, these inputs were single but in the case of room temperature thermocouples, these signals were multiplexed due to:

1. physical limitation of the DAS
2. the numerous amount of temperature measurements.

The thermocouples were of the type T with an accuracy of ± 0.2°C. These thermocouples were calibrated at various times during the experimental period by utilizing a thermocouple calibrator.

Type: T.C. type T

Accuracy: ± 0.2 °C

Calibration: via Doric T.C. Calibrator Model 477

The gas meters at MEGA house were equipped with a cubic meter pulser which sent a binary signal to the DAS which inturn converted this binary signal, to a cumulative volumetric flow by means of the software

counter. The calibration consisted of dividing this counter reading by 100 to convert to m^3.

Model: ALM 225

Manufacturer: Canadian Meter Company

Accuracy: ± 0.001 m^3

Calibration: DAS reading/100 (m^3)

As a further check, the gas meters readings were verified throughout the duration of the experimental period by manually recording the gas meter readings, as will be discussed in Chapter 4.

Similarly, the water meters also were equipped with pulsers which converted a binary code, via the DAS software, to a cumulative total water flow. The calibration consisted of dividing the reading recorded from the DAS by 88 to convert to gallons.

Model: Style 430

Pulser Model: Hersey R-38

Manufacturer: Canadian Water Meter

Accuracy: ± 0.005 gallons

The accuracy of the water flow meters was verified from time to time by utilizing a precision graduated cylinder and physically measuring a collected water volume in a measured time lapse. This was then compared to the flow as recorded by the DAS.

The pressure transducers which were placed in the supply ducts on the warm-air system recorded voltage readings which were stored on the DAS. The calibration of the pressure transducers was done, with the help of manometers, at the beginning of the experimental set-up and the following relationship was determined:

$$V = 0.842 * P + 0.2$$

where, V is the voltage (DAS reading)

P is the pressure (" w.g.)

The final equipment which had to be calibrated was the gas analyzer. The first step was to zero with the use of the zero gas (N_2) which was accomplished by supplying approximately 500 cc/min. of the zero gas at 10 psig, into the analyzer, and the zero control was adjusted such that it read 0. Next, the span was checked by allowing the span gas (CO_2, or O_2) at approximately 500 cc/min. and 10 psig., and the span control was adjusted

such that it indicated the value corresponding to the concentration of the span gas.

Model: Horiba PMA-200

Object of measurement: O_2, CO_2 % in flue gases.

Scale: 0 to 25%, 0-100%

2.6 Physical and Cost Comparison

Having described the heating systems and the distribution network, it will be interesting to compare the physical characteristics of the systems as well as the costs in relation to each other.

Many factors are influential when rating a gas-fired heating system. The actual physical size may be important if space is limited, for example, most single unit apartments do not have mechanical rooms to accommodate the relatively cumbersome warm-air furnace and air duct distribution network assemblies. Another factor which is important is zone control. If a central unit such as a furnace or boiler is utilized, room by room control can be obtained, but adds extensively to the initial cost of the set up. Thus in most cases when a central system is utilized, one single thermostat control is employed. In cases where individual control is desired for each room, the modular system is best suited. Table 2.12

shows a summary of the major physical characteristics, capacities, as well as electro-mechanical details of each system.

The ignition type of the furnace and boiler is of a spark ignition type, thus there are little off-cycle or standby losses since these systems do not have a continuous pilot as in the modular. On the other hand, the modular does not require any alternative source of energy such as electricity to be lit, and furthermore, the mode of heat transfer is by natural convection and radiation thus working one hundred percent of the time, even in instances of power failures and blackouts.

Table 2.12 Physical characteristics of three systems.

Description	W.Air-Furnace	Modular	Boiler
Make	Coleman	Auer	Celtic
Model	2960-656		50FF
Country	United States	France	France
Size(h,w.d)	60"x20"x36"	24"x28"x7"	32"x15"x14"
Input (BH)	65000	13200	50000
Output (BH)	57500	10200	42000
Ignition	spark	pilot	spark
Control	on/off	modulating	on/off
Venting	mechanical	direct vent	direct vent
H-X Type	condensing	un-condensing	condensing
Rated Eff.	86	75	80
Weight (lbs)	n.a.	55	115

The warm-air furnace utilizes mechanical venting in order to minimize off-cycle and on-cycle losses. With this strategy come benefits of savings, but also entails a major drawback. The furnace requires energy, in the form of electricity, to power the vent fan; in addition the system becomes more dependant on auxiliary electrical energy. The furnace and boiler also have in common a condensing heat-exchanger core. This provides for a more efficient system from the point of view of energy usage, but special plumbing services must be installed to collect and dispose of the condensate, thus initial cost of the system increases.

Another factor which is important is the country of origin of the system. The warm-air furnace is manufactured and assembled in the United States, while the modular and boiler are a product of France. While the gas-technologies have excelled in Europe and particularly in France, Belgium and the Scandinavian countries, these systems are imported and thus carry some tariffs or taxes which are passed on to the consumer.

Cost is a very important factor when choosing a heating system. The initial cost of the system is not always the most expensive part of the system. The distribution, ie piping, fans, pumps, ducts, accessories such as programmable thermostats, electronic air cleaners, humidifiers, and also

the supply gas piping, make up most of the initial investment. For instance, the distribution system of the furnace cost nearly double the furnace itself, while the distribution of the boiler cost nearly five times the initial cost of the boiler. A complete breakdown of the initial costs can be seen in Table 2.13.

Table 2.13 Cost comparisons for the three systems. ($ 1989)

Description	W.Air-Furnace	Modular	Boiler
Unit Cost	$ 2480.00	5@ $ 394.00	$ 2214.00
Installation & Accessories	$ 3666.00	$ 1570.00	$ 9380.00
Gas Supply Main	$ 640.00	$ 1480.00	$ 639.00
Total Cost	$ 6786.00	$ 4920.00	$12233.00

In addition to the initial cost, the running or operational costs, must also be looked at and investigated. In the case of the modular, the auxiliary costs are non-existent because the heat is transferred to the room passively by convection and radiation. The furnace, on the other hand, requires an electronic spark to start-up the burners, and also a fan to blow the warm-air through the distribution ducts, to the various rooms. The boiler also

requires electricity to light the burners and to circulate the hot water to the various convectors/radiators in each room. Other hidden costs such as servicing costs are greatly increased with the furnace and boiler since mechanical wear of fans, fan motors, pumps and relays is an operational characteristic of these systems and thus cannot be avoided.

2.7 Summary

Initial cost is very important when comparing heating systems. Other costs such as operating, ie. electrical energy charges for fans, and pumps, and costs arise from mechanical wear. Another form of cost is directly associated with the ignition type of the heating system. For instance, the furnace and hydronic boiler utilize a spark ignition, thus off-cycle losses are minimized to jacket losses. The modular, on the other hand, has a continuous pilot ignition, which wastes energy at all times. One advantage to the modular is that it does not require electrical energy to be lit, nor does it use mechanical means to transfer the heat to the room, thus providing heat at all times, even during power failures.

Other energy saving features such as mechanical venting, as in the furnace, further reduce the off cycle losses through the flue. The

condensing heat-exchanger design is employed in both the furnace and boiler, and recovers heat from the flue gases. This has its drawbacks in the form of initial cost, since plumbing lines must be placed close to the heating system in order to evacuate the condensate. One drawback to the modular system was directly related to its non-condensing heat-exchanger design. Since the flue gas temperatures were quite high and there was no heat recovery in the form of condensing water, on very cold days, it was noted that ice build-up occurred at the exit of the flue-pipe.

The modular system uses very long on-cycles which creates certain problems such as casing could reach high temperatures in the range of 70-80°C, which is dangerous for homes with young children. Another drawback to the modular is that it achieves very high room temperatures, over 23°C. The best room temperature control from the point of view of variance was provided by both the hydronic boiler and the warm-air furnace, followed by the modular.

CHAPTER 3

NORMAL DAILY OPERATION AND TRANSIENT TESTS

In this chapter, the heating systems are examined closely from two different points of view. First the heating systems operation on typical days, under normal operation is examined. Second, the manner in which the systems performed under various transient field tests is analyzed. The results presented in this chapter, will provide a basis upon which all three systems will be compared in relation to one another.

The first part of this chapter (section 3.1) examines the daily operation of the heating systems under normal operating conditions. This is achieved by analyzing the system operation on three days in the heating season, namely a mild day (T_{out}=2 to 5°C), a cool day (T_{out}=0 to -6°C), and a cold day (T_{out}=-2 to -10°C). Typical daily profiles of gas consumption, and room temperatures are plotted for three days. In section 3.2 the cyclic operation of the system is studied by examining the sequential switching of the burner, the fan, and the pump as applicable.

Section 3.3 of this chapter is concerned with specific transient field tests which were performed in order to study the warm-up time. In the warm up test, the systems were shut off for a period of time, usually till

room temperatures reached approximately 10°C, then the systems were turned on. At this time, the heating systems worked at full load to raise the room temperature from 10 to 21°C. Under these full-load conditions, gas analysis was also performed in order to determine the steady-state efficiency of the heating systems.

3.1 Normal Daily Operation

The daily operation of the three heating systems on three typical days in the heating season are compared in this section. The average hourly temperature profile for these 3 days is shown in Figure 3.1. The first day was a relatively mild day with a temperature range of 2-5°C and an average temperature of 3°C. The second day was slightly cool with temperatures ranging from -6 to 0°C with an average of -3°C. The third day was the coldest of the 3 days with temperatures ranging from -10 to -2°C with an average daily temperature of -8°C.

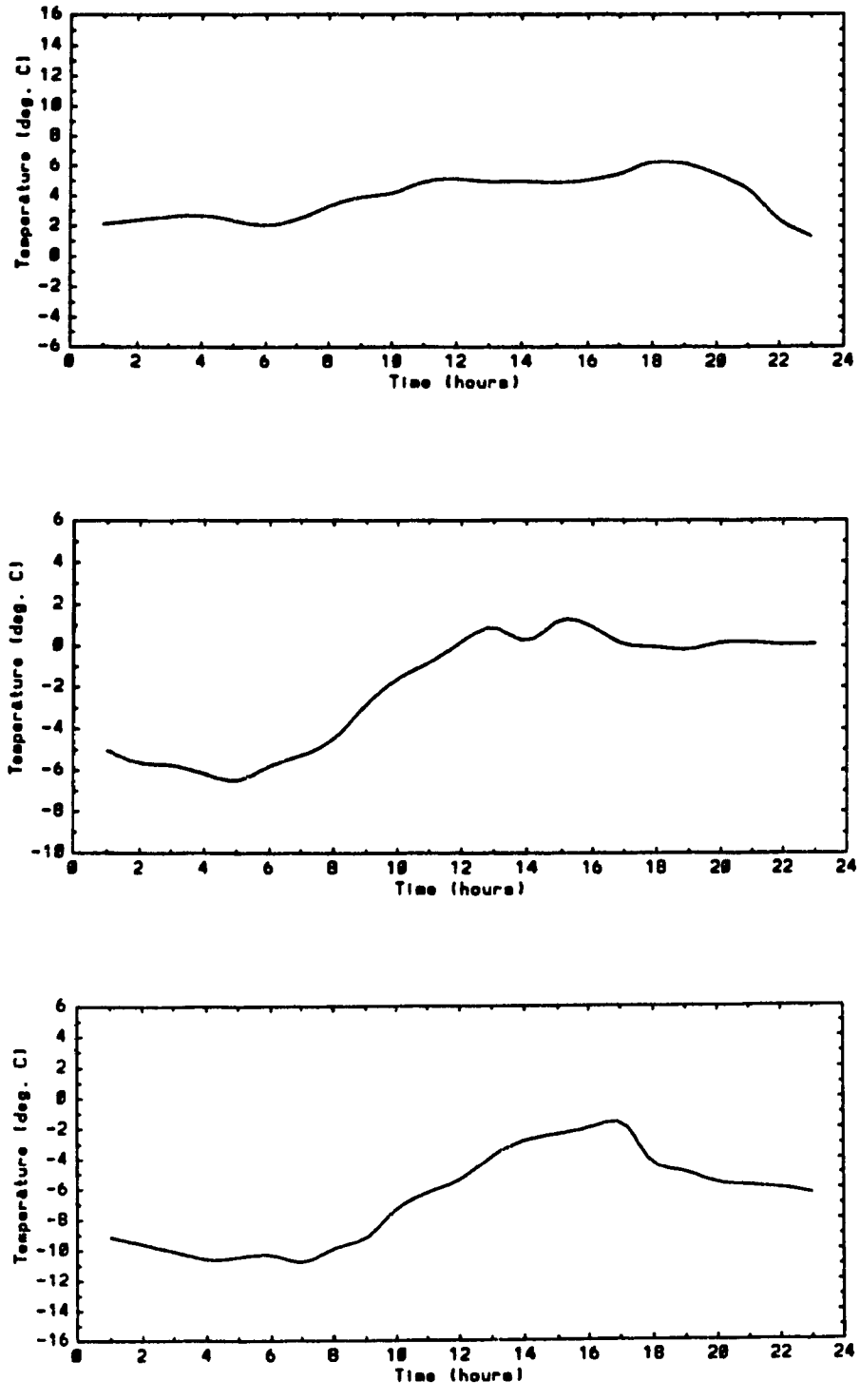

Figure 3.1 Daily temperature profiles of mild, cool, cold days.

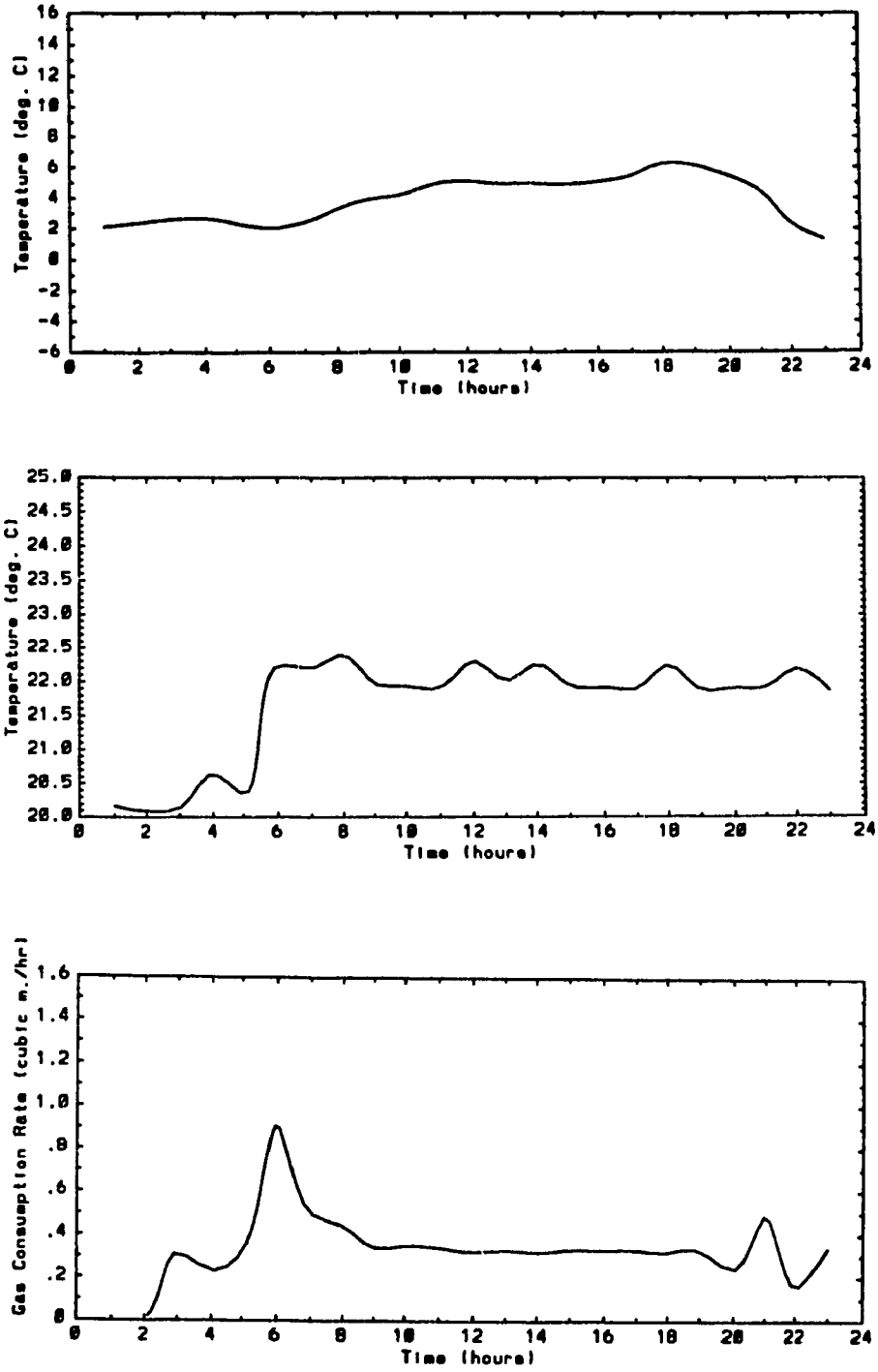

Figure 3.2 Zone temperature and gas consumed on mild day (floor 1)

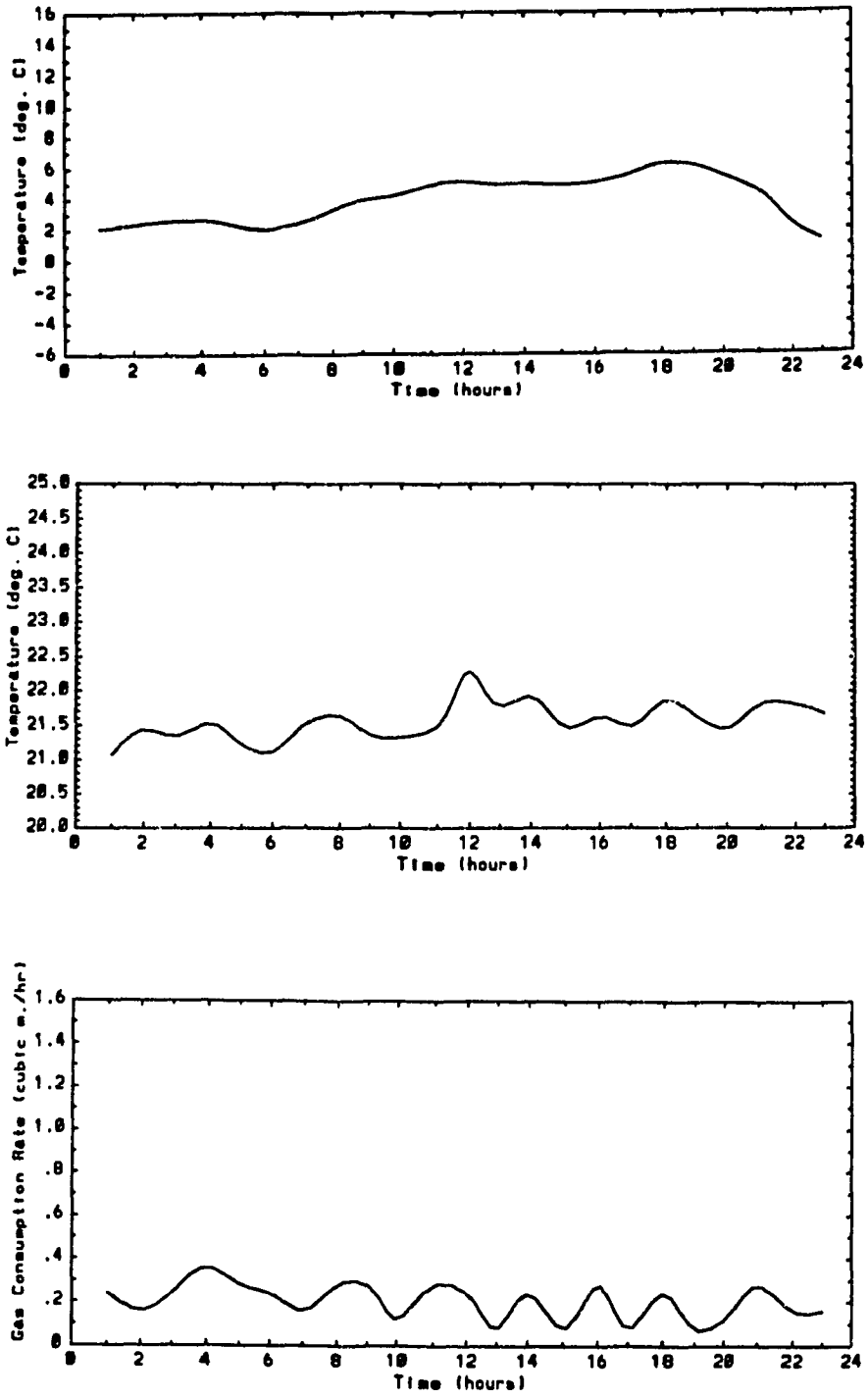

Figure 3.3 Zone temperature and gas consumed on mild day (floor 2).

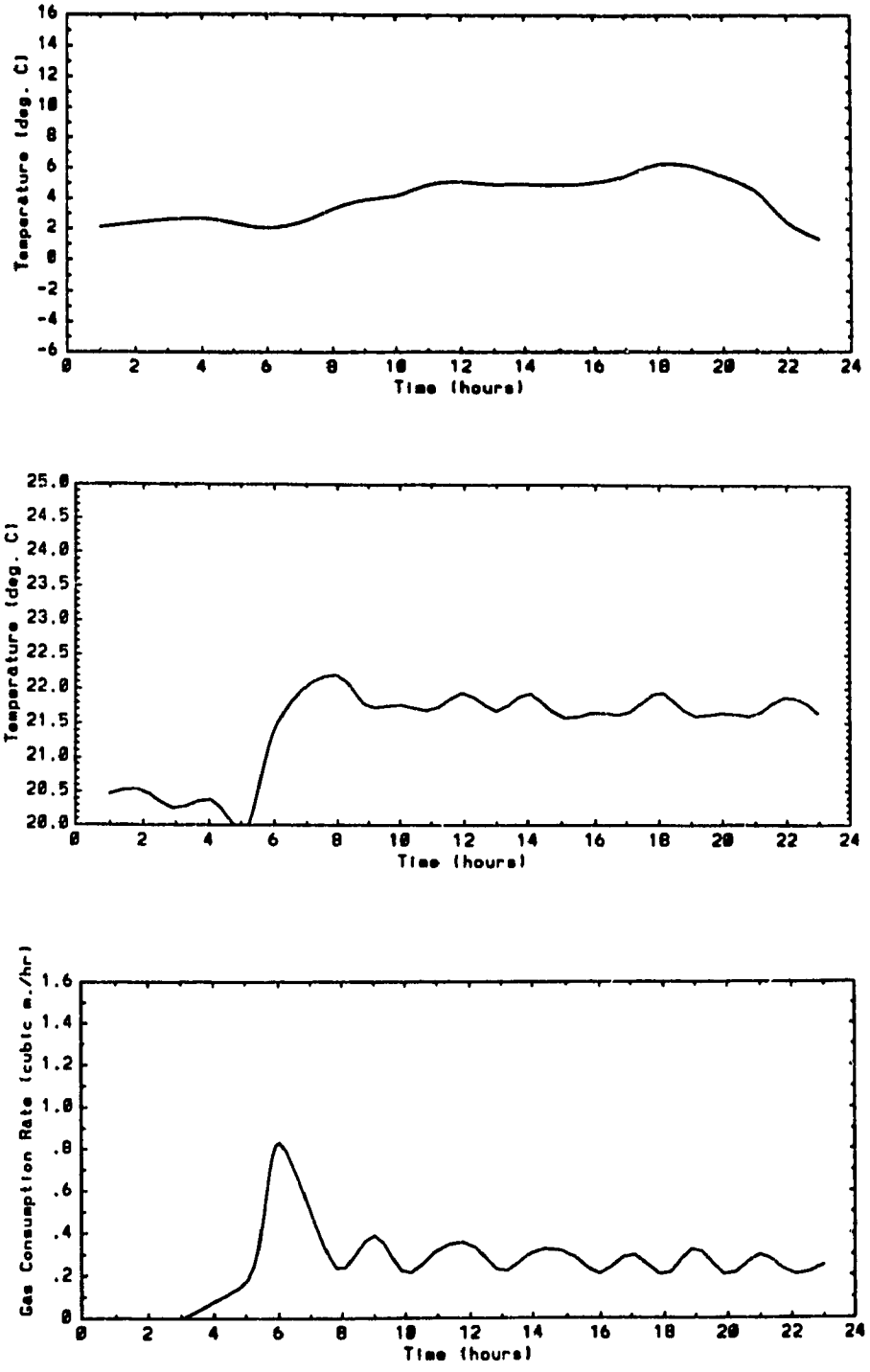

Figure 3.4 Zone temperature and gas consumed on mild day (floor 3).

During these 3 days, the room temperature as well as gas consumption rate were plotted. For the mild day and warm-air system, these plots can be seen in Figure 3.2. It is noticed that for the warm-air system, peak demand for gas-consumption occurs in the hours directly preceding the end of night set back, ie. @ 6:00 A.M. This peak gas consumption of 0.9 m^3/hr then drops to an average of 0.35 m^3/hr for the bulk of the day since the outdoor temperature also remained relatively constant between the hours of 8:00 A.M. to 6:00 P.M. After 6:00 P.M. the outdoor temperature begins to drop, and thus the gas consumption rate increases to 0.5 m^3/hr and begins to cycle as does the furnace. Similarly, during this day, the room temperature follows closely the gas consumption profile. The rise in room temperature from 20 to 22.3°C following the night set-back, can also be seen in the figure. The room temperature is maintained between 21.9°C to 22.4°C for the remainder of the day.

On this mild day, the modular system performed quite differently as seen in Figure 3.3. Unlike the furnace and boiler, night set back was not attainable with the modular system, thus the gas consumption rates are proportional to the space load. From these plots, we see that room temperatures fluctuate between 21 and 22°C. It is worth noting that the rate of gas-consumption of the modular heating system which ranges from between 0.33 to 0.1 m^3/hr is much less than those of the warm-air system.

Thus the low gas consumption rate is one of the main advantage of the moduiar heating system.

The outdoor temperature, room temperature and gas consumption rate for the boiler on this mild day are shown in Figure 3.4. Note that as in the warm-air furnace, night set-back is utilized. At 6:00 A.M., a peak heating demand is achieved, which corresponds to a rate of 0.8 m^3/hr of gas consumption. What is worth mentioning is that unlike the warm-air furnace where the peak room temperature and peak gas consumption rate occur almost simultaneously, in the boiler, the room temperature rises about 2 hours after the peak demand, ie. at 8:00 A.M. This is due to the thermal capacitance of the working medium, and also because of the means by which the useful heat is transferred to the space which is mostly by convective and radiative heat exchange. The warm air system on the other hand uses forced convection as the means of heat transfer, and therefore room temperature rises more rapidly as compared to the hydronic boiler.

The results from the cool day for the warm air furnace are shown in Figure 3.5. It can be seen that after 6:00 A.M., the outdoor temperature begins to rise until it settles at around 0°C. During this time period, the gas consumption decreases from the peak established due to the night set-back.

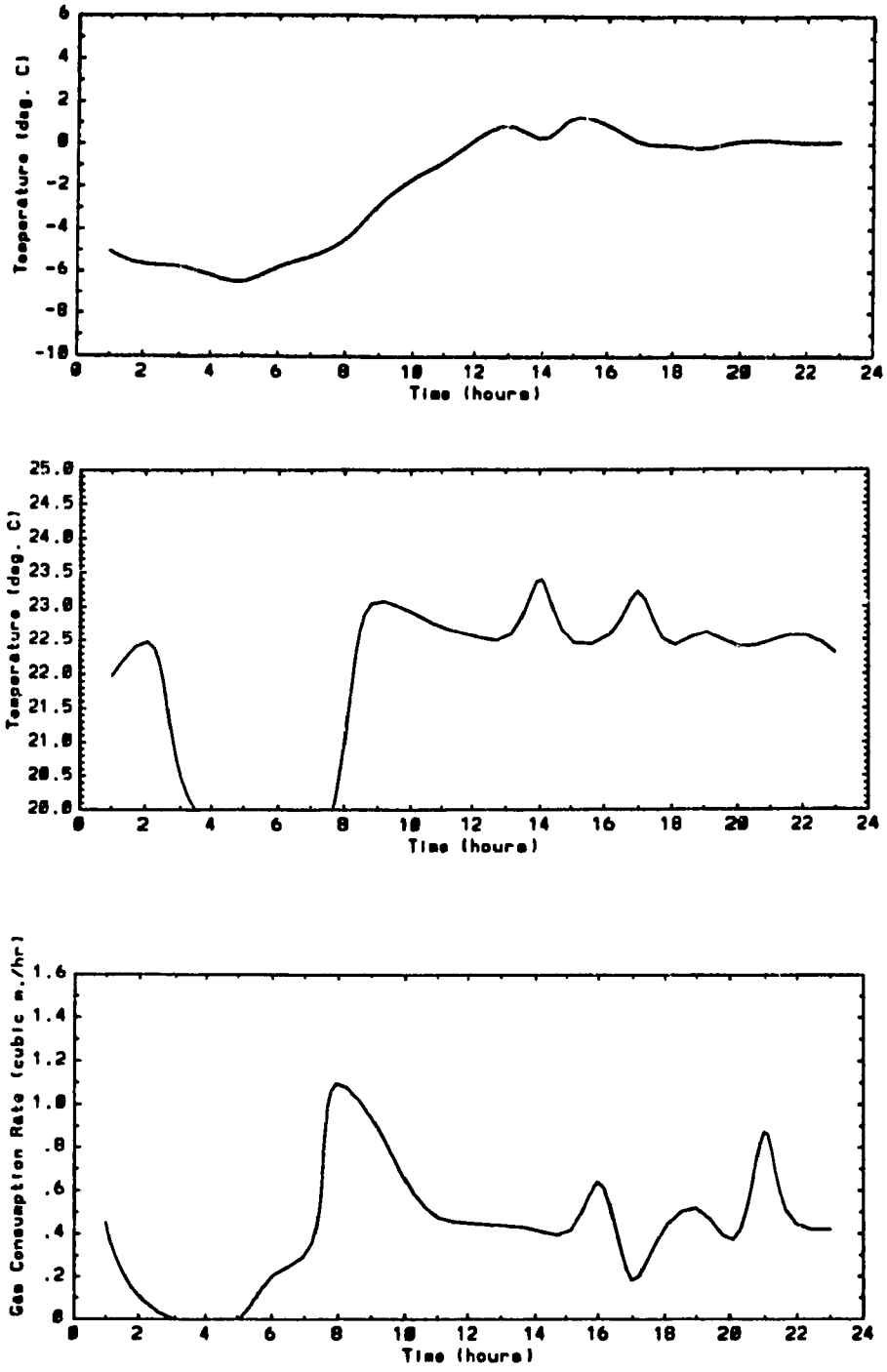

Figure 3.5 Zone temperature and gas consumed on cool day (floor 1).

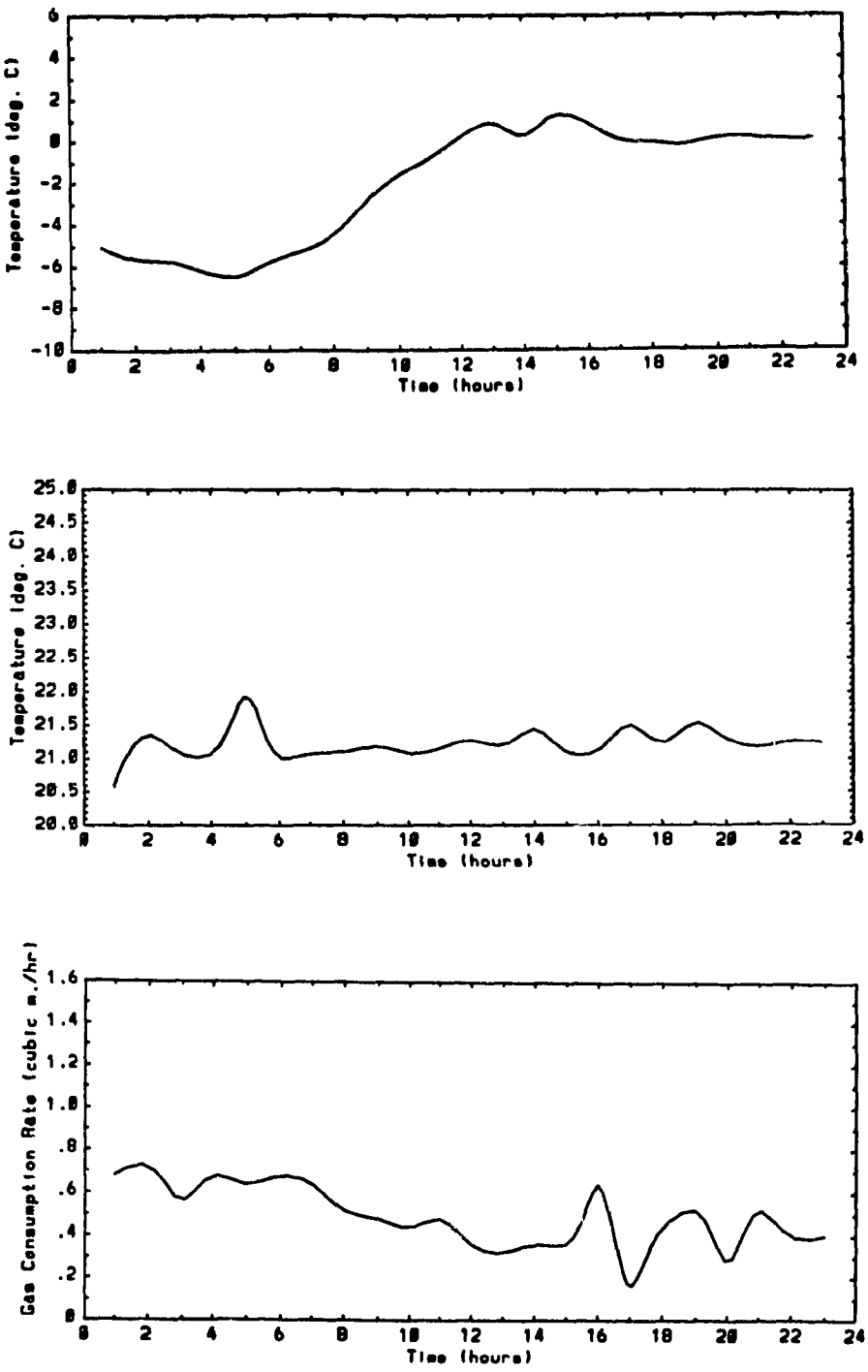

Figure 3.6 Zone temperature and gas consumed on cool day (floor 2).

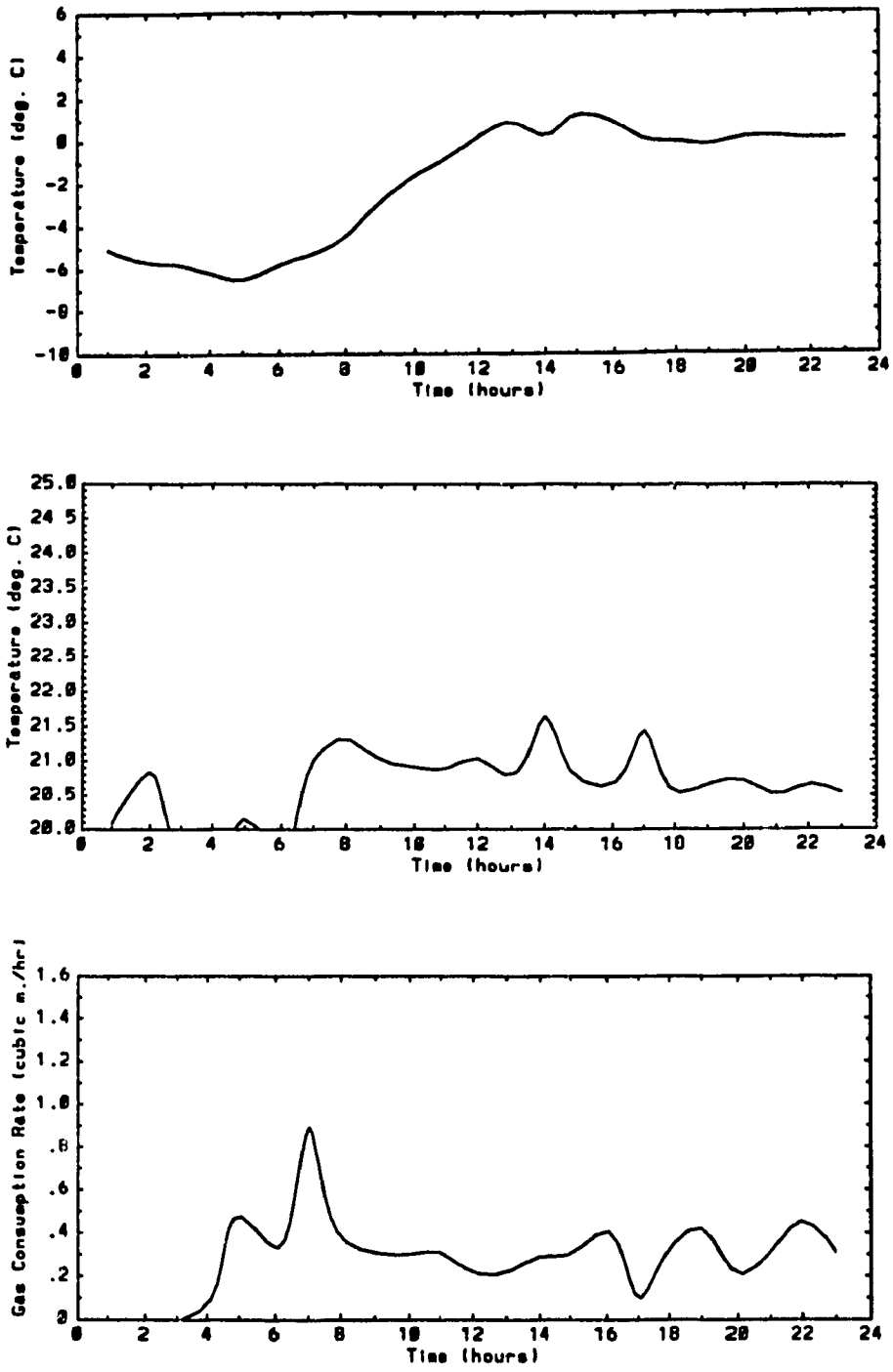

Figure 3.7 Zone temperature and gas consumed on cool day (floor 3).

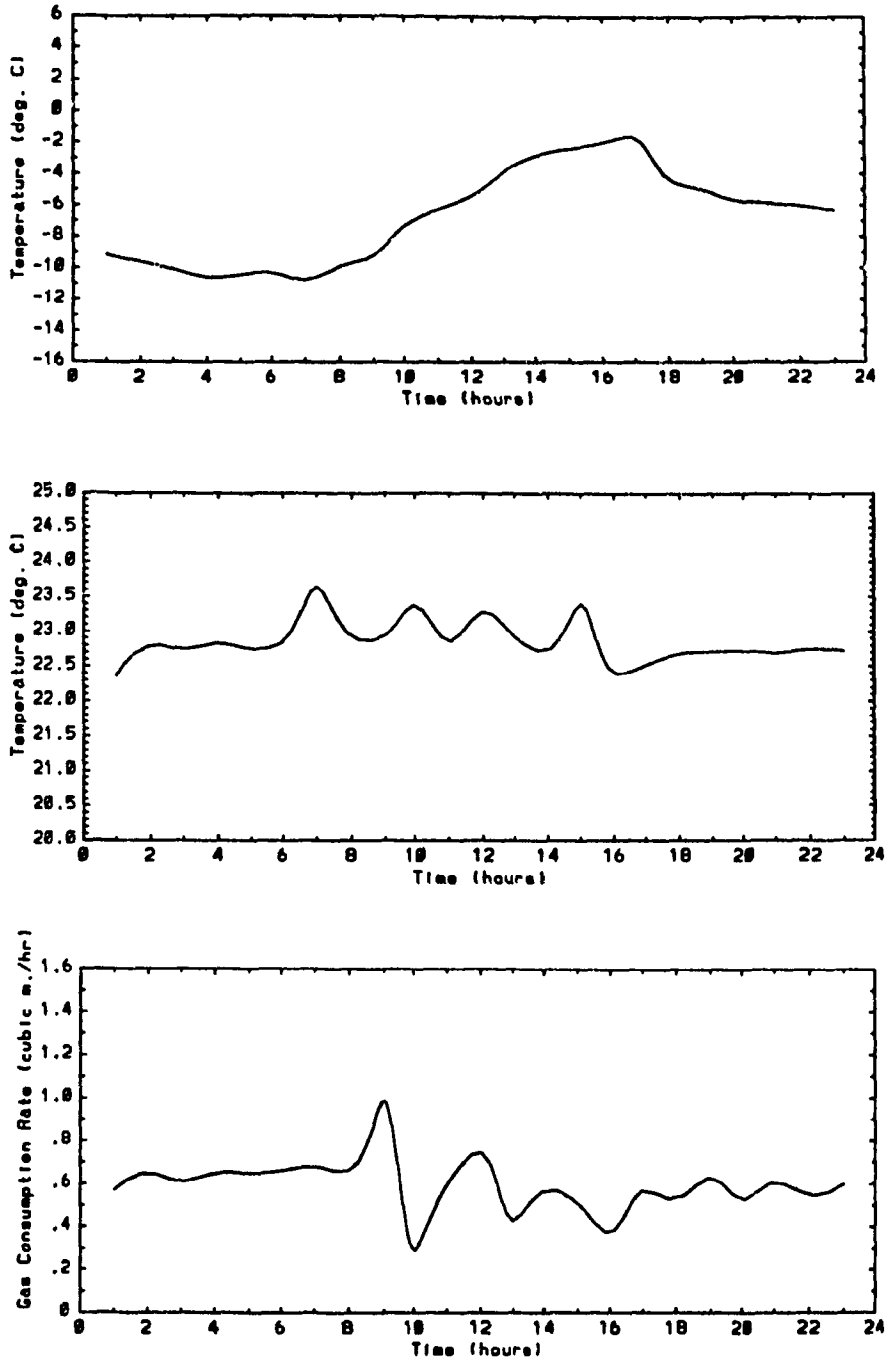

Figure 3.8 Zone temperature and gas consumed on cold day (floor 1).

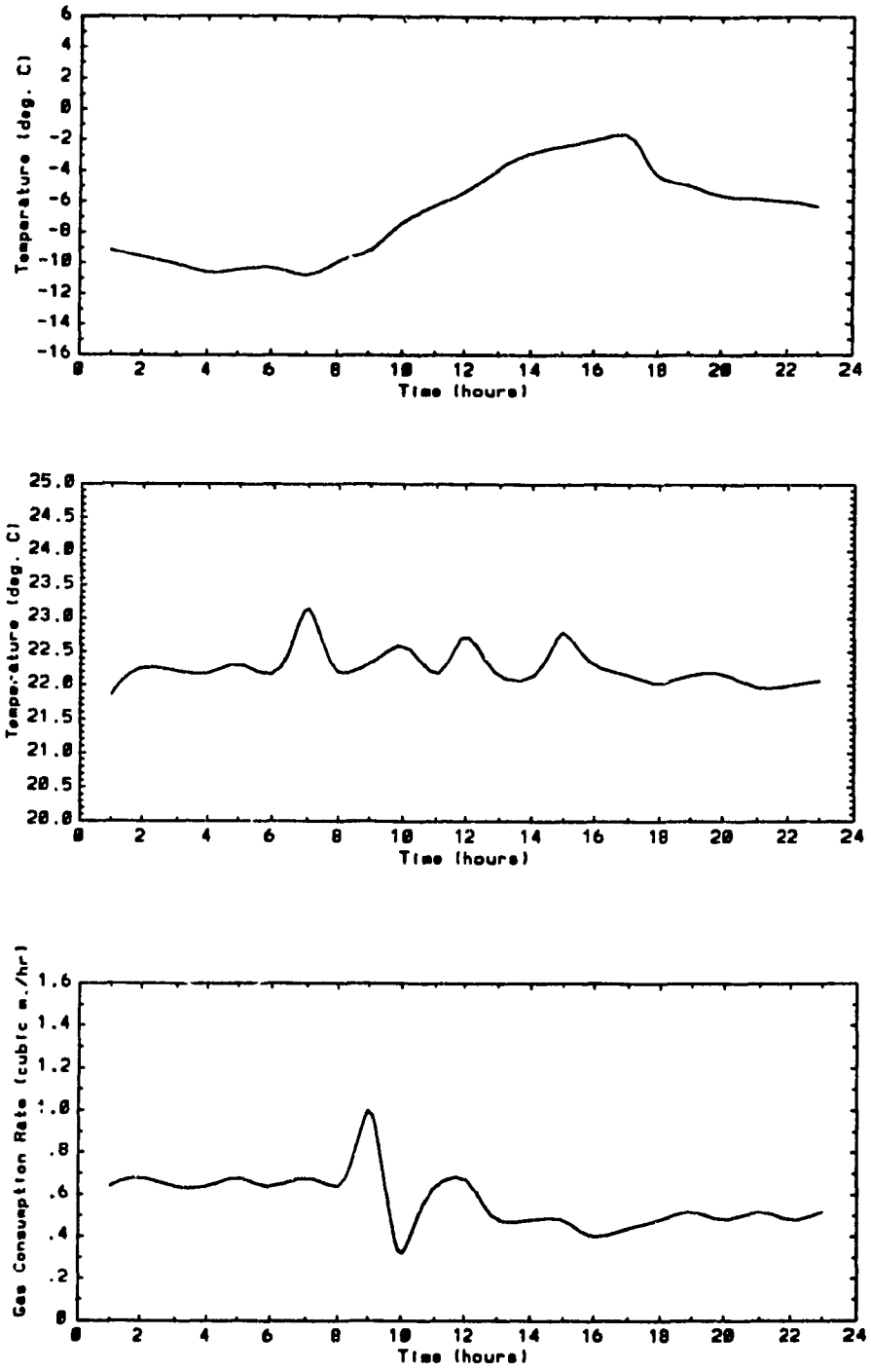

Figure 3.9 Zone temperature and gas consumed on cold day (floor 2).

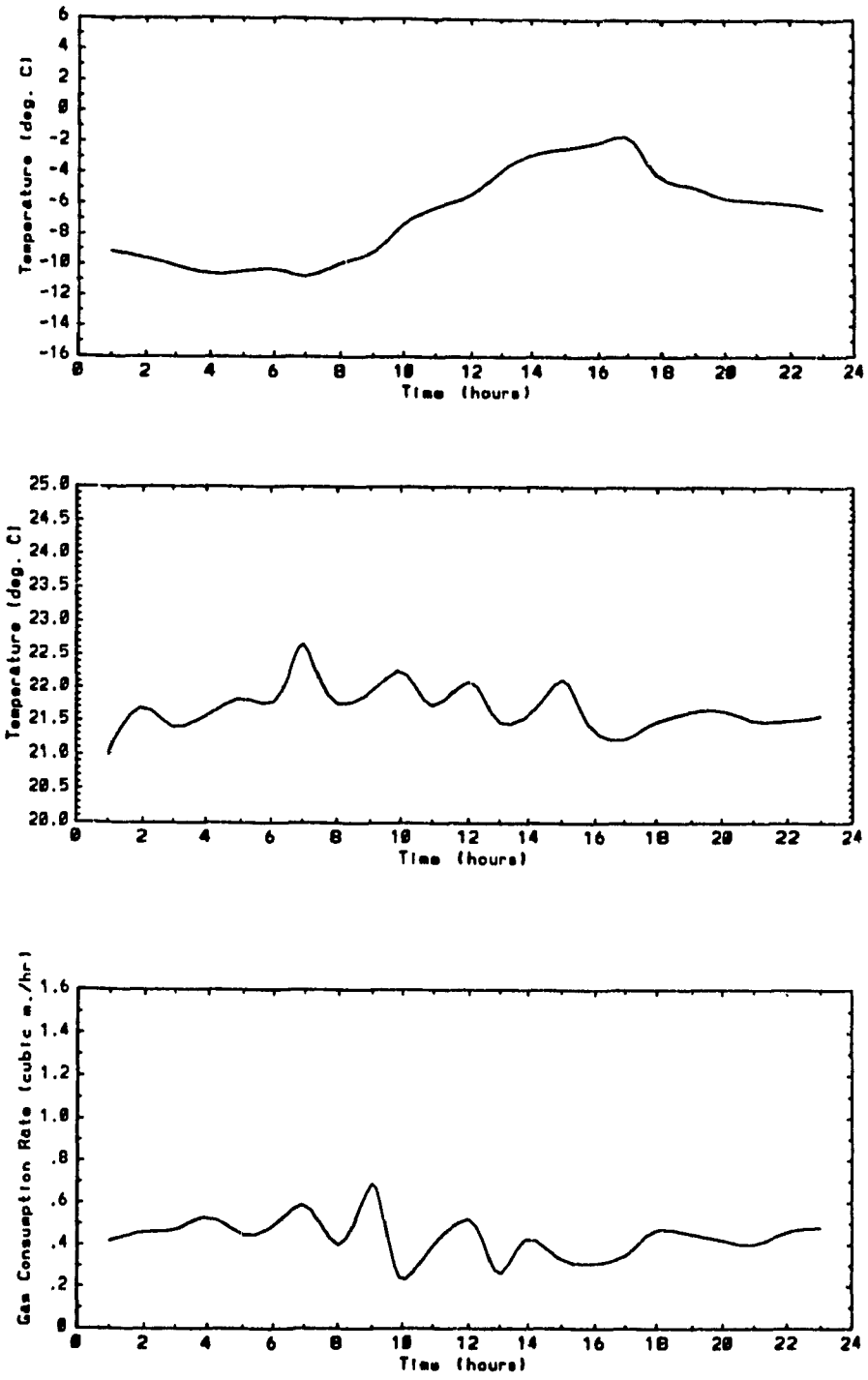

Figure 3.10 Zone temperature and gas consumed on cold day (floor 3).

The room temperature fluctuated between 22.5 and 23°C, and remained relatively constant throughout the day.

The results for the modular system are plotted in Figure 3.6. It may be noted that although the day warms up, the modular system continues to operate at a constant frequency. The corresponding gas consumption rate varies from 0.7 to 0.4 m^3/hr during this time period. After 2:00 P.M., the modular system begins to modulate its gas consumption rate from 0.6 to 0.3 m^3/hr for the remainder of the day.

For the boiler, similar plots are given in Figure 3.7. It is noticed that as the space load decreases, ie. the outdoor temperature increases, the gas consumption rate is gradually decreased between 0800 and 1400 hours while holding the room temperature close to 21°C.

The results for the coldest of the 3 days with the coldest hours occurring between midnight and 9:00 A.M. (minimum temperature around -10°C) are shown in Figure 3.8 (warm-air system), Figure 3.9 (modular system), and Figure 3.10 (hydronic boiler). A summary of typical daily operation characteristics of the three systems are depicted in Table 3.1. It may be noted that the warm-air system had peak gas consumption rate of 1.1 m^3/hr. Results also show that the daily gas consumption of warm-air

system is somewhat higher than the other two systems. This because of the higher space load of the first floor. In terms of temperature regulation, all systems were able to maintain room temperatures within ± 0.5°C of the setpoint.

Table 3.1 Typical daily operating characteristics.

1	Peak gas Consumption	Furnace	Modular	Boiler
	Mild day	0.9	n/a	0.81
	Cool day	1.1	n/a	0.90
	Cold day	n/a	n/a	n/a
2	Gas Consumption	m^3/day	m^3/day	m^3/day
	Mild day	7.5	4.8	6.3
	Cool day	9.7	8.8	7.4
	Cold day	13.2	12.0	11.0
3	Room Temperature Swings	(°C)	(°C)	(°C)
	Mild day	22.1±0.22	21.5±0.5	21.7±0.2
	Cool day	22.8±0.5	21.3±0.5	21.0±0.5
	Cold day	23.0±0.5	22.5±0.5	21.8±0.5
4	% Time on during day			
	Mild day	29%	33.5%	25%
	Cool day	33.5%	44.3%	29.5%
	Cold day	38.5%	46.2%	33.3%

3.2 Typical Cyclic Operational Characteristics

For the mild day, the supply and return duct temperatures for the warm-air system were plotted. These plots can be seen in Figure 3.11. It is noticed that the supply temperature starts at 30°C and increases to 40°C while the burner is on. Then the temperature decreases back down to 31°C when a secondary cycle begins.

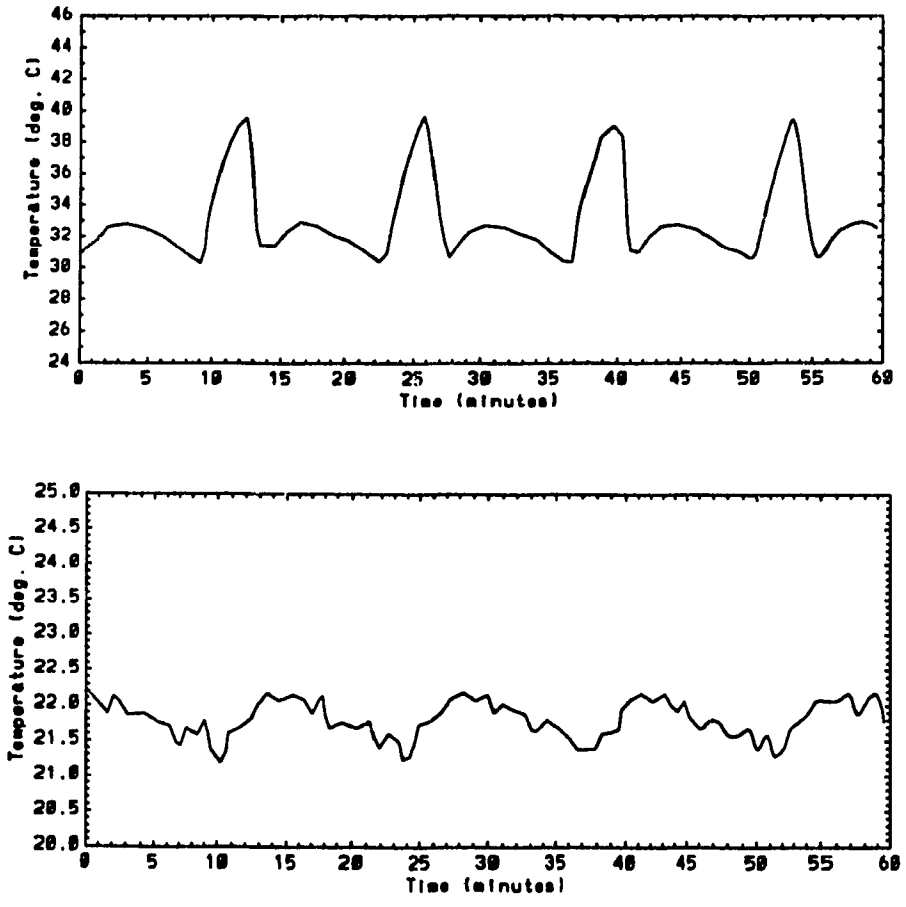

Figure 3.11 Typical cyclic behaviour of warm-air furnace.

The secondary cycle corresponds to a cycle where the residual heat from the heat exchanger is extracted after the burner is shut off. The secondary cycle is 8.5 minutes long while the primary cycle is 4 minutes long. The corresponding return duct temperature varies from 22.2 to 21.2°C as shown in Figure 3.11.

In order to understand the sequence of events that take place, one complete cycle must be examined closely. The burner begins its operation at 8 minutes real time. One minute later, (i.e. at 9 minutes), the temperature of the supply air begins to increase at which time the blower also begins to function. At 12 minutes real time, the burner shuts off which is followed by a sharp drop in the supply air temperature. The blower then shuts off at 14 minutes at which time there still remains some residual heat on the heat-exchanger surface. The supply air temperature thus increases slightly although the burner and blower are off, and at 16 minutes, the supply air temperature decreases until the burner operation repeats. A summary of the cycle times, temperature rises for warm, cool and cold days are shown in Tables 3.2 and 3.3.

Table 3.2 Typical supply and return air temperatures.

Day	Max. T_{supply} (°C)	Max. T_{return} (°C)	Min. T_{supply} (°C)	Min T_{return} (°C)
mild	39.8	22.2	30.5	21.2
cool	40.5	22.6	31.0	21.6
cold	41.0	22.8	31.0	22.0

Table 3.3 Typical cycle times warm-air furnace.

Day	Burner on time (min.)	Burner off time (min.)	Blower on time (min.)	Blower off time (min.)	Delay Burner/Blower (min.)
mild	4.0	10.0	5.5	8.5	1.0
cool	5.0	6.5	7.0	5.0	1.0
cold	6.0	4.5	6.5	4.0	0.5

On the cool day it was noticed that the temperature rise for the supply air is from 31 to 40.5°C. The corresponding duration of the burner on time is 5 minutes. The return air temperature varies from 21.6 to 22.6°C.

On the coldest day the burner on time (burner cycle) lasted for 6 minutes with temperature of supply air ranging from 31 to 41°C. The corresponding return air temperature ranged from 22 to 22.8°C.

Space heating with the modular heating system is achieved by natural convection and radiation heat transfer mechanisms. In other words, there is no fan to deliver supply air as in the warm air system. The cyclic operation of the modular heating system is controlled by room thermostat which turns the burner on or off. Figure 3.16 shows the on-off cyclic operation of the burner as indicated by the flue gas temperature profile.

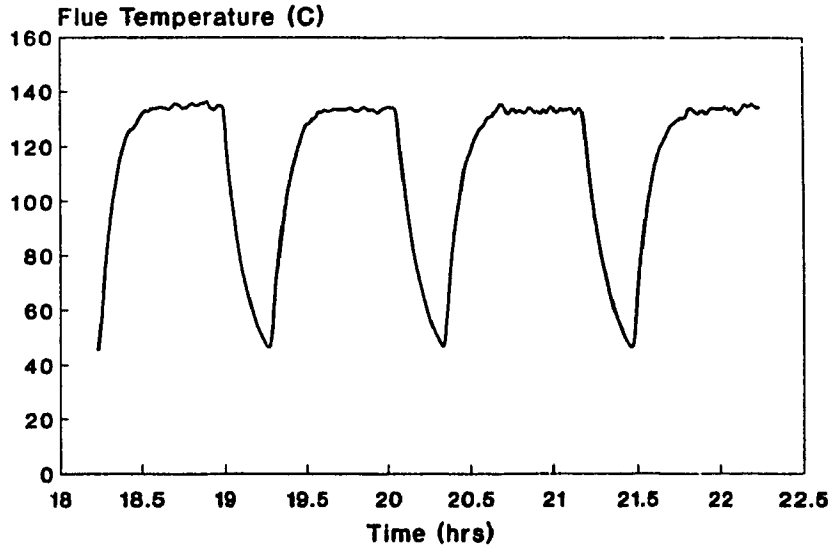

Figure 3.12 Flue gas temperature profile of the modular.

For example, on a cool day, the burner on cycle time is about 45 minutes followed by 15 minute off cycle. As the space load decreases, the on time decreases. For instance, on a mild day, as shown in Table 3.4, the burner on time was 30 minutes and corresponding off time was 35 minutes. Thus the on-off times are varied in accordance with load. It may be noted that compared to the warm-air system, the cycle time of modular system is almost three times longer. The temperature of flue gas and cycle times for three days are summarized in Table 3.5.

Table 3.4 Flue gas temperatures from the modular system.

Day	Max. T_{flue} (C)	Min. T_{flue} (C)
Mild	140	45
Cool	135	45
Cold	140	45

Table 3.5 Cycle times for modular system.

Day	t_{on} (minutes)	t_{off} (minutes)
Mild	30	35
Cool	45	20
Cold	45	20

The cyclic operation of the hydronic boiler is examined next. The supply and return water temperatures are plotted for the mild day as depicted in Figure 3.17. Unlike the warm-air system, many short cycles occur within the larger boiler cycle. If we look closely to one particular cycle we note that the burner begins the cycle at approximately 15 minutes on the real-time scale. The circulation pump begins at approximately 17 minutes but the supply water temperature peaks at 20 minutes. This is because of the thermal mass of the water in the circuit which invokes a certain delay or lag. At 21 minutes, the burner shuts off which can be clearly seen in the figure especially in the burner operation, at which point the water temperature begins to decrease. This natural decrease in water temperature continues until the cycle repeats itself again.

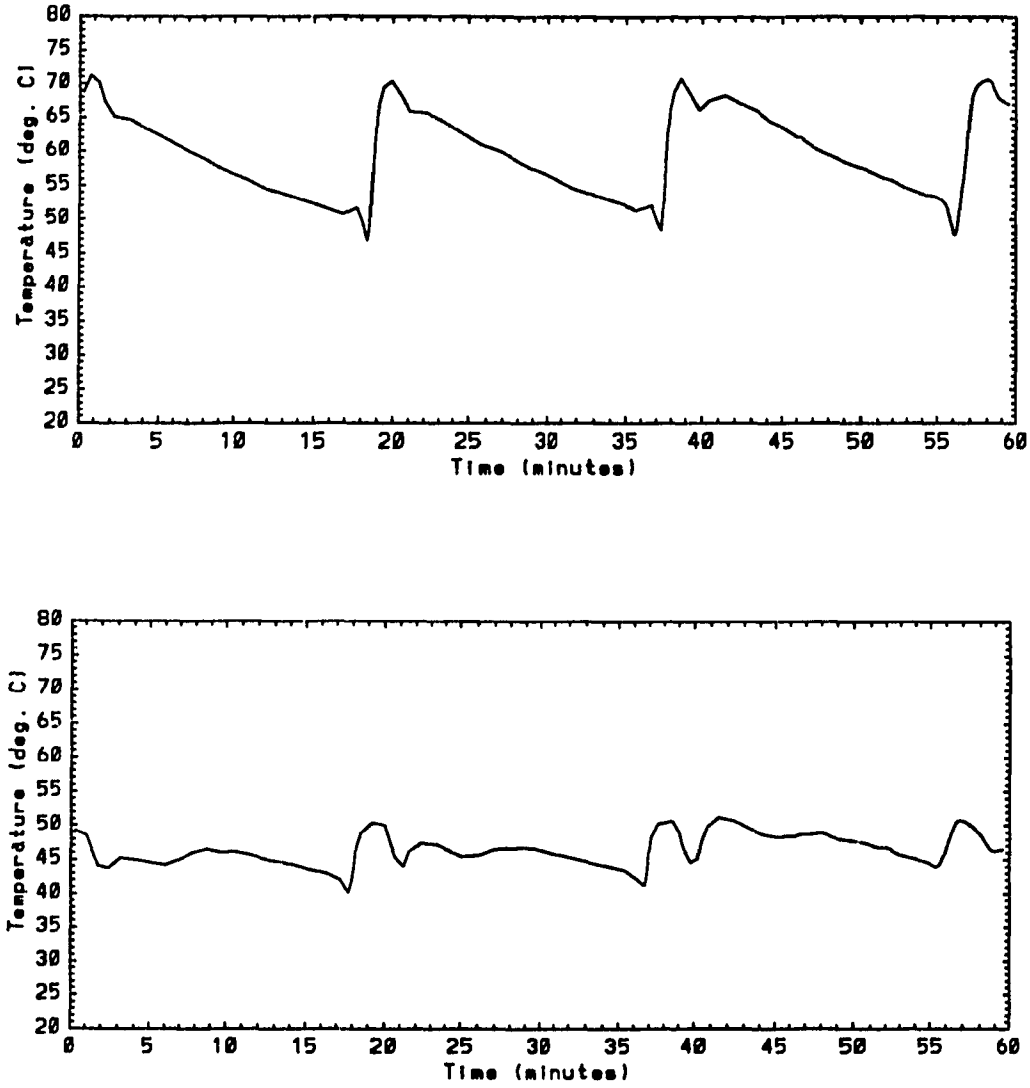

Figure 3.13 Typical cyclic response of hydronic boiler.

The results for the cool and cold days are summarized in respectively in Tables 3.6 and 3.7. It may be noted that as the space load increases, the

burner on time increases, consequently, the supply water temperature increases as well.

Table 3.6 Typical supply and return water temperatures of boiler.

Day	Max. T_{supply} (°C)	Max. T_{return} (°C)	Min. T_{supply} (°C)	Min T_{return} (°C)
mild	67.0	46.0	43.0	39.0
cool	71.0	51.0	48.0	41.0
cold	72.0	52.0	51.0	47.0

Table 3.7 Typical cycle time during boiler operation.

Day	Burner on time (min.)	Burner off time (min.)	Pump on time (min.)	Pump off time (min.)	Delay Burner/Pump (Sec.)
mild	2.0	17.0	4.0	15.0	30
cool	4.0	14.5	4.5	14.0	30
cold	4.5	14.0	5.5	13.0	30

3.3 Warm Up/Cool Down Tests

The purpose for doing the cool down test was twofold. The first reason was to get an indication of the time constant of the building, and second was in order to be guaranteed of full load when taking flue gas sampling. Two types of cool down tests were performed. The first cool down test was a forced cool down in which the heating system was shut off and simultaneously the windows and doors were opened for 45 minutes.

After analyzing the data from these tests, which were repeated many times during the heating season, it was concluded that these tests could not be utilized because of the stratification of room temperatures, ie. cool spots, hot spots. The second manner in which these tests were performed was by natural temperature decay. This was accomplished by turning the heating system off for approximately 10 hours, and then the heating system was turned on. The room temperature for one particular test was approximately 10°C. The warm up test results for all three heating systems can be seen in Figure 3.23. The warm-air system, as expected, attained steady-state conditions in approximately 6 hours, while the other two systems took somewhat longer. This is as expected since the warm-air system uses forced convection as its method of heat transfer while the other two systems rely solely on natural convective process. All three systems performed satisfactorily by bringing the zone temperature from 10°C to steady-state conditions (≈22°C) in about 6 to 8.5 hours.

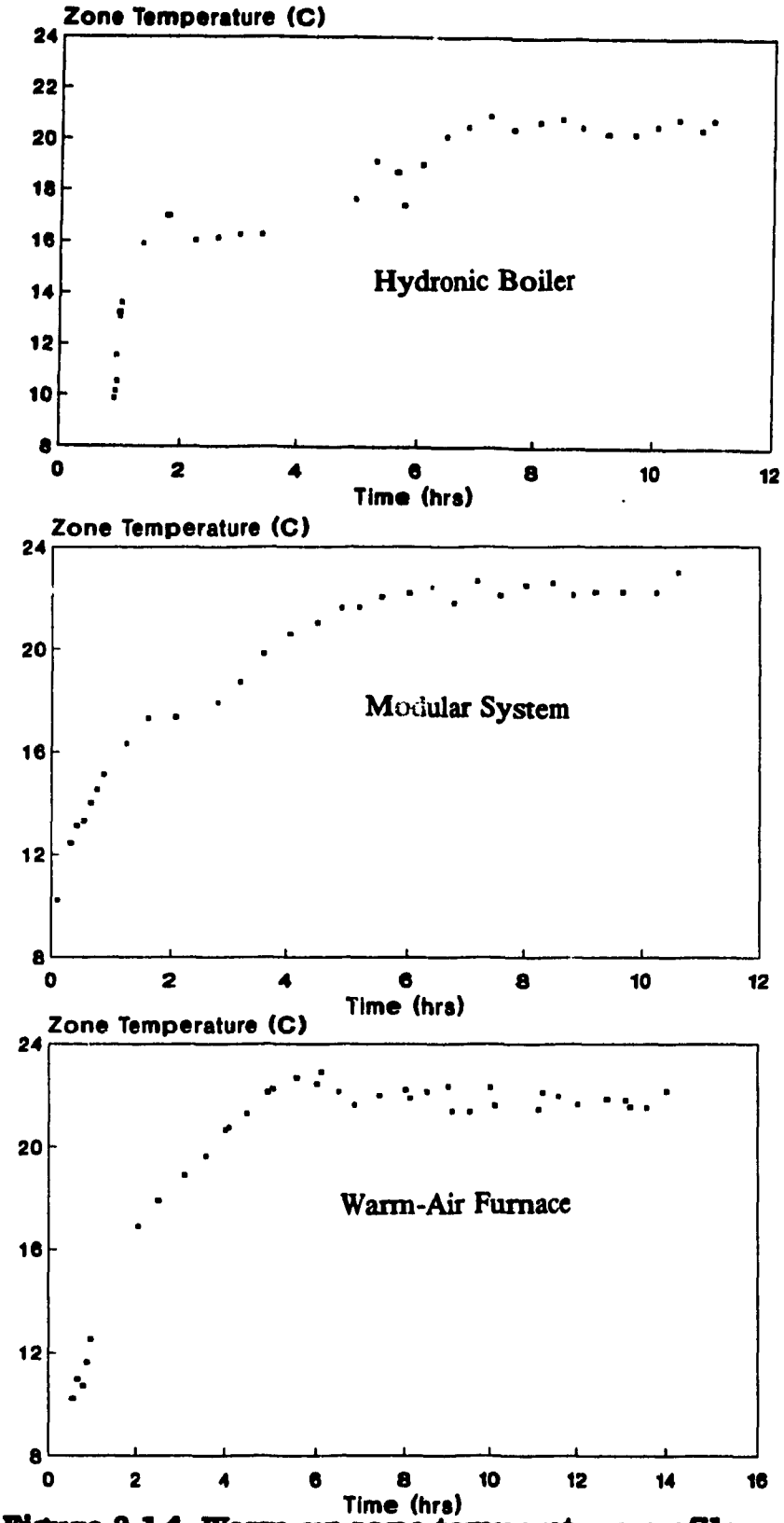

Figure 3.14 Warm up zone temperature profiles.

3.3.1 Steady-State Efficiency Tests

The warm up tests were performed simultaneously with the steady-state efficiency test. The reason for doing the steady-state efficiency test simultaneously with the warm-up test was to ensure that the heating system was performing at or near full load. It was assumed that if the space was cooled down enough and the heating system was turned on, that the full load would be obtained.

By plotting the O_2, CO_2, and temperature profile of the flue gas during the warm-up, the steady-state efficiency was obtained by correlations given in ASHRAE Fundamentals. The plots for the warm-air furnace, modular and hydronic boiler can be seen respectively in Figure 3.26, Figure 3.27 and Figure 3.28. The computed efficiencies were then compared to those given by the manufacturer's specifications and are summarized in Table 3.10.

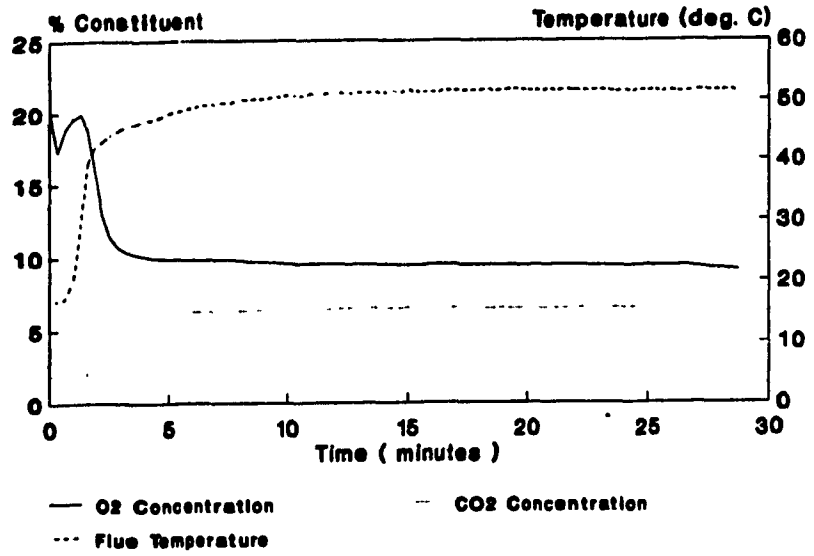

Figure 3.15 Flue gas analysis of warm-air furnace.

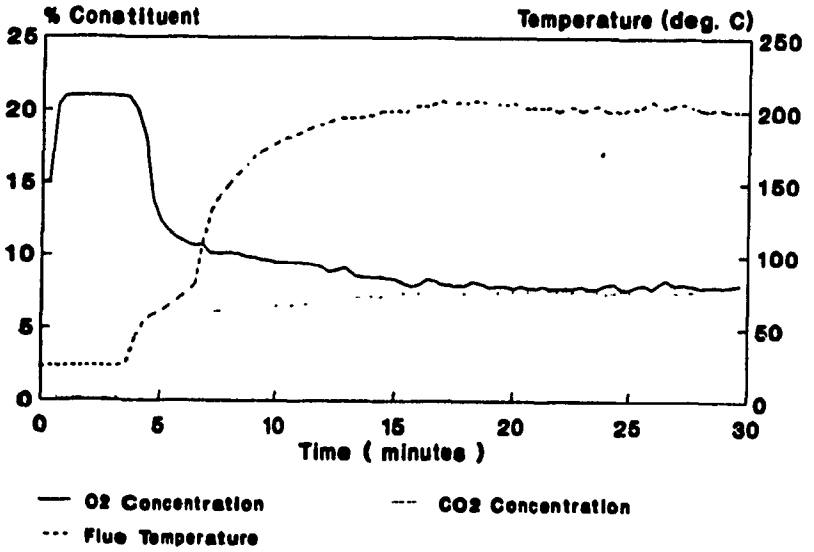

Figure 3.16 Flue-gas analysis of modular system.

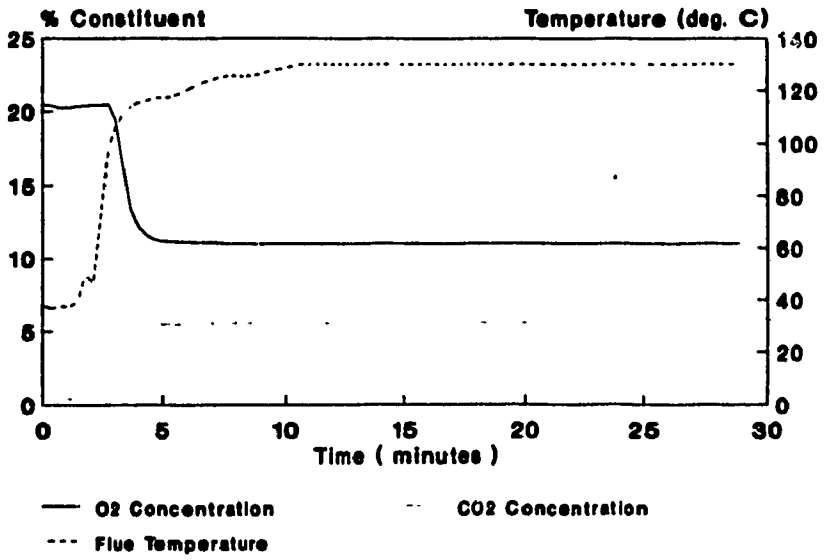

Figure 3.17 Flue-gas analysis of hydronic boiler.

Table 3.8 Steady-state efficiency results.

System	Steady State Efficiency Computed (%)	Rated Efficiency (%)	% difference
Furnace	86.0	86.0	0.0
Modular	80.0	80.0	0.0
Boiler	83.0	80.0	3.8

The warm-air furnace obtained a steady-state efficiency of 86% while the boiler obtained a value of 83% and the modular 80%. These values are as expected because the furnace was both a condensing furnace and also had mechanical venting thus the flue-temperature was quite low. The boiler was also a condensing unit but had no mechanical venting, thus the steady-state efficiency was slightly lower. In the case of the modular, it was neither of condensing heat-exchanger design, nor did it have mechanical venting and therefore the steady state efficiency of the system is lower compared to the warm-air system and hydronic boiler.

3.3 Summary

Normal operation of the 3 heating systems on 3 days, namely a mild winter day (T_{out}=3°C), a cool day (T_{out}=-2°C), and a cold day (T_{out}=-6°C), is examined. Gas consumption rate, peak demand and room temperature profiles were among specific system performance characteristics which were studied. Mass effects and time delays associated with these mass effects were also shown for the boiler and warm-air furnace for these 3 typical winter days.

In the second section, specific transient tests which were performed are discussed and their results shown. The transient tests included warm up tests which give an indication of the lead time required for heating the

space from about 10°C to the set temperature. The second type of test that was conducted is the full load or steady state efficiency test. The steady state efficiency results obtained from this test were as follows: warm-air furnace 86%, modular system 80%, and the hydronic boiler 83% which are very close to the manufacturer's specifications.

CHAPTER 4

SEASONAL PERFORMANCE OF THE HEATING SYSTEMS

The main objective of this chapter is to establish the operating characteristics of the systems based upon seasonal measurements. The results from this chapter enable a better comparison of the three heating systems.

In section 4.1, frequency distributions which indicate the characteristic of each system are shown. These include the variation in room temperature for each heating system, the cycle time as a function of average outdoor temperature, and the frequency of occurrence as a function of on/off times and as a function of outdoor temperature. In addition, the distribution of cycle times over the duration of the heating season will be examined.

Section 4.2 of this chapter deals with the seasonal gas consumption of each system. The seasonal gas consumption is determined by two methods. The first method involves utilizing the numbers recorded by the DAS, then plotting cumulative gas consumption as a function of heating degree days. As a check, gas consumption of each heating system was also recorded manually once a day. Using these manual readings, the

cumulative gas consumption as a function of cumulative heating degree days recorded by Dorval weather office were plotted. Both results compare favourably.

Section 4.3 describes the seasonal efficiency and also gives some indication of the part-load efficiency of the systems. The daily efficiency of the warm air furnace and the hydronic boiler is examined as a function of average outdoor temperature. The overall seasonal performance is then shown for the above mentioned systems by plotting the cumulative efficiency as a function of time.

4.1 Seasonal Frequency Distributions

In Chapter 2 (section 2.5), the initial cost and physical characteristics of each system were compared. However, cost is not the only major concern when assessing the performance of a heating system. By analyzing the total data over the entire heating season, some very distinct relationships were established.

The on-off cycle time for the heating systems is an important characteristic in terms of assessing thermal comfort and also the rate of gas consumption [14]. To this end, the frequency distribution of the cycle on and off times were plotted for the heating season. The results of these plots

can be seen in Figures 4.1 to 4.3.

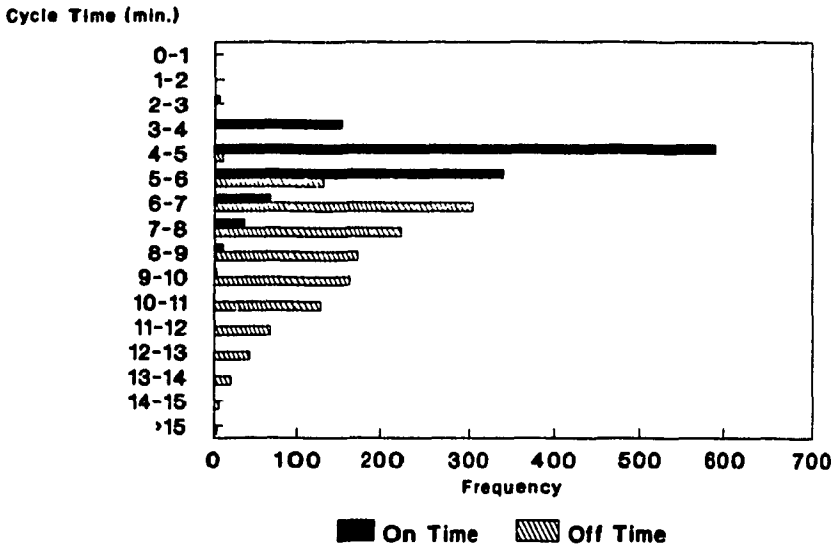

Figure 4.1 Frequency distribution of on/off times (warm-air system).

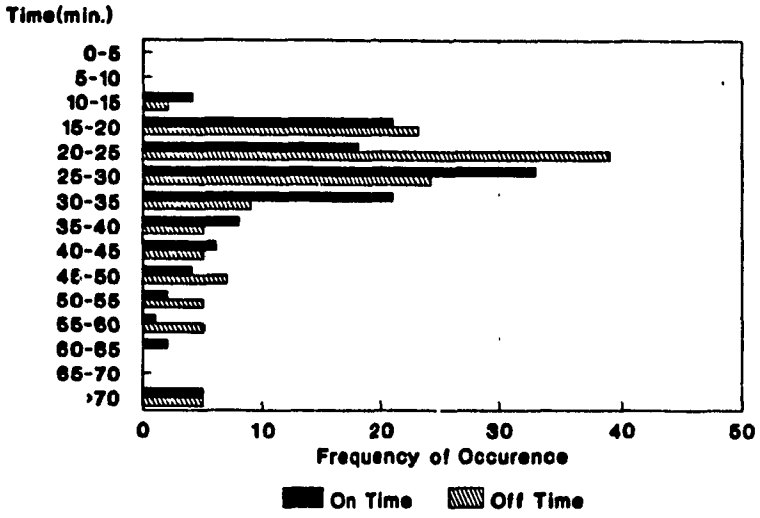

Figure 4.2 Frequency distribution of on/off times (modular system).

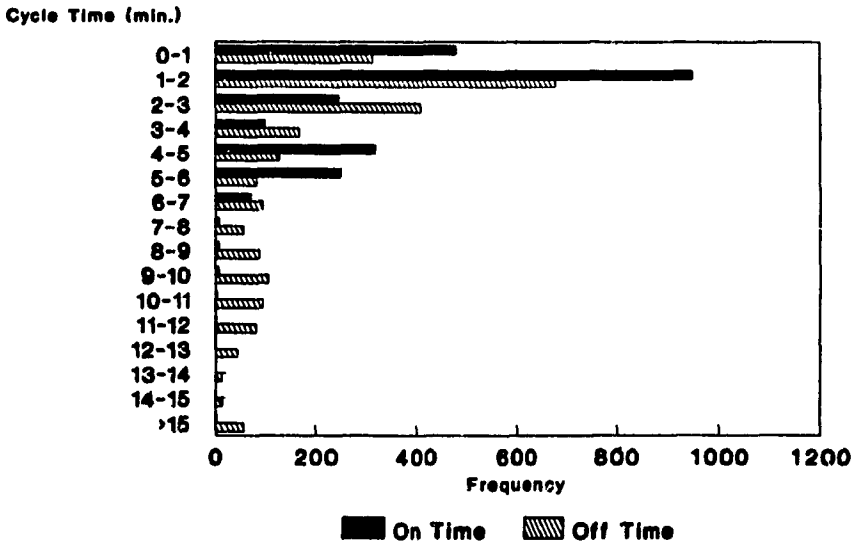

Figure 4.3 Frequency distribution of on/off times (hydronic boiler).

The on-off time frequency distribution for the warm air furnace is shown in Figure 4.1. The on cycle times range from 2-8 minutes with highest frequency occurring between 4-5 minutes. The off times which range from 4-15 minutes with a maximum frequency at 6-7 minutes. It is also noticeable that there exist very few occurrences, less than 10, for on/off times greater than 15 minutes. This behaviour can in part be explained by the set back at 12:00 a.m., when the room temperature is allowed to drop from 21 to 18°C, and the on times are explained by the morning set forward from 18 to 21°C. Also on very warm and cold days such large on/off times are likely to occur.

The Frequency distribution of on-off times for the modular system are shown in Figure 4.2. The ranges for the on-cycle time is from 10-65 minutes with the maximum frequency occurring at 25-30 minutes. The off-cycle times (at 30% capacity) of the modular range from 10-60 minutes and obtaining a maximum frequency at 20-25 minutes. Unlike the furnace and boiler, the modular heating system was not equipped with night set-back so that the cycle times of greater than 70 minutes were actual times under normal operating conditions, rather than under special set back/set forward situations. It should be noted at this point that for long durations of on cycle time, the casing on the modular attained very high temperatures, namely in the range of 70-80°C, and thus it poses some

danger to the occupants especially young children and therefore requires special attention.

The frequency distribution plot for the hydronic boiler is shown in Figure 4.3. What is interesting about this system is that it obtained two somewhat distinct distribution curves for both the on and off cycle times. The first "on" distribution had a range from 0-3 minutes with maximum frequency occurring at 1-2 minutes, while the second distribution ranged from 3-11 minutes with a maximum occurrence at 4-5 minutes on. The first off time distribution ranged from 0-7 minutes and occurred most frequently at 1-2 minutes, while the second distribution ranged from 7-15 minutes with maximum occurrence at 9-10 minutes. The reason for these distinct distributions is due to the fact that the system works in two modes. A space heating mode and a DHW mode. One on/off cycle time distribution is associated with the space heating side of the hydronic boiler while the other distribution are related to the DHW side. The short bursts of on/off times distribution is associated with the DHW. The short on/off cycles are mainly due to jacket losses from the DHW tank and thus the boiler shuttles between the space heating mode and the DHW mode, in order to satisfy both loads.

Another relationship of interest which was obtained from the data

analysis was the dependence of cycle on and off times with outdoor temperature. This result is shown in Figures 4.4 to 4.6.

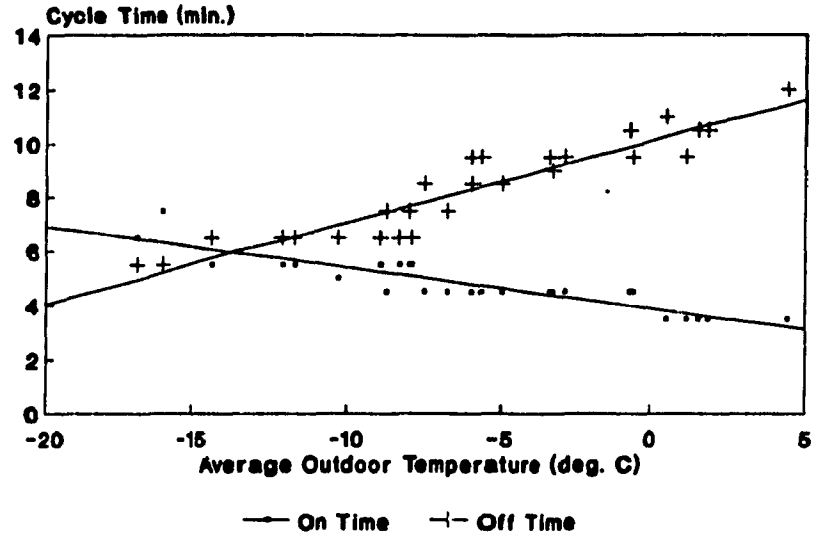

Figure 4.4 Cycle time vs T_{out}(warm-air system).

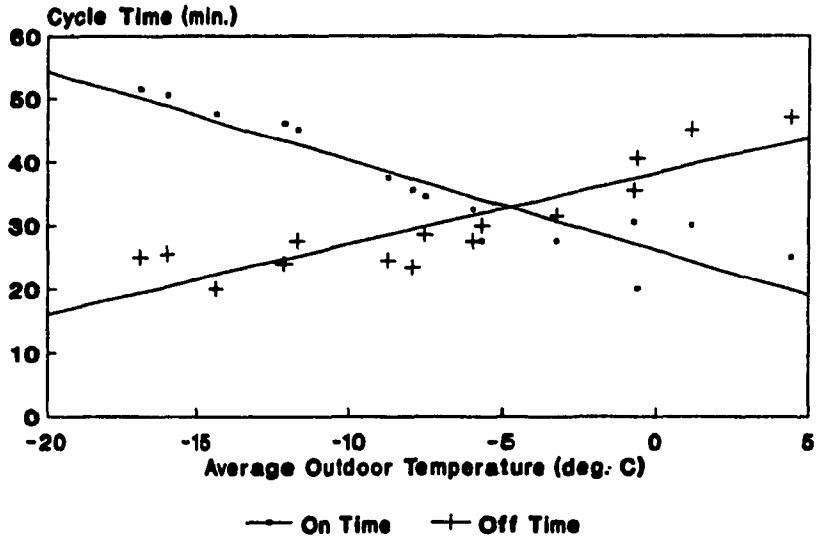

Figure 4.5 Cycle time vs T_{out}(modular system).

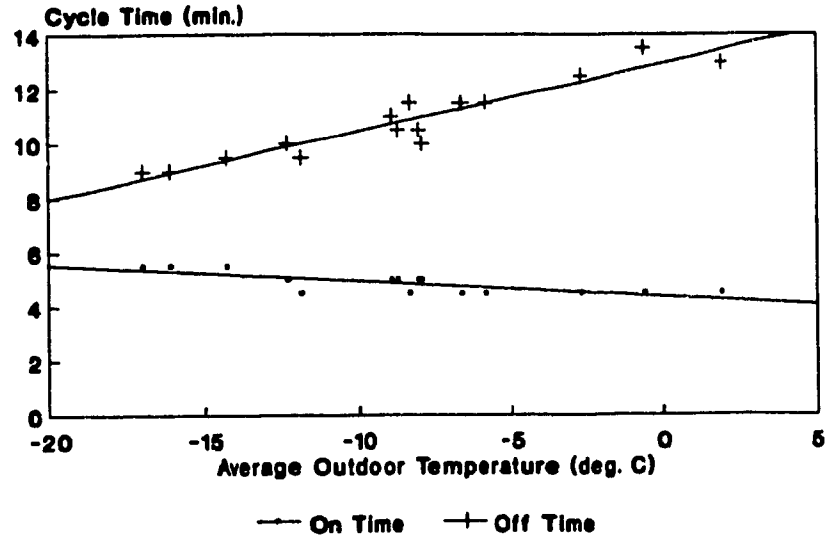

Figure 4.6 Cycle time vs T_{out} (hydronic boiler).

For an average outdoor temperature of -10°C, we see that the warm air furnace achieves a 5.5 minute on time and a 7 minute off time. The results for all systems at -10°C, are given in Table 4.3. The results show that as the outdoor temperature decreases, the on-cycle time increases and the off-cycle time decreases. The results shown in Figures 4.3 thru 4.6 quantify the characteristics for the three heating systems.

Table 4.1 Average on and off times.

System	Average On-Time (min.)	Average Off-Time (min.)
Warm-Air Furnace	5.5	7.0
Modular System	40.0	25.0
Hydronic Boiler	5.7	10.0

Another way in which the performance of the systems can be compared is from the point of view of room temperature control. Each of the three systems was set at 21°C, with the furnace and boiler also utilizing a 3°C night set-back. The room temperature distributions were plotted versus frequency of occurrence when the systems were in normal operation. These frequency distributions are shown in Figures 4.7 - 4.9.

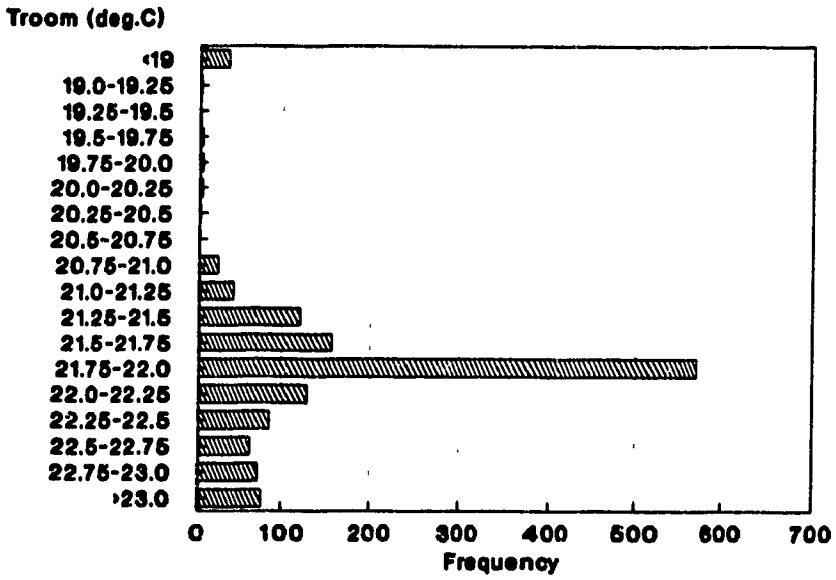

Figure 4.7 Room temperature variations (warm-air system)

The room temperature distribution of the warm air furnace is shown in Figure 4.7. The temperatures range from 19-23°C with maximum

frequency occurring at 21.75 to 22.0°C temperature range. It may be noted during certain times, the room temperatures were less than 19°C and greater than 23°C. These are related to night set back and overshoot directly related to set forward. The bulk of the distribution was between 21.25 to 22.5°C, which is within 1°C, from the set-point.

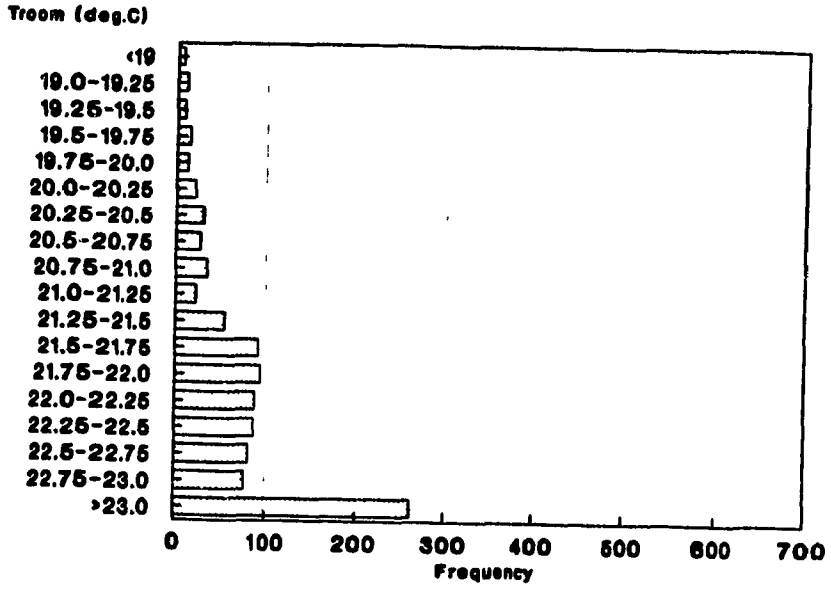

Figure 4.8 Room temperature variations (modular).

In the case of the modular, Figure 4.8, the bulk of the room temperatures ranged from 21.5 to 23°C. What is very important to mention is the fact that the maximum occurrence occurred for temperatures exceeding 23°C. This deviates by more than 2°C from the "set point" and

provides the occupant with an uncomfortable environment. Thus compared to the warm air system, the temperature control characteristics of the modular system were not satisfactory.

The temperature distribution of the hydronic boiler is shown in Figure 4.9. The room temperatures ranged from 19-23°C with the bulk occurring between 20.75 to 22°C. Temperatures of less then 19°C were non-existent, while temperatures higher than 23°C were minimal with less than 10 occurrences throughout the entire heating season. Therefore, it can be concluded that both the warm-air system and the hydronic boiler performed well in terms of maintaining good room temperature control.

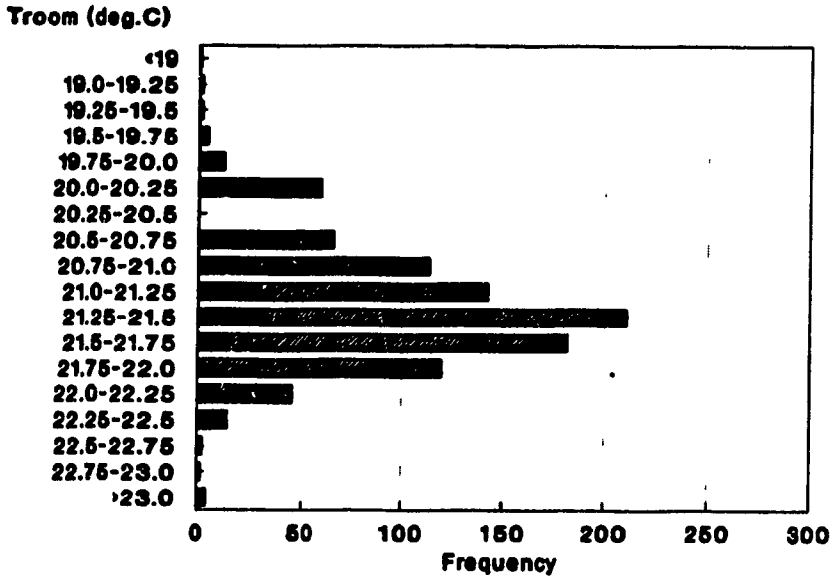

Figure 4.9 Room temperature variations (boiler).

4.2 Seasonal Gas Consumption

This section deals with data analysis to determine correlations between gas consumption and heating degree-days for each of the three heating systems. This is shown in Figure 4.10. The cumulative gas consumption is the integrated value of the gas consumption which is plotted as a function of cumulative heating degree-days (base 18°C). It may be noted that all three heating systems show more or less a linear relationship. This is also the basis for energy calculation using degree-day method [26] which assumes a linear relationship. For the data collection period which spanned from November 1988 to April 1989, the cumulative degree-days were about 3600, which represented about 80 % of an average heating season.

The gas consumption was also recorded manually once a day as a check. These results are plotted in Figure 4.11. They compare well with readings gathered from the DAS. The seasonal gas consumption from Figure 4.11 for each of the three systems is as follows:

1. Warm-air furnace = 1625 m^3
2. Modular = 925 m^3
3. Hydronic boiler = 1275 m^3

Another important factor namely the UA-value of each of the three

floors can be obtained from Figures 4.10 and 4.11. For example, the slope of the line in Figure 4.11 is proportional to the UA-value which is characteristic of the enclosure and as well as includes the effects of the seasonal efficiency of the heating systems. The measured slopes obtained from Figure 4.11 in units of m^3/DD were converted to W/°C. These are given below:

1. Floor 1 = 368.6 W/°C
2. Floor 2 = 213.0 W/°C
3. Floor 3 = 291.0 W/°C

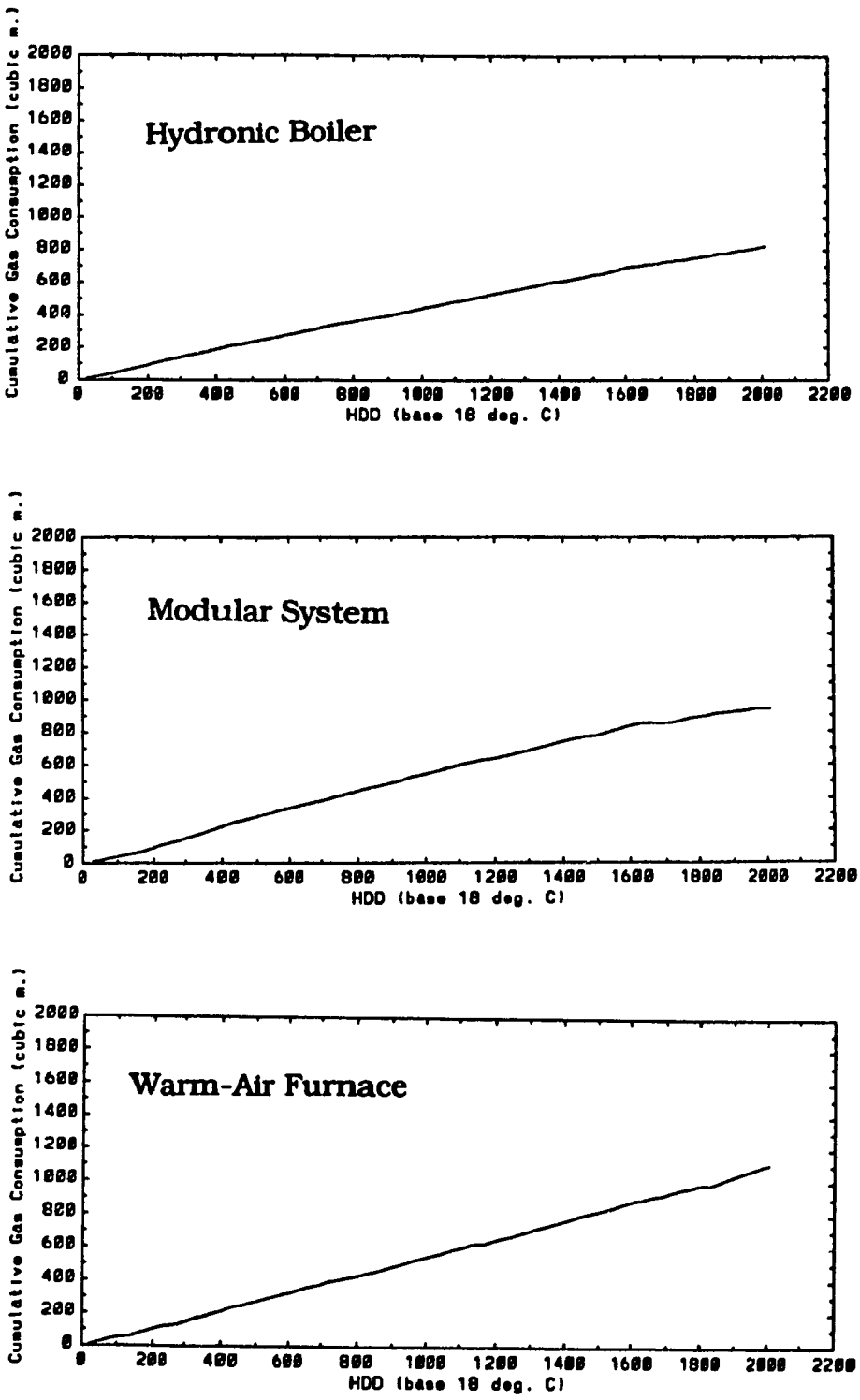

Figure 4.10 Gas consumption as a function of degree days for three systems.

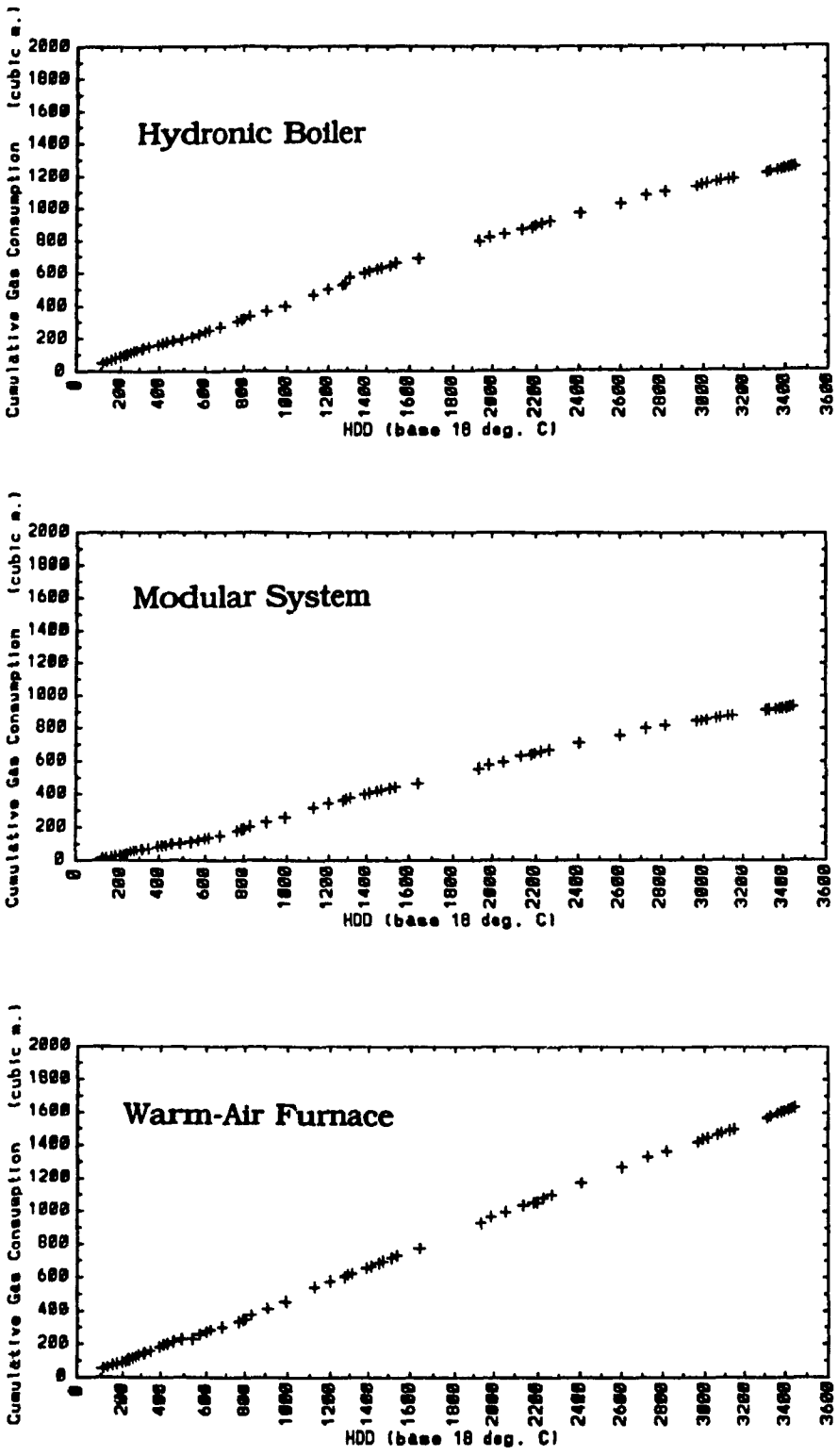

Figure 4.11 Manual measurements of gas consumed.

4.3 Cumulative Efficiency

The cumulative efficiency gives an indication of the useful energy that is utilized to heat the space, while the steady-state efficiency, which was determined in chapter 3, gives only the full-load efficiency of the heating system. In other words, the steady-state efficiency does not include the off-cycle losses considered in the computation of the seasonal efficiency. Both the seasonal and daily cumulative efficiencies will be discussed in the subsequent two sections.

4.3.1 Seasonal Cumulative Efficiency

By taking the ratio of integrated output to input heat fluxes, the cumulative efficiency of the heating systems was obtained. This is shown in Figure 4.12(a) (warm-air) and 4.12(b) (boiler). As seen from the figures, the cumulative efficiency attains a constant value in about 250-400 hours. The magnitude of the cumulative efficiency for the warm-air system and hydronic boiler are respectively 0.80 and 0.78. Since it is based on integrated heat fluxes, it takes into account the effects of off-cycle losses and the part load characteristics of the heating system. The cumulative efficiency gives a measure of seasonal performance of the system as shown in previous study [27].

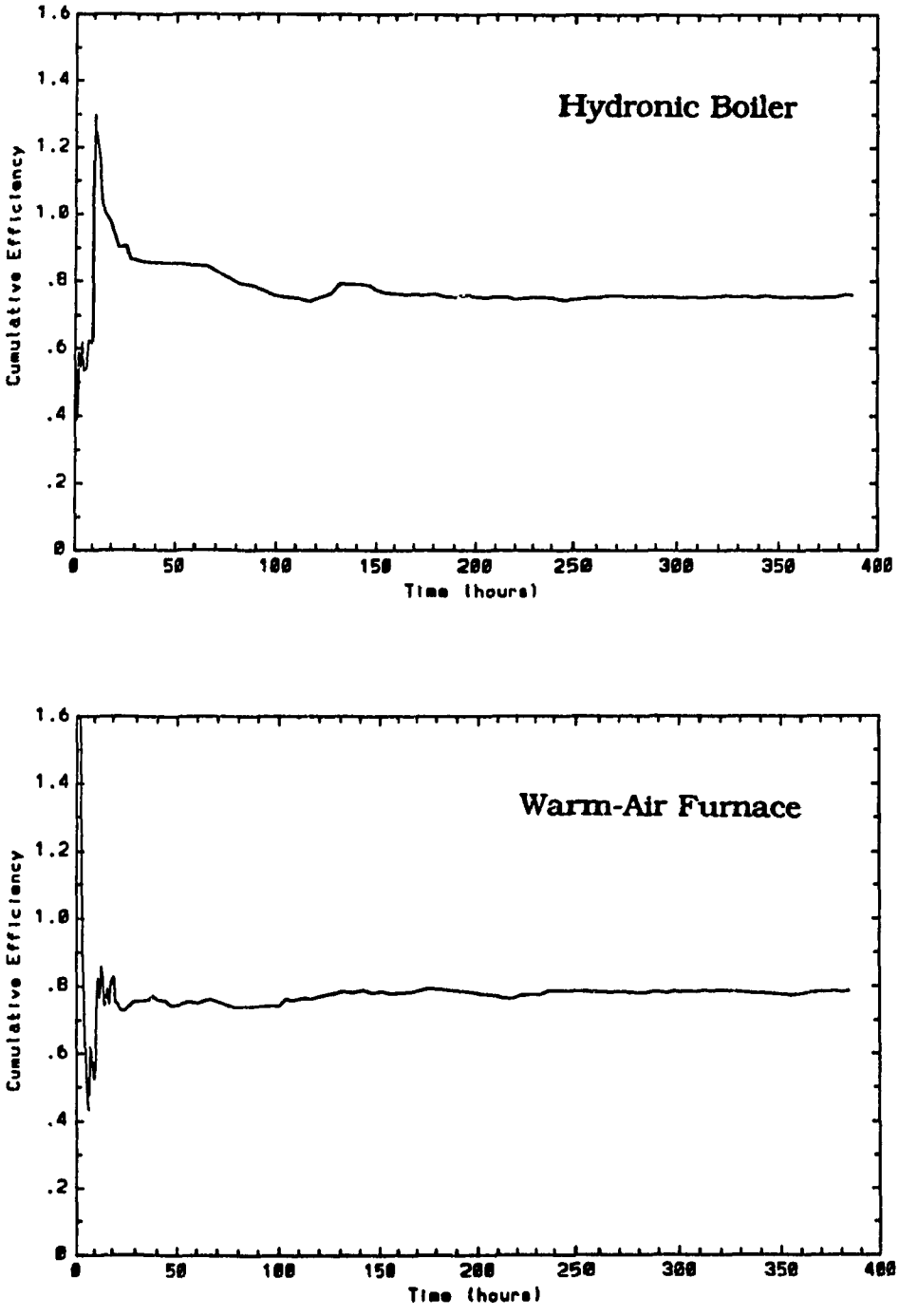

Figure 4.12 Cumulative efficiencies of two heating systems.

It is to be expected that the cumulative efficiency will be less than the steady-state efficiency of the system. Our results show that the cumulative efficiency of the warm-air system is about 6% less than the corresponding steady-state efficiency where as for the boiler it is about 5%.

In the case of the modular heating system, the measurement of output heat fluxes is difficult and therefore were not made. Instead, an alternative method of determining the cumulative efficiency was utilized. In the method used, the second floor was heated with modular heating system for one week and with electric baseboard heaters the following week. By alternating the heating between modular and electric baseboards, the gas consumption and electric energy used by the baseboards was recorded. By assuming that the heating with electric baseboards is 100% efficient, the cumulative efficiency of the modular heating system was determined. This is shown in Figure 4.13, in which the ration of UA-electric to UA-modular system is plotted as a function of cumulative heating degree-days. This ratio which gives the cumulative efficiency of the modular heating system was found to be 77%. Thus about 3% less than the steady-state efficiency of the modular heating system. A summary of cumulative efficiency of al three heating systems is given in Table 4.2.

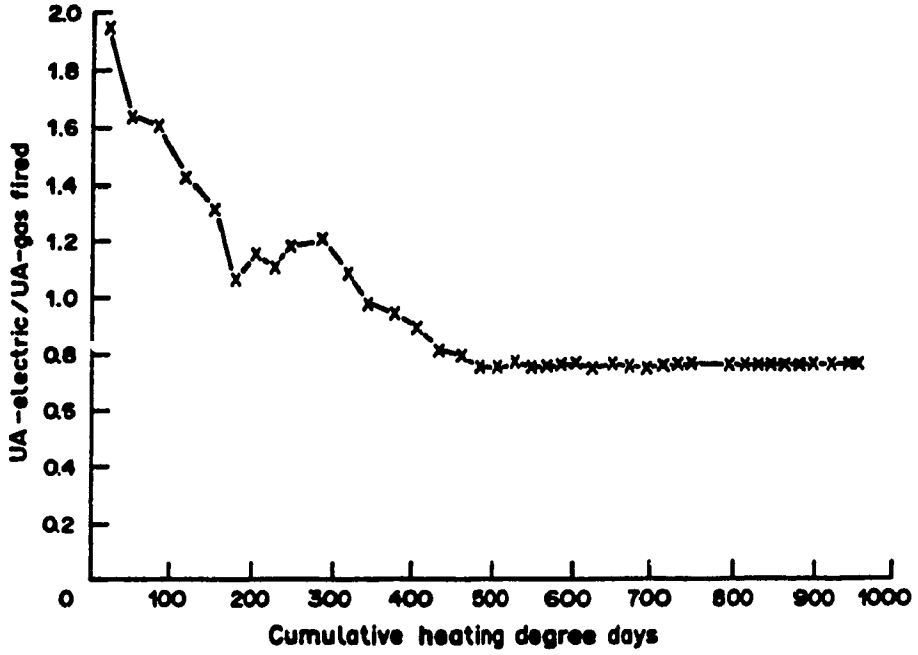

Figure 4.13 Cumulative efficiency of modular system.

Table 4.2 Summary of cumulative efficiencies.

System	Cumulative efficiency %
Warm air furnace	80
Modular	77
Boiler	78

4.3.2 Daily Cumulative Efficiency

In order to assess the part load performance, the daily efficiency was analyzed as a function of average daily outdoor temperature, as shown in Figure 4.14 and 4.15. For the warm-air system (Figure 4.14) , we see that for an outdoor temperature range of -16 to -6°C, the daily efficiency is approximately 80%. Similarly, for the temperature ranges of -6 to +10°C, the daily efficiency decreases linearly from 80 to 75%.

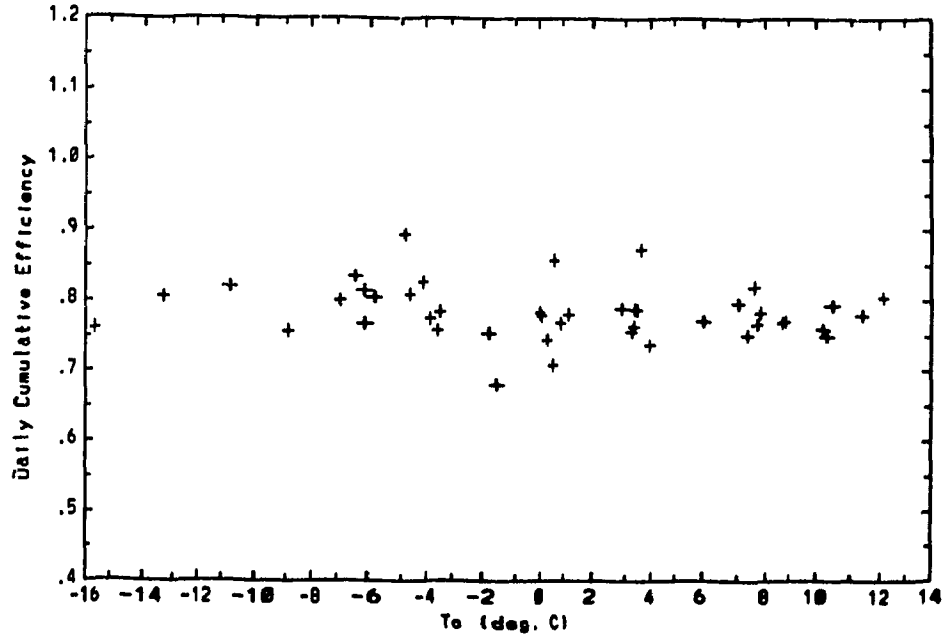

Figure 4.14 Daily cumulative efficiency (w.a system).

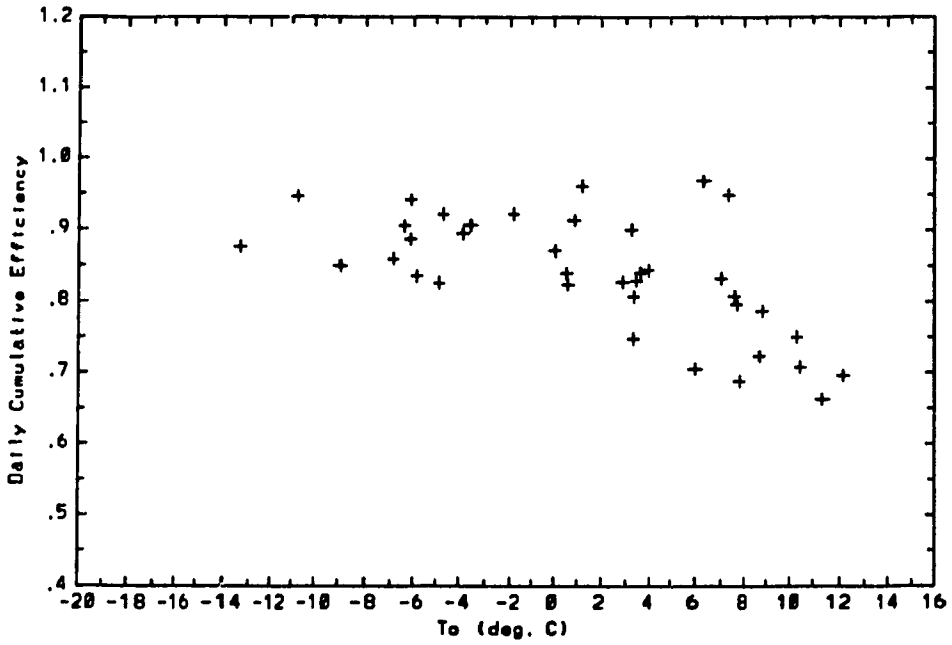

Figure 4.15 Daily cumulative efficiency (boiler).

In the case of the hydronic boiler (Figure 4.15), for a temperature of about -10°C, the cumulative efficiency is about 90%, while for a temperature of +10°C, the efficiency drops to 75%. These results point to the fact that energy utilization efficiency of the gas-fired heating systems could vary as much as 10-15% depending on the load imposed on the system.

4.5 Summary

The frequency plots of on-off times for the boiler showed that two distinct cycle-on/off time distributions existed. One was very similar to that of the warm-air furnace, while the other consisted of short on/off times. These short on/off times are directly related to the DHW side of the energy balance. The short on/off times are caused by the cycling of the boiler in order to maintain both the space and DHW load. The short cycles are explained by small bursts of heat being transferred to the DHW in order to maintain a set temperature. The small bursts are due to jacket losses from the DHW storage tank. At the highest frequency, the on-off time of the three heating systems compared as follows:

	on-time (minutes)	off-time(minutes)
Warm air furnace	4-5	6-7
Modular	25-30	20-25
Boiler	4-5	9-10

From the view point of temperature regulation, the three heating systems ranked as follows: warm-air furnace, hydronic boiler and the modular heating system.

The cumulative gas consumption of each heating system over the same duration of time (3400 °C days) varied as a function of heat loss

characteristics of each floor. The measured cumulative gas consumptions of the three heating systems were as follows:

Warm-air furnace: 1625 m^3

Modular: 925 m^3

Boiler: 1275 m^3

The cumulative efficiencies for the furnace, the modular and the boiler were respectively 80, 77 and 78%. It was also shown that the cumulative daily efficiency is a function of outdoor air temperature increasing as the outdoor temperature decreases and vice versa. In other words, this relationship describes the part load characteristics of the heating system.

CHAPTER 5

DYNAMIC MODEL FOR INTEGRATED HYDRONIC HEATING SYSTEM

5.1 Introduction

The motivation for developing an analytical model of the hydronic heating system comes from the fact that there is a need to develop good operating strategies for these systems in order to achieve good zone temperature control. Good zone temperature control translates into energy savings and better thermal comfort. Thus, the final aspect of the present study deals with development of an analytical model for hydronic heating system. Predictions from the model will be compared with measured data. The validated model will be used to study various control strategies in order to improve the operating performance of the system.

The hydronic heating system installed at the MEGA House combines both space heating and domestic hot water (DHW) functions. Such systems are well suited for the residential applications and are known as Integrated Hydronic Heating Systems or IHHS. The rationale for developing the model of the IHHS was due to the fact that they are widely used and found to be economical compared to conventional systems [23].

A typical Integrated hydronic heating system as shown in Figure 5.1

consists of a boiler unit, baseboard heater, a DHW tank, a distribution network of piping equipped with circulation pump, and flow control valves. The system operates in a simple on/off mode, which means that the room thermostat switches the burner and the pump on/off in response to a fluctuation in room temperature and/or DHW temperature from their desired settings.

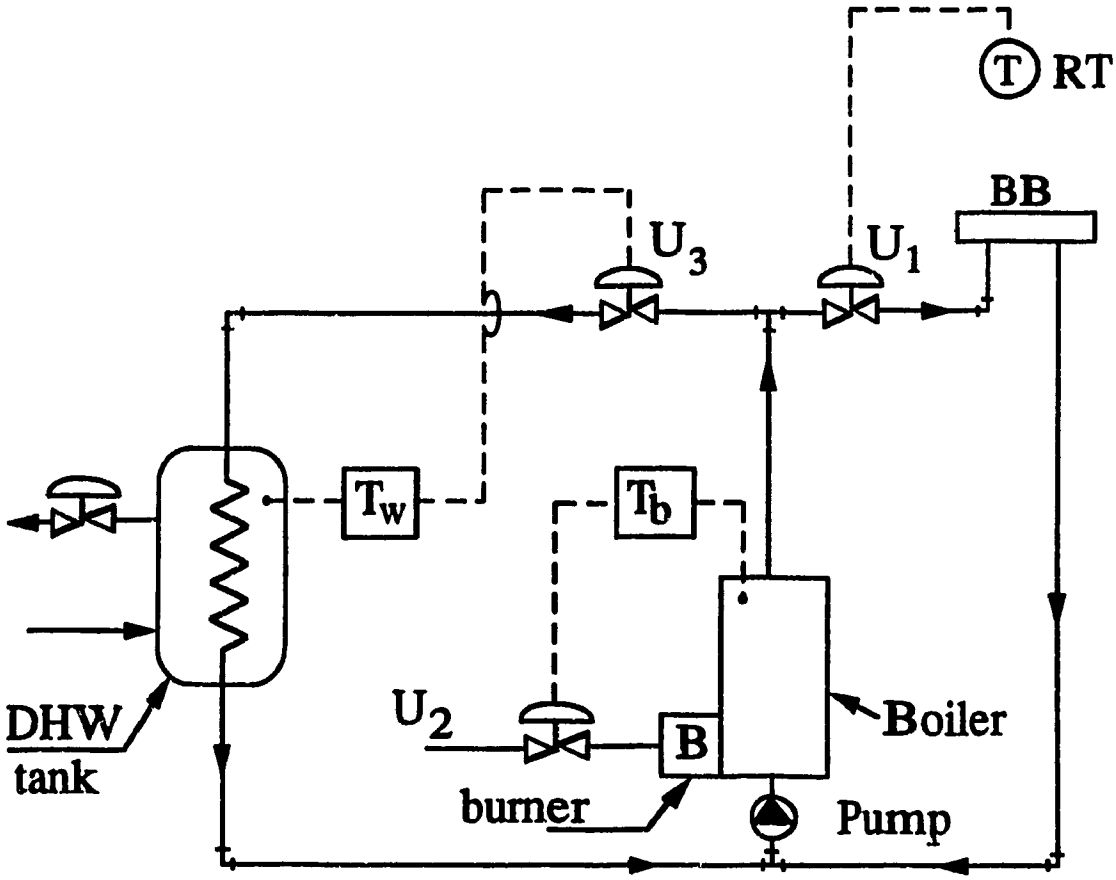

RT: Room thermostat
BB: Baseboard

Figure 5.1 Schematic diagram of Integrated hydronic heating system.

To avoid frequent switching, also known as "shuttling", the burner remains on until the boiler temperature reaches a high limit and turns off and thus continues to be off until the low limit is attained. Note that the pump and burner are interlocked meaning that the pump is first turned on followed by the burner (the delay or lag time varies between 30 to 60 seconds). The reverse also occurs after the burner is shut off. The former action ensures that the heat transfer to the water is complete thus preventing overheating of the combustion chamber and the latter action allows the withdrawal of stored heat from the heat exchanger surfaces.

This two position control works fairly well and has the advantage of being very simple. The major disadvantage of this control strategy is that when the heating load decreases, the standby losses are greatly increased due to the high and low limit of the boiler. Furthermore, it is well known that an increase in off-cycle losses decreases the seasonal efficiency of the boiler [14].

From temperature control viewpoint, the on/off control gives rise to cyclic variations in room and DHW temperatures which exceed the setpoint differential due to factors such as thermal capacity of the boiler-convector unit. For this reason, close control of temperature about a setpoint cannot be achieved with the two-position control.

In order to achieve good room temperature control, it is proposed to replace the two position control by a proportional-integral (PI) controller. In other words, the burner is continuously controlled to match the heating load (load-matching burner), and the flow rate of the hot water is controlled by variable flow pumping, thus maintaining good room temperature control. Both actions are concurrent and require feedback signals from room thermostat and boiler temperature sensor (aquastat).

The following illustration will help clarify the proposed control scheme. Consider the single zone IHHS as shown in Figure 5.1. The room temperature is maintained close to the setpoint by regulating the flow rate of the hot water via controller C_1. Likewise, the boiler temperature is maintained close to the aquastat setpoint by regulating the burner capacity via controller C_2. A third controller C_3 is used to control the DHW temperature at some chosen setpoint. The optimum aquastat temperature can be determined by optimizing the boiler temperature as a function of heating load, thereby minimizing any standby losses that occur due to higher boiler temperatures at part load. In other words, in the proposed control strategy, the boiler setpoint is not fixed but rather variable.

To design such energy efficient strategies, the first step is to develop a transient model of a single zone Integrated hydronic heating system. To

this end, this chapter is organized as follows. The first section describes the model with respect to dynamic heat transfer processes as taking place in the boiler, the fin-tube convectors, the DHW tank and in the environmental zone. The system operating performance will be simulated using on-off control and the predicted results will be compared with measured data. To improve the operating performance of the system, PI controllers will be designed using the validated model. The PI controllers will be used to simulate the system operation. The use of forecasted load to determine the boiler temperature setpoint and its implementation using the designed controller will be illustrated.

5.2 Analytical Model of a Single Zone IHHS.

A transient model of the IHHS is developed by writing energy balance equations for the boiler, the baseboard heat distribution system the DHW tank, and the space.

5.2.1 Boiler Model

For the boiler model, the energy balance equation can be expressed as follows:

$$C_b \frac{dT_b}{dt} = U_2 U_{2_{max}} \left(1 - \alpha \frac{T_b}{T_{b_{max}}}\right) - U_1 U_{1_{max}} C_{pw} (T_b - T_r) - U_3 U_{3_{max}} C_{pw} (T_b - T_{dhw}) - a_b (T_b - T_e) \quad (1)$$

where U_1, U_3 and U_2 are the normalized mass flow rates corresponding to hot circulating water, and burner capacity (in heat units) respectively. In Equation 1, the rate of heat stored in the boiler is equated to the net energy input to the water, minus the rate of heat supplied to the radiator, the DHW coil and the jacket heat losses to the boiler room at temperature T_e. All other terms are defined in the nomenclature.

5.2.2 Baseboard Model

The heat transfer between the hot water and the room air occurs in the baseboard heat exchanger. This is described by energy balance on the hot water in the tubes and the fin-tube temperature.

$$\frac{\partial T_w}{\partial t} + V_w \frac{\partial T_w}{\partial y} = \frac{h_{it} A_{it}}{m_w C_{pw}} (T_t - T_w) \qquad (2)$$

$$\frac{\partial T_t}{\partial t} = \frac{1}{C_t}[\eta_{s,ov} h_{ta} A_c (T_z - T_t) + h_{it} A_{it} (T_w - T_t)] \qquad (3)$$

In Equation 2 the rate of change of energy stored in the hot water (unsteady and convective components) in the baseboard unit is equated to the net rate of heat transfer between the inside tube surface and the hot water.

The tube temperature in Equation 3 was computed by equating the rate of energy stored in the tube metal to the rate of heat transfer between the room air and the tube surfaces and also between the tube and the hot water flowing inside the tube.

The water-side and air-side heat transfer coefficients are obtained from the following correlations [26]:

$$\frac{h_{it} d_i}{K_w} = 0.023 R_{e_w}^{0.8} P_{r_w}^{0.3} \qquad (4)$$

$$h_{t_a} = 1.32 \left(\frac{T_w - T_z}{d} \right)^{\frac{1}{4}} \qquad (5)$$

The fin-tube surface effectiveness is calculated by using the following correlations [28]:

$$\eta_s = \frac{\mathrm{Tanh}(ml_f)}{(ml_f)} \tag{6}$$

$$\eta_{s,ov} = 1 - \frac{A_f}{A}(1-\eta_s) \tag{7}$$

$$m = \left[\frac{2h_{ta}}{K_f y_f}\right]^{\frac{1}{2}} \tag{8}$$

5.2.3 Zone Model

There exist several different models for predicting zone loads [29]. For simplicity, the following lumped capacity model expressed by :

$$C_z\frac{dT_z}{dt} = h_{ta}A_o l_z \eta_{s,ov}(\overline{T}_t - T_z) - a_z(T_z - T_a) \tag{9}$$

is considered. The rate of heat stored in the zone air in Equation (9) is equated to the rate of heat transfer from the baseboard unit and the rate of heat loss to the outdoor at temperature T_a.

In equation (9) T_t is the average fin-tube surface temperature given by:

$$\bar{T}_t = \frac{1}{N}\sum_{i=1}^{N} T_{ti} \qquad (10)$$

Since the water temperature in the baseboard unit changes as it flows through it along the length, so does the tube temperature T_t. By dividing the length of the baseboard in n equal segments, T_t was computed and averaged by using Equation (10).

5.2.4 DHW Model

The energy balance equation describing the heat transfer between the DHW tank and the boiler can be described by the following equations.

$$C_{dhw}\frac{dT_{dhw}}{dt} = m_{dhw}C_{pw}(T_m - T_{dhw}) + a_{dhw}(T_e - T_{dhw}) + h_t A_d l_c (\bar{T}_c - T_{dhw}) \qquad (11)$$

$$C_c\frac{d\bar{T}_c}{dt} = h_t A_{po}(T_{dhw} - \bar{T}_c) - h_{it}A_{pi}\left(\bar{T}_c - \frac{T_b + T_{c,w}}{2}\right) \qquad (12)$$

$$C_{cw}\frac{dT_{c,w}}{dt} = U_3 U_{3_{max}} C_{pw}(T_{c,w} - T_b) - h_t A_d l_c (\bar{T}_c - T_{dhw}) \qquad (13)$$

In equation (11) the rate of heat stored in the DHW is equated to the rate of energy lost in the DHW consumption, rate of heat losses through the tank exterior surfaces, and the rate of heat transfer between the DHW coil surface and the DHW.

The DHW coil was assumed to be at a uniform temperature T_c and therfore the rate of energy stored in the DHW coil metal is equated in Equation (12) to the rate of heat transfer between T_c and T_{dhw} and the rate of energy transfer between the boiler water and T_c.

Equation (13) states that the rate of heat stored in the return water from the coil is equal to the rate of energy supplied from the boiler water via the valve U_3 and the rate of heat transferred to the DHW via the coil surfaces.

Equations 1 through 13 were discretized in space and time. For this purpose, the baseboard length was divided into three equal segments and nodal equations, for each segment, were derived. A total of nine non-linear differential equations were solved by using finite difference methods. To check the system responses, realistic design parameters given in Table 5.1 were chosen and simulation runs were made.

Table 5.1 Design Parameters of boiler used in computer simulations.

Variable	Magnitude	Variable	Magnitude
a_b	3.33 J/s°C	c_{pw}	4180 J/kg°C
a_{dhw}	3.33 J/s°C	c_t	384 J/kg°C
a_z	1462 J/s°C	ρ_{fin}	2787 kg/m³
C_b	450 KJ/°C	c_f	896 J/kg°C
C_{dhw}	168 KJ/°C	l_r	6.0 m
C_z	374 KJ/°C	k_f	236 J/s m°C
d	22.22 mm	k_w	0.658 J/s m°C
d_i	19.94 mm	y_f	1.56 mm
l_c	2.0 m	T_e	20 °C
m_{wdhw}	0.028 kg/s	T_∞	18 °C
U_{1max}	0.3 kg/s	T_{bmax}	90 °C
U_{2max}	105 KJ/s	α	0.12
U_{3max}	0.1 kg/s		

Figures 5.2a-d show the temperature responses of the space heating part of the circuit to constant inputs (valve lift U_1=0.521 and burner capacity U_2=0.527) at constant outdoor temperature T_a=-5°C. Starting from arbitrarily chosen initial conditions, the system output temperatures rise exponentially and attain steady state conditions as shown in the figures.

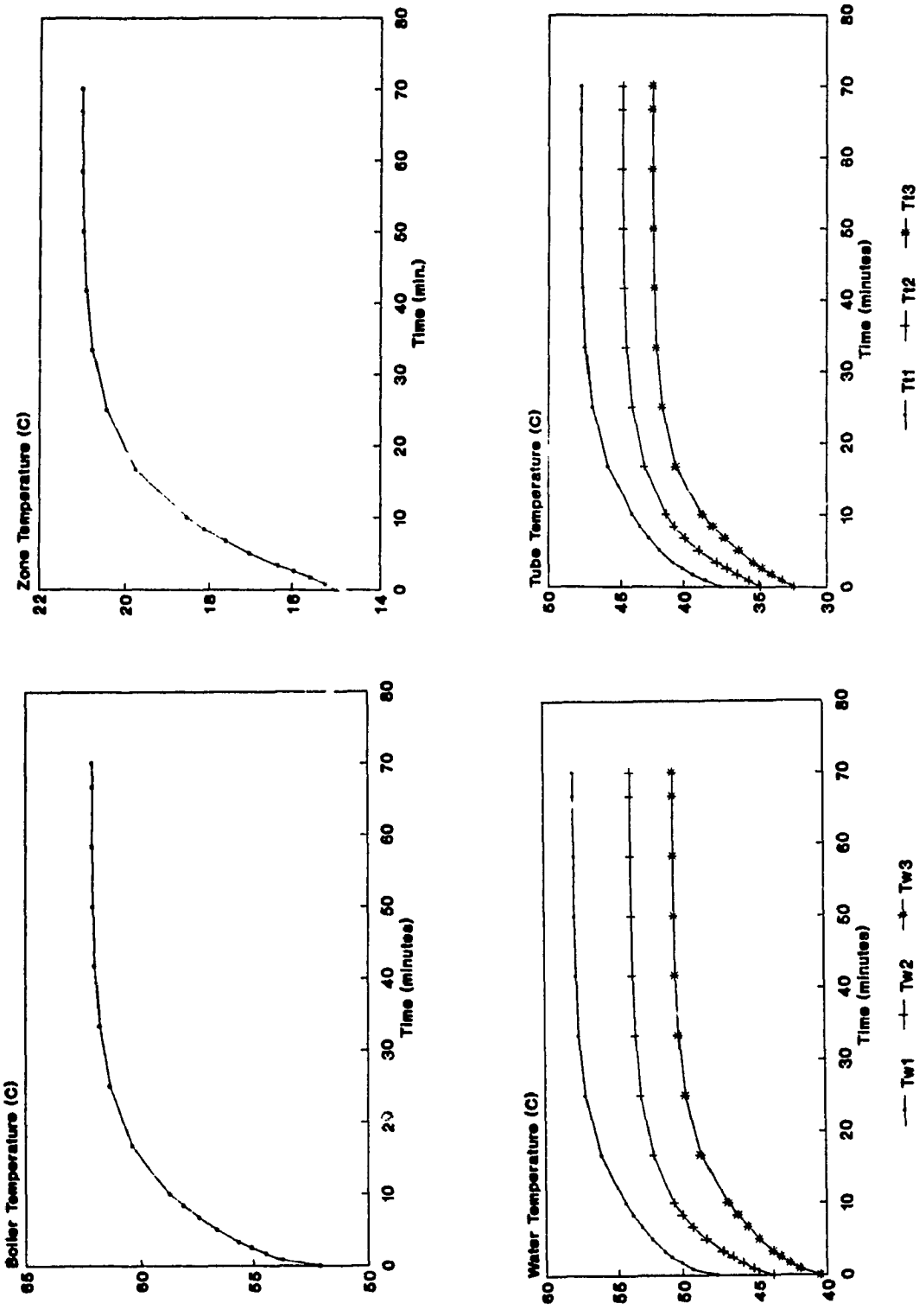

Figure 5.2 Response of IHH system to constant inputs.

The time required to attain steady state is of the order of 1 hour. This delay is mainly due to the thermal capacity of the boiler water and the natural convection heat transfer process which occurs between the room air and the baseboard units. When steady state conditions are attained, the boiler temperature T_b=62.1°C, the zone temperature T_z=21°C as shown in Figure 5.2a-b. Also shown in Figure 5.2 c are the temperatures of the hot water at each of the three nodes along the length of the baseboard. These three temperatures are defined as T_{w1}, T_{w2} and T_{w3}. It is evident that the water temperature drops along the length of the baseboard. The corresponding fin-tube temperature at these same three nodes are depicted in Figure 5.2 d. It is also observed that the fin-tube nodal temperatures are less than the corresponding water temperatures. This is expected since the heat is transferred from the water to the room air via the fin-tube surfaces. The temperature responses obtained from Figures 5.2 a-d show expected trends from a HHS and therefore it is concluded that the model equations and design parameters are suitable for simulation studies, but must be validated utilizing the actual in-situ data from the experiments conducted in Mega house.

5.3 Model Validation

In order to validate the model given by equations (1-13), simulation tests

were conducted and predictions from the model were compared with in-situ measurements.

For this purpose, the IHHS model parameters were chosen from the manufacturers specifications. For example, the burner capacity, pump capacity, DHW tank size, high and low limit temperatures for the boiler and the length of baseboard radiators etc... are known accurately. However, other parameters such as boiler thermal capacity, and heat loss rates and heat exchanger effectiveness were chosen based on steady state sizing methods. These latter parameters were fine tuned during comparison with actual data.

For the purpose of comparisons simulation tests were conducted corresponding to a day on March 26, 1989. The outdoor temperature on this day remained within -5°C ±0.5°C. The predicted outputs such as boiler temperature, zone and DHW temperatures were compared with the measured data.

5.3.1 Boiler Temperature Validation

The first operating characteristic to be simulated was the boiler temperature. The results of the simulation and of the actual measured

data (T_{out}= -5°C) are shown in Figure 5.3.

As is clearly evident from the figure, the model performed quite well in simulating the actual boiler temperature, with only small deviations from the measured data. These deviations are due to the fact that the thermal capacity of the boiler and the distribution piping and heat loss parameters are not accurately known. However, the predictions with the chosen parameters appears to be reasonable.

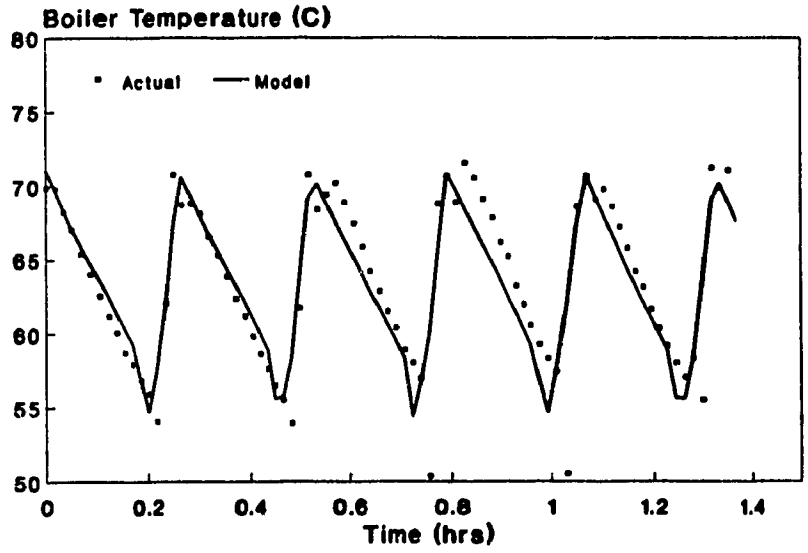

Figure 5.3 Predicted and Actual Boiler Temperature.

5.3.2 Zone Temperature Validation

The next operational characteristic which had to be looked at in order

to validate the analytical model was the room temperature response. This response can be seen in Figure 5.4. For this simulation, the same outdoor temperature conditions (T_{out} = -5°C) were chosen.

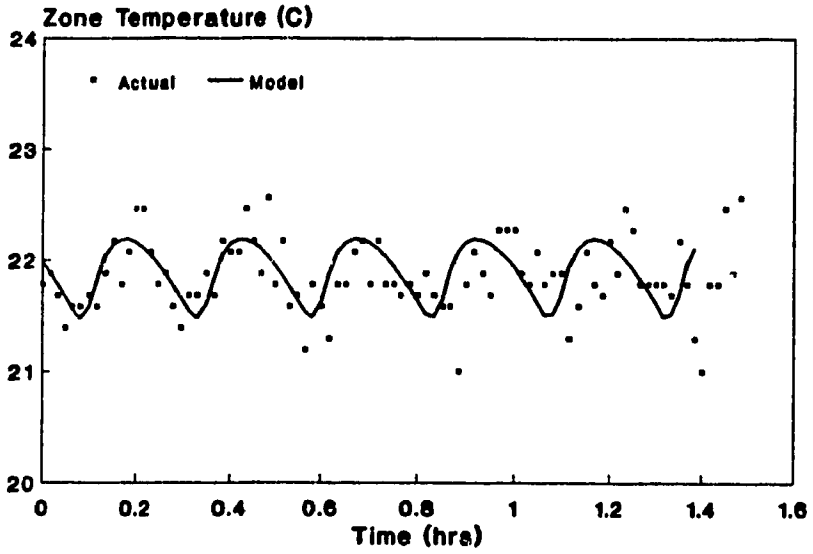

Figure 5.4 Simulated and Actual Zone Temperature.

The general trend expected of a two position control is evident from Fig. 5.4. The predicted and measured data follow cyclic pattern associated with on-off control. Differences in the predicted and measured data are expected due to several factors. The primary source of the error is due to the fact that the measured data represented an average of five readings taken on the third floor at Mega House rather than one room temperature reading at the thermostat location. Another source of error is that the heat loss rate parameter used in the model does not accurately represent the actual

thermal dynamics of the building. Nevertheless, results show that the differences in the measured and predicted temperatures are within ±0.5°C.

5.3.3 DHW Model Validation

The third operational characteristic which was looked at was the domestic hot water temperature. The plot of both boiler and DHW temperature obtained during a typical experiment together with the predicted values are shown in Figure 5.5.

This test was conducted under the following operating conditions.

DHW setpoint = 60°C

DHW mass flow rate (load) = 0.5 G.P.M.

City water Temperature = 12°C

Outdoor Temperature = -5°C

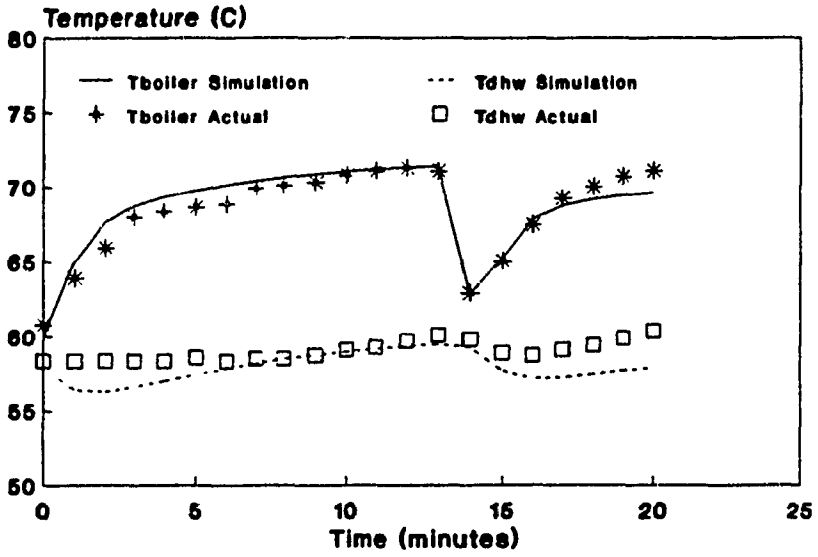

Figure 5.5 Simulated and Actual DHW and Boiler Temperature.

For clarity, one typical cycle results of the boiler and DHW temperature profile are plotted. The predicted boiler temperature profile is close to the measured data during on and off periods. The cycle time also matches quite well. The DHW cycle also shows the general trend (cycle time matches the measured data), but the predicted DHW temperature shows an undershoot for the first 5.5 minutes of the cycle. This can be attributed to a low initial DHW temperature value at the start of the simulation and also due to the errors in the magnitude of the heat transfer coefficients used in the model.

The results depicted in Figures 5.3 - 5.5 show that the predictions from the model are in general agreement with the measured data. As such,

the developed model can be used as a useful guide to develop different operating strategies for improving the performance of the IHHS.

5.4 Proportional and Integral Control of IHH System

As discussed in the Introduction to this chapter, the practical IHHS are mainly controlled by using on-off control action. As a result, good temperature control cannot be achieved. Since temperature deviations from the setpoint often translate into energy losses, it is necessary to control the boiler temperature and other output temperatures as close to the setpoint as possible. To this end, it is proposed to simulate the system response using PI controllers. To illustrate the system response with PI control, first the space heating function will be considered. In other words, controllers C_1 and C_2 will be designed for the system shown in Figure 5.1 assuming that the DHW circuit is off.

5.4.1 Tuning of PI Controllers

There are several methods available for the tuning PI controllers [30]. The basic equation describing PI control action is given by:

$$U(t) = K_p\left[e + \frac{1}{T_i}\int e dt\right] \qquad (14)$$

This equation can also be expressed as:

$$U(t) = K_p e + K_i \int e dt \qquad (15)$$

where K_p is the proportional gain, K_i is the integral gain time and e is the error defined as:

$$e = T - T_{set} \qquad (16)$$

The controller constants K_p and K_i were chosen by trial and error until smooth responses were obtained. First, Kp was chosen and then the magnitude of Ki was gradually increased until smooth responses were obtained.

Sets of K_p and K_i, one for each controller, were obtained and the system response with these controllers was simulated. Figure 5.6 shows the block diagram of the closed loop system.

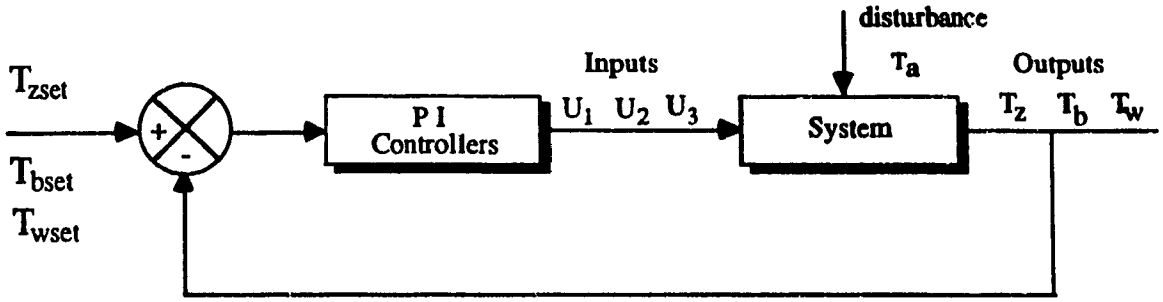

Figure 5.6 Block Diagram of the Closed Loop System

To better illustrate the controller response, consider a case in which the heating load on the zone increases due to a step change in outdoor temperature (say from -5°C to -7.5°C). Figure 5.7a-c depicts how the controllers restore the zone and the boiler temperatures to their respective setpoints following this step disturbance. As shown in Figure 5.7a the boiler temperature reaches close to its setpoint (T_{bset}=62.1°C) after approximately 9 minutes. On the other hand, zone temperature drops to 20.5°C initially, as shown in Figure 5.7b, and then gradually reaches close to the setpoint (T_{zset}=21°C) in approximately 20 minutes. The modulation of the mass flow rate of hot-water, U1, and burner capacity, U2, during this time are depicted in Figure 5.7c. The temperature responses depicted in Figures 5.7a-c show that the controller responses are smooth and the effect of the step changes in outdoor temperatures on the output responses are

rejected, thus restoring T_b and T_z to their respective setpoints in a reasonable time.

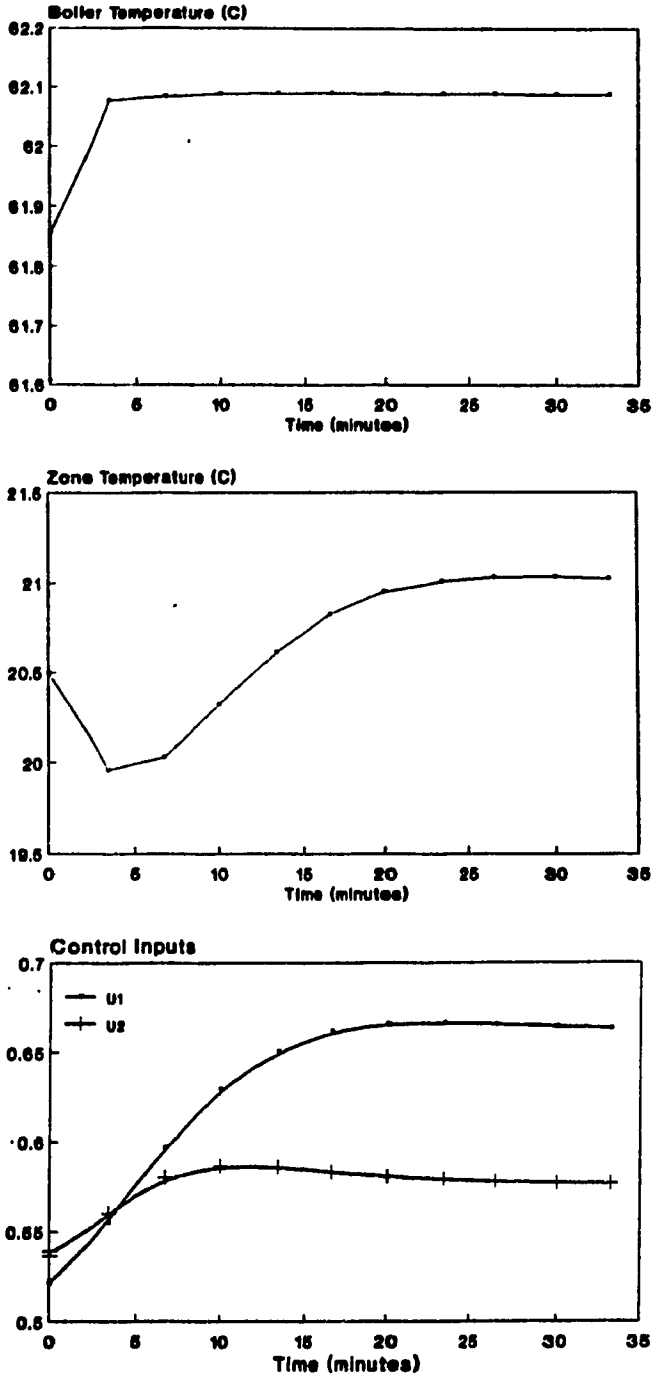

Figure 5.7 Temperature responses of the closed loop system due to a step change in T_{out}

5.5 Outdoor Air Temperature based Control Strategy

By continuously matching the burner capacity with the heating load, the overall efficiency of the boiler can be kept high at all load conditions. To this end, a scheme which can be used to continuously vary the boiler setpoint temperature as a function of load is proposed. In this regard, it is necessary to determine the steady-state boiler temperature as a function of outdoor temperature. This functional dependence is shown in Figure 5.8a-b. Note that under steady state conditions, T_b is a linear function of T_a which can be expressed by:

$$T_{bset} = T_{bo} + f'(T_a - T_{ao}) \qquad (17)$$

where, T_{bo} and T_{ao} represent a known operating point.

As the outdoor temperature varies, the control strategy will automatically match the boiler setpoint to the new load condition and consequently the burner capacity is regulated to bring the boiler temperature close to the new set-point. The following example illustrates how the control scheme can be implemented.

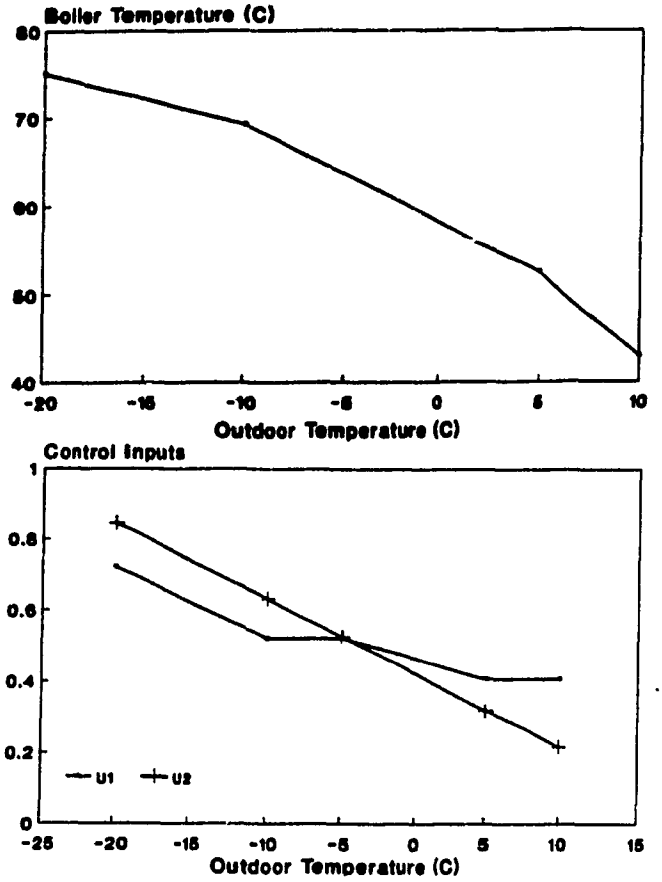

Figure 5.8 Control Inputs and Boiler Temperature as a function of T_{out}

Consider the current outdoor temperature is -5°C and the forecasted outdoor temperature suggests that the approaching warm front raises the outdoor temperature to 5°C in a short time. Given this forecast, we can determine the new set-point temperature for the boiler from Equation (17) and reduce the current boiler setpoint gradually to the new setpoint using an exponential profile, such as

$$T_{bnew} = T_{bold} - \Delta t(1 - e^{-bt}) \qquad (18)$$

where, b is a coefficient and t is time.

In the example considered, b was chosen such that the transition time is of the order of 13 minutes. In other words, the boiler temperature should be decreased to the new setpoint in about 13 minutes. The results of this simulation are depicted in Figures 5.9a-b.

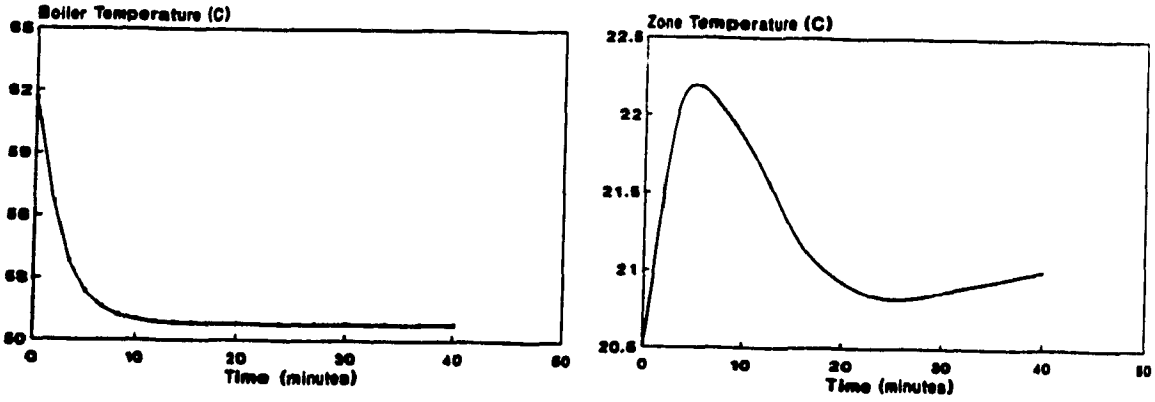

Figure 5.9 Boiler and Zone Temperature Profiles

It is apparent from Figure 5.9a that the boiler temperature is decreased from 62°C to the new setpoint of 50.8°C in about 13 minutes. The zone temperature response during the transition is shown in Figure 6b. Note that some overshoot in T_z occurs because of the fact that while the heating load on the zone is decreasing, the stored heat in the distribution system is released thus causing a 1°C overshoot. This is not unreasonable with

baseboard heating systems. Also note that the example we have considered is a worst case scenario in which the outdoor temperature is assumed to undergo a 10°C change in less than 20 minutes, which is somewhat severe. The results show that the proposed controller can be used to implement the outdoor air temperature based setpoint control schemes.

5.5.1 Closed-Loop Response of the IHHS with three Controllers

Utilizing the method described in section 5.4, PI constants for the three controllers (one each for U_1, U_2 and U_3) were determined. These controllers were used to simulate the IHHS with step changes in space heating and DHW loads. It is assumed that a 15% increase in space heating load and 25% increase in the demand for DHW occur simultaneously. The results are shown in Figures 5.10a-d. As seen in Figure 5.10a, the boiler temperature rises quickly and attains its setpoint (T_{bset}=82°C) in less than 10 minutes. The zone temperature, Figure 5.10b, overshoots by 0.5°C and reaches close to the setpoint (T_{zset}=21.0°C) in approximately 25 minutes. The DHW temperature as seen in Figure 5.10c, takes longer to reach the setpoint (T_{wset}=60°C). However, DHW temperature reaches within ±0.2°C of the setpoint in approximately 25 minutes. How the inputs are regulated during this time is shown in Figure 5.10d. Although the responses are not optimal, it is worth mentioning that the controllers are able to regulate the

system outputs close to the setpoints, in the presence of realistic changes in space heating and DHW loads.

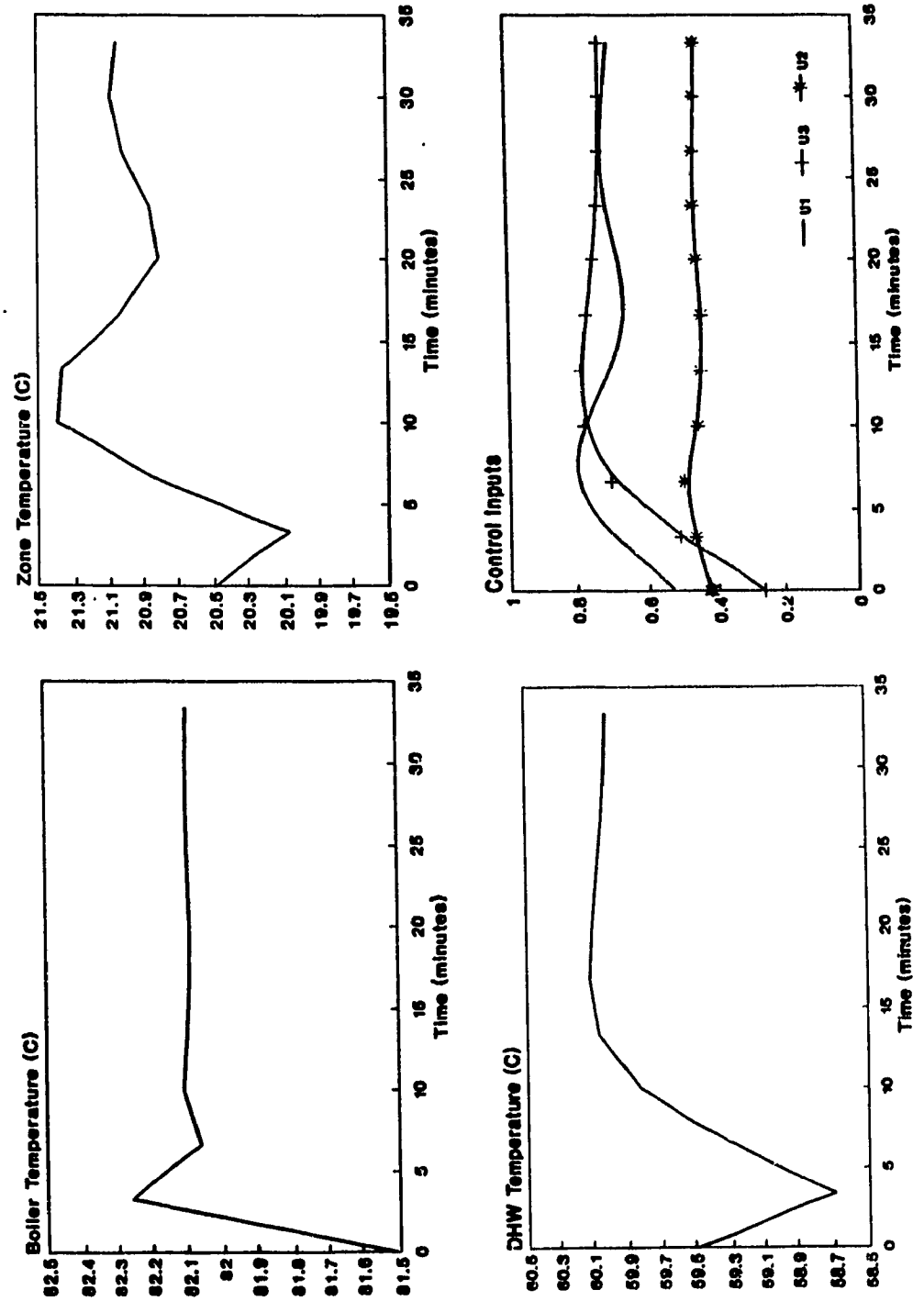

Figure 5.10 Closed loop response of IHHS.

5.6 Summary

A transient model of an IHHS was developed and validated. The transient response results to step changes in inputs show that the single zone HHS takes about one hour to reach steady-state. It has also been shown that the PI controllers are able to maintain boiler, zone, and DHW temperatures close to their respective setpoints in the presence of realistic step changes in space heating and DHW loads.

CHAPTER 6

CONCLUSIONS AND RECOMMENDATIONS

6.1 Conclusions

The literature review showed us that field data on high efficiency gas-fired heating systems was lacking. For this reason, a study was initiated by the Centre for Building Studies (Concordia University) in conjunction with Gas Metropolitain Inc.

The relative performance of three heating systems in a multi-unit apartment building (Mega House) was assessed and evaluated. Cyclic and daily operational characteristics, steady-state and seasonal performance, initial cost and physical practicality were some of the characteristics which were studied.

1. **Comparisons based on Physical characteristics**

   (a) The modular system has most stand by losses, due to its continuos pilot ignition.

   (b) The condensing heat exchanger design as found in the furnace and hydronic boiler recovers heat from the flue gases but has increased initial cost due to extra plumbing.

(c) Long on cycles results in high temperatures on the modular casing.

2. <u>Comparisons based on operational characteristics</u>

(a) Steady-state efficiencies for the furnace, modular and boiler were 86, 80 and 83 % respectively.

(b) For a given cold day, the furnace, modular and boiler on-times were 38.5, 46.2, and 33.3 % of the day.

3. <u>Comparisons based on seasonal performance</u>

(a) At the highest frequency of occurence, the furnace, modular and boiler had on/off times of 4-5/6-7, 25-30/20-25, and 4-5/9-10 minutes respectively.

(b) From the view point of temperature regulation, the three systems ranked as follows: 1-warm-air furnace, 2-hydronic boiler, and 3-modular system.

(c) Cumulative gas consumptions over the entire heating season were as follows: 1625, 925, and 1275 m^3 for the furnace, modular and boiler respectively.

(d) The seasonal efficiency of the warm-air system, modular and boiler were 80, 77, and 78 % respectively.

The final objective of the Thesis was to develop an analytical model for the hydronic heating system. The choice of the boiler model was due to the fact that it was an integrated system. That is, a system which satisfies both space heating and domestic hot water load demand.

Models for the boiler, zone, space, and DHW load were developed from basic heat transfer principles and validated using in-situ measured data. Once the overall model was validated, the simple on-off control strategy was replaced with a PI controller. Simulation results show that the PI controllers are able to maintain boiler, zone, and DHW temperatures close to their respective setpoints in the presence of realistic step changes in space and DHW loads. For example, the effect of a -2.5 °C step change in outdoor temperature was corrected in about 30 minutes.

6.2 Recommendations

Many previous studies have focused attention on more industrial and commercial sized hydronic heating systems. More focus should be applied to smaller units such as in single unit homes and apartments, more particularly in combined space/DHW load heating systems, since this is a rapidly growing trend. Experimental work on developing improved controllers for IHHS will be valuable.

REFERENCES

1. Supply and Services Canada, "Energy conservation in residential apartment buildings: policy discussion paper", Project 3-3878, 1983.

2. Becker, F.E. and Searight E.F., "Development of a High-Efficiency, Gas-Fired, Warm Air Heating System Utilizing Heat Pipe Technology", *ASHRAE Transactions* 1983, Vol. 89, Part 1b, pp. 708-714.

3. Ontario Energy, "Energy conservation building operations demonstration: forty high, medium and low-rise multi-unit residential buildings", Ministry of Municipal Affairs, Energy Ontario, 1984.

4. Macriss, R.A. and Zawacki T.S., "Effect of Retrofits on Combustion Characteristics and Seasonal Efficiency of Gas-Fired Furnaces and Boilers", *ASHRAE Transactions* 1981, Vol. 87, Part 1, pp. 805-816.

5. Zawacki, T.S., Cole J.T., Huang V., and Macriss R.A., "Effects of Building Structure and Space Heating Installation on Furnace/Boiler Retrofit Effectiveness", *ASHRAE Transactions* 1983, Vol. 89, Part 1b, pp. 735-750.

6. Macriss, R.A., Zawacki T.S., and Cole J.T., "Residential Gas Furnace Retrofit in 150 Homes in Illinois", *ASHRAE Transactions* 1987, Vol. 93, Part 4, pp. 1490-1498.

7. Lee, W.D., Delichatsios M.M., Hrycaj T.M., and Caron R.N., "Review of Furnace/Boiler Field Test Analysis Techniques", *ASHRAE Transactions* 1983, Vol. 89, Part 1b, pp. 700-707.

8. Gable, G.K. and Koenig K., "Seasonal Operating Performance of Gas Heating Systems with Certain Energy-Saving Features", *ASHRAE Transactions* 1977, Vol. 83, Part 1, pp. 850-864.

9. Hise, E.C. and Holman A.S., "Heat Balance and Efficiency Measurements of Central, Forced-Air, Residential Gas Furnaces", *ASHRAE Transactions* 1977, Vol. 83, Part 1, pp. 865-880.

10. Grot, R.A. and Harrje D.T., "The Transient Performance of a Forced Warm Air Duct System", *ASHRAE Transactions* 1981, Vol. 87, Part 1, pp. 795-804.

11. Janssen, J.E., Torborg R.H. and Bonne U., "Measurement of Heating System Dynamics for Computation of Seasonal Efficiency", *ASHRAE Transactions* 1977, Vol. 83, Part 2, pp. 159-169.

12. Bonne, U. and Langmead J.P., "A Short Method to Determine Seasonal Efficiency of Fossil-Fired Heating Systems for Labeling Purposes", *ASHRAE Transactions* 1978, Vol. 84, Part 1, pp. 422-446.

13. Chi, J. and Kelly G.E., "A Method for Estimating the Seasonal Performance of Residential Gas and Oil-Fired Heating Systems", *ASHRAE Transactions* 1978, Vol. 84, Part 1, pp. 405-421.

14. Kweller E.R., "Off-Cycle Energy Loss Measuring Methods for Vented Heating Equipment", *ASHRAE Transactions* 1985, Vol. 91, Part 2b, pp. 773-787.

15. Bonne, U., "Furnace and Boiler System Efficiency and Operating Cost Versus Increased Cycling Frequency", *ASHRAE Transactions* 1985, Vol. 91, Part 2, pp. 109-130.

16. Bonne, U. and Patani A., "Combustion Controls for Alternative Fuels", *ASHRAE Transactions* 1981, Vol. 87, Part 1, pp. 361-380.

17. Caron, R.N. and Wilson R.P., "Water-Heating Efficiency of Integrated Systems Designed for Space and Water Heating", *ASHRAE Transactions* 1983, Vol. 89, Part 1b, pp. 18-29.

18. Claus, G. and Stephan W., "A General Computer Simulation Model for Furnaces and Boilers", *ASHRAE Transactions* 1985, Vol. 91, Part 1b, pp. 47-59.

19. Malmstrom, T.G., Mundt B., and Bring A.G., "A Simple Boiler Model", *ASHRAE Transactions* 1985, Vol. 91, Part 1b, pp. 87-108.

20. Lebrun, J.J., Hannay J., Dols J.M., and Morant M.A., "Research of a Good Boiler Model for HVAC Energy Simulation", *ASHRAE Transactions* 1985, Vol. 91, Part 1b, pp. 60-86.

21. Pedersen, C.O., McCulley M.T., and Nicol J.L., "A Mechanistic Model for Warm-Air Furnaces", *ASHRAE Transactions* 1985, Vol. 91, Part 1b, pp. 131-141.

22. Kusuda, T., Alereza T., and Hovander L., "Development of Equipment Seasonal Performance Models for Simplified Energy Analysis Methods", *ASHRAE Transactions* 1982, Vol. 88, Part 2, pp. 249-262.

23. Caron, R.N., Demetri, E.P., and Wilson, R.P. Jr., "Integrated appliances for Hot-Water and Space Heating", Symposium on Future Alternatives in Residential/Commercial Space Conditioning, June 12-14 (1980), Chicago, Illinois.

24. *ASHRAE Handbook-1985 Fundamentals*, American Society of Heating, Refrigeration and Air-Conditioning Engineers, Inc., Atlanta, 1985.

25. Zaheer-uddin, M., Fazio P., Roozmon P., and Monastiriakos P., "Heating Multiple-Unit Apartment Building with Gas-Fired Heating Systems: Description of the Facility and 1987-88 Heating Season Results", CBS Report 118, Concordia University, July 1988.

26. McQuiston, F.C, and Parker, "Heating, Ventilation and Air-Conditioning Analysis and Design", 2nd edition, John Wiley & Sons, 1982.

27. Zaheer-uddin, M, Fazio P., and Monastiriakos P., "Heating Multiple-Unit Apartment Buildings with Gas-Fired Heating Systems: Experimental Strategy and Results", *ASHRAE Transactions* 1989, Vol. 95, Part 1, pp. 687-696.

28. Bhalchandra, V.K, and Desmonde R.M., Heat Transfer, 2nd edition, West Publishing Company, St-Paul, Minnesota, 1982.

29. Borresen, B.A., "Thermal Room Models for Control Analysis", *ASHRAE Transactions* 1981, Vol. 87, Part 2, pp. 251-260.

30. Ogata, K., *Modern Control Engineering*, Prentice-Hall, Englewood New Jersey, 1990.

31. Ziegler, J.G. and Nichols, "Optimum Settings for Automatic Controllers", *ASME Transactions* 1942, Vol. 64, pp. 759-768.

APPENDIX

```
************************************************************************
************************************************************************

                HYDRONIC HEATING SYSTEM MODEL FOR
                    SPACE HEATING LOADS

************************************************************************
************************************************************************


      REAL L,M,MU,K,NUO,NUI,MWDHW,MT,LR
      REAL MW1,MW2,LC,LF,MF,MW,KF

      open(1,file='fin.out',status='unknown')
      open(2,file='fin.sim',status='unknown')

      WRITE(*,*)'WHAT IS THE OUTDOOR TEMPERATURE ?'
      READ(*,*)TA


************************************************************************

                        DESIGN DATA

************************************************************************


      CPW = 4180.
      RHOW = 983.0
      QDHW = 41.0 / 1000.
      TE = 20.0
      TCITY = 15.0
      DO = 22.23 / 1000.
      DI = 19.94 / 1000.
      lc=2.0

      AC = LC * 3.14159 * (DO)**2
```

```
**********************************************************************

                    INITIAL CONDITIONS

**********************************************************************


      TDHW = 58.0
      TTC = 65.0
      T3 = 50.0
      T1 = 60.0
      TW1 = 60.0
      TW2 = 55.0
      TW3 = 50.0
      TT1 = 65.0
      TT2 = 60.0
      TT3 = 55.0
      TZ = 18.0
      TW = 60.0

      mw1 = 0.363

c     MW2 is the mass flow rate of water in radiator coil. This rate
c     corresponds to 0.2 kg/sec.

      MW2 = 0.20


**********************************************************************

              RATE OF HOT WATER USED = 1GPM

**********************************************************************

      Tmax = 71.5
      Tmin = 63.0

      mwdhw = 0.028

        U1MAX = MW2
        U2MAX = MW1 - MW2
        U3 = 0.01

       u11 = u1max
```

```
      DO 100 I=1,40000

        IF(TDHW.GE.61.)  U2 = U2MAX * 0.05
        IF(TDHW.LT.60.0) U2 = U2MAX


       IF(T1.GE.Tmax) U3 = 0.0
       IF(T1.LE.Tmin) U3 = 1.0

       if(tz.gt.21.85) u1 = u1max * 0.2035
       IF(TZ.LT.21.50) U1 = U1MAX

*************************************************************************

              HOT IS THE HEAT TRANSFER COEEFICIENT
          FROM COIL SURFACE TO THE DHW WATER  NU = f(Gr Pr)

*************************************************************************


       G = 9.8
       L = 2.0
       K = 0.658

       AD = 3.14159 * DO

c      B = ((2.4/40.)*(TDHW-40.0)+3.9)*0.0001
c      MU = ((-306./40.)*(TDHW-40.)+658.)*1.0E-06
c      PR = ((-2.05/40.)*(TDHW-40.)+4.3)
c      GR = (B*G*(RHOW**2)*(TTC-TDHW)*(DI**3))/(MU**2)
c      NUO = 0.555*(GR*PR)**0.25

       b = 0.00054
       mu = 0.00046675
       pr = 3.01875
       gr = 1360626.864
       nuo = 0.555 * (gr*pr)**0.25

       HOT = NUO * K / DI
```

```
*************************************************************************

                    DHW COIL CHARACTERISTICS

*************************************************************************


      RHOT = 8927.0
      MT = RHOT * 3.14159 * 0.5 * (DO+DI) * 0.5 * (DO-DI)
      CT = 384.0
      AI = 3.14159 * DI


*************************************************************************

        HITC INSIDE HEAT TRANSFER COEEFICIENT FOR DHW
                    NUw= f(Re Pr)

*************************************************************************


c     PR = ((-2.05/40.)*(TDHW-40.)+4.3)
c     MU = ((-306./40.)*(TDHW-40.)+658.)*1.0E-06
      ACI = 3.14159 * (DI)**2 / 4.
      VW = U2 / (RHOW*ACI)
      RE = (RHOW*VW*DI) / MU
      NUI = 0.023 * (RE**0.8) * (PR**0.3)
      HITC = NUI * K / DI


*************************************************************************

      HITR INSIDE HEAT TRANSFER COEEFICIENT FOR RADIATOR
                    NUw= f(Re Pr)

*************************************************************************


      PR = ((-2.05/40.)*(TW2-40.)+4.3)
      MU = ((-306./40.)*(TW2-40.)+658.)*1.0E-06
      ACI = 3.14159 * (DI)**2 / 4.
      VW = U1 / (RHOW*ACI)
      RE = (RHOW*VW*DI) / MU
      NUI = 0.023 * (RE**0.8) * (PR**0.3)
      HITR = NUI * K / DI
```

```
************************************************************************

                AIR-SIDE HEAT TRANSFER COEFFICIENT

************************************************************************


C     HA = 1.32 * ((TW2-TZ)/DO)**0.25
      HA = 8.4

      RHOF = 2787.0
      CF = 896.0
      FT = 1.56 / 1000.
      KF = 236.
      LF = 4. * 25.4 / 1000.
      WF = 4. * 25.4 / 1000.


************************************************************************

                   120 FINS PER METER LENGTH

************************************************************************


      p = 120.
      LR = 8.0

      AF = (LF*WF-(3.14159*0.25*DO**2)) * P * 2 * LR
      MF = RHOF * AF * FT / 2.


************************************************************************

                        FIN EFFICIENCY

************************************************************************


      M = 2. * HA / (KF*FT)
      HF = LF / 2.
      EF = (EXP(M*HF)-EXP(-M*HF)) / (EXP(M*HF)+EXP(-M*HF))
      AS = AF
```

```
      AP = 3.14159 * DO * LR * (1.-P*FT)
      AO = AS + AP
      EFO = (1.-(AF/AO) * (1-EF))

*****************************************************************************

                    INTEGRATE THE EQUATIONS

*****************************************************************************


      DT = 0.03
      LC = 2.0 * 4.0
      DY = 2.0


      cb = 60000.

c     H is the maximum rate of gas consumption corresponding to 0.028
c     cu.m/min. The unit of H is joules/sec.


      h = 0.789 * 17682

      MW = 3.14159 * 0.25 * DI**2 * RHOW * lc

c     AB is the rate of heat loss of the boiler jacket. The unit is
c     joules/sec.

      AB = 12000. / 3600.
      UADHW = 1200. / 3600.
      ALPHA = 0.12


      UAZ = 1.18 * 574000.0 / 3600.
```

```
**************************************************************************

RC IS DHW COIL DIAMETER AND XNC IS NUMBER OF DHW COIL
LOOPS

**************************************************************************


      RC = 0.15
      XNC = 10. * 4.

      AD = 3.14159 * DO
      XLC = 3.14159 * DO * 3.14159 * RC * XNC


**************************************************************************

                    EQUATION 1  FOR TDHW

**************************************************************************


        A1 = (RHOW*CPW*QDHW)
        A2 = MWDHW * CPW
        A3 = UADHW
        A4 = HOT * XLC


        TDHW=TDHW+(DT/A1)*(A2*(TCITY-TDHW)+A3*(TE-TDHW)+
             A4*(TTC-TDHW))

      AI = 3.14159 * DI


**************************************************************************

                    EQUATION 2  FOR TTC

**************************************************************************


        B1 = (1./(MT*CT))
        B2 = HOT * AD
        B3 = HITC * AI
```

```
c      TTC=TTC+(DT*B1)*(-B2*(TDHW-TTC)-B3*(TTC-0.5*(T1+T3)))

       ttc = (b3*0.5*(t1+t3)-b2*tdhw)/(b3-b2)

*****************************************************************************

                          EQUATION 3 FOR T3

*****************************************************************************


         C1 = (RHOW*AC*LC*CPW)
         C2 = U2 * CPW
         C3 = HOT * XLC

c      T3=T3+(DT/C1)*(C2*(T1-T3)-C3*(TTC-TDHW))

       t3 = (c2*t1-c3*(ttc-tdhw))/c2


      T1IN = (U1*TW3+U2*T3)/(U1+U2)

*****************************************************************************

                          EQUATION 4  FOR T1

*****************************************************************************


         D1 = CB
         D2 = H * U3
         D3 = (U1+U2) * CPW
         D4 = AB

     T1=T1+(DT/D1)*(D2*(1.-(ALPHA*T1/TMAX))-D3*(T1-T1IN)-D4*(T1-TE))


*****************************************************************************

          WATER AND TUBE TEMPERATURE IN THE RADIATORS
          EQUATION 5 FOR TW1 THRU TW3

*****************************************************************************
```

```
      VW = U1 / MW

      E1 = (HITR*AI/(MW*CPW))

    TW1 = TW1+(DT)*(-VW*(TW1-T1)/DY+E1*(TT1-TW1))

    TW2 = TW2+(DT)*(-VW*(TW2-TW1)/DY+E1*(TT2-TW2))

    TW3 = TW3+(DT)*(-VW*(TW3-TW2)/DY+E1*(TT3-TW3))

*************************************************************************

                EQUATION 6 FOR TT1 THRU TT3

*************************************************************************

     F1 = (1./(MT*CT+EF*MF*CF))
       F2 = EFO * HA * AO
       F3 = HITR * AI

    TT1 = TT1+(DT*F1)*(F2*(TZ-TT1)+F3*(TW1-TT1))

    TT2 = TT2+(DT*F1)*(F2*(TZ-TT2)+F3*(TW2-TT2))

    TT3 = TT3+(DT*F1)*(F2*(TZ-TT3)+F3*(TW3-TT3))

    TTAVG = (TT1+TT2+TT3) / 3.

*************************************************************************

                EQUATION 7 FOR TZ

*************************************************************************

    G1 = 1.2 * 374000.0

    G2 = HA * AO * LR * EFO

    TZ = TZ+(DT/G1)*(G2*(TTAVG-TZ)+UAZ*(TA-TZ))
```

```
c      If(i.gt.260000) then
      write(1,*)i*dt/3600.,t1,tdhw,tz
      write(2,*)i*dt/60.,t1,tdhw

c      write(*,*)hot,ttc,t3
c      else
c      goto 100
c      endif


100   CONTINUE
     STOP
     END
```